TECHNISCHE UNIVERSITÄT MÜNCHEN

Klinik und Poliklinik für Strahlentherapie und Radiologische Onkologie

Klinikum rechts der Isar

(Direktor: Univ.-Prof. Dr. M. Molls)

Interaction of Endothelial Cells and Natural Killer Cells

Isabelle Marie Mathilde Riederer

Vollständiger Abdruck der von der Fakultät für Medizin
der Technischen Universität München
zur Erlangung des akademischen Grades eines Doktors der Medizin
genehmigten Dissertation.

Vorsitzender: Univ.-Prof. Dr. E. J. Rummeny

Prüfer der Dissertation: 1. Univ.-Prof. Dr. G. Multhoff

2. Univ.-Prof. Dr. M. Molls

3. Univ.-Prof. Dr. U. Protzer

Die Dissertation wurde am 04.10.2012 bei der Technischen Universität München eingereicht und durch die Fakultät für Medizin am 07.05.2014 angenommen.

Τόλμα πρήξιος ἀρχή, τύχη δὲ τέλεος κυρίη

Courage is the beginning of an action, but chance is the master of the end.
(Demokrit)

Dedicated to my family.

List of contents

Appendix

(i) Riederer I, Multhoff G.
The human microvascular endothelial cell line HMEC presents activatory NK ligands. Abstract and presentation.
Molekulare Bildgebung (MoBi) p14, 2009.

(ii) Multhoff G, Riederer I, Andratschke N.
Effects of irradiation on endothelial cells and interaction with the immune system. Abstract and Poster.
12. Jahrestagung der Gesellschaft für Biologische Strahlenforschung (GBS) Essen p133, P6.09, 2009.

(iii) Riederer I, Sievert W, Eissner G, Molls M, Multhoff G.
Irradiation-induced up-regulation of HLA-E on macrovascular endothelial cells confers protection against killing by activated natural killer cells.
PLoS ONE 5(12): e15339, 2010.

(iv) Stangl S, Gehrmann M, Riegger J, Kuhs K, Riederer I, Sievert W, Hube K, Mocikat R, Dressel R, Kremmer E, Pockley AG, Friedrich L, Vigh L, Skerra A, Multhoff G.
Targeting membrane heat-shock protein 70 (Hsp70) on tumors by cmHsp70.1 antibody.
Proc Natl Acad Sci U S A. 108(2): 733–738, 2011.

(v) Riederer I, Molls M, Sievert W, Multhoff G.
Endothelial cells cultured under flow. Poster.
Symposium of CARDIORISK, Munich, June 2011.

Abbreviations

APC	allophycocyanin
BSA	bovine serum albumin
CAM	cell adhesion molecule
CD	cluster of differentiation
cmHsp70.1	cell membrane-bound heat shock protein 70
cpm	counts per minute
Cr	Chromium
d	day
DAPI	4′,6-diamidino-2-phenylindole
DMEM	Dulbecco's modified Eagle medium
DMSO	dimethyl sulfoxide
EA.hy 926 cells	a cell line derived from the fusion of HUVECs with the epithelial lung tumor cell line A549-8
ECs	endothelial cells
EGF	endothelial growth factor
E:T	effector to target ratio
FCS	fetal calf serum
FITC	fluorescein isothiocyanate
g	gravitational constant
Gy	Gray
h	hour
hCMV	human cytomegalovirus
HLA	human leukocyte antigen
HLAE	human leukocyte antigen E
HMEC	human microvascular endothelial cell
HSP	superfamily of heat shock proteins
Hsp70	major stress-inducible heat shock protein 70

HUVEC	human umbilical vein endothelial cell
ICAM	intercellular adhesion molecule
Ig (G)	immunoglobulin (G)
IL	interleukin
IU	international unit
kDa	kilodalton
mAb	monoclonal antibody
mfi	mean fluorescence intensity
mg	milligramm
MHC	major histocompatibility complex
MICA/B	MHC class I polypeptide-related sequence A/B
min	minute
µl	microliter
mM	millimolar
ng	nanogramm
NK cells	natural killer cells
NKR	natural killer cell receptor
P	passage
PBMC	peripheral blood mononuclear cell
PBS	phosphate-buffered saline
PE	phycoerythrin
PECAM	platelet endothelial cell adhesion molecule
RPMI	Roswell Park Memorial Institute, medium for cell culture
SEM	standard error of the mean
TKD	Hsp70-derived peptide with the amino acid sequence TKDNNLLGRFELSG
TNF	tumor necrosis factor
TPBS	tween phosphate-buffered saline
ULBP1, 2, 3	UL16-binding proteins 1, 2, 3

1 Introduction

1.1 Blood vessels and endothelial cells (ECs)

An intact vascular system is essential for the delivery of oxygen and nutrients to organs and to remove carbon dioxide and waste products. Furthermore, the vasculature interacts with cells of the immune system and therefore, plays an important role in immune surveillance. The wall of a larger blood vessel consists of three major parts (see Figure 1): The luminal section is termed tunica intima which is composed of endothelial cells (ECs), basal lamina, and the subendothelial connective tissue. The next layer is the tunica media consisting of smooth muscle cells, collagen, connective tissue, and elastic fibers. Arterial vessels contain more smooth muscle cells and collagen in their tunica media than venous vessels because these have to tolerate higher blood pressure. The tunica adventitia forms the outer layer and consists of collagen, connective tissue, few smooth muscle cells, blood vessels (vasa vasorum), and nerves.

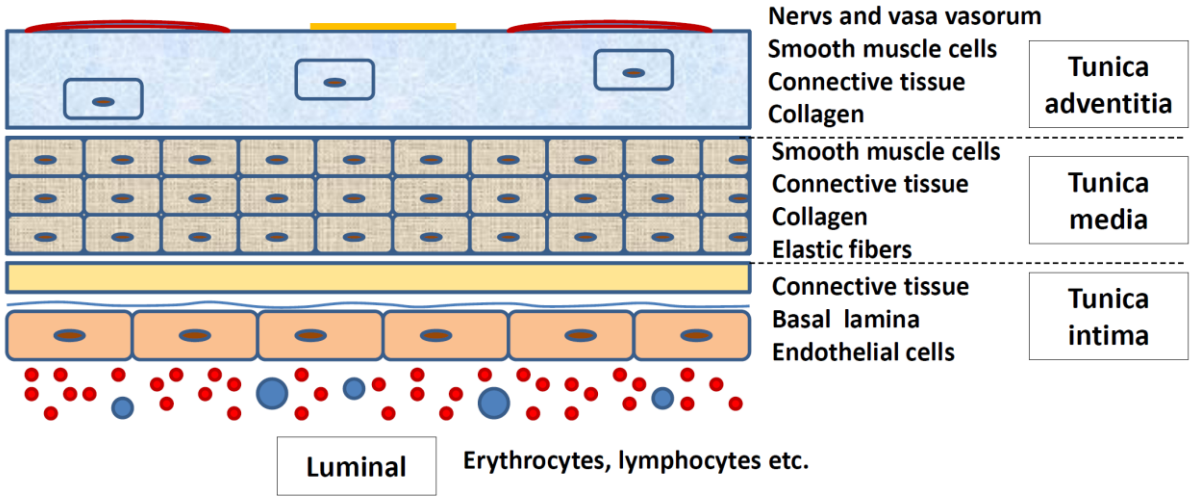

Figure 1: Wall structure of a larger blood vessel consisting of three layers: tunica intima with endothelium, basal lamina and subendothelial connective tissue, tunica media with smooth muscle cells, connective tissue, collagen and elastic fibers, and tunica adventitia containing collagen, connective tissue, few smooth muscle cells, vasa vasorum and nerves.

The most important functions of ECs are summarized in Figure 2. ECs are connected with zonulae occludentes (tight junctions) and provide a barrier between the blood and the tissue. Depending on its location and function, the endothelium can be

classified in the continuous, fenestrated or discontinuous endothelium. All three subtypes exhibit different permeability for substances. Another major task of ECs is the regulation of blood homeostasis by secreting prothrombotic substances, such as the von Willebrand factor (vWF), tissue factor (TF), and plasminogen activator inhibitor (PAI), or antithrombotic acting molecules, such as prostacycline and thrombomodulin. The regulation of the vascular tone is supported by vasodilatory acting NO and prostacycline or vasoconstrictively acting endothelin and angiotensin converting enzyme (ACE). In addition, ECs play an important role in the paracrine regulation of cell growth, e.g. by secreting platelet derived growth factor (PDGF), basic-fibroblast growth factor (bFGF), and macrophage colony-stimulating factor (M-CSF) as stimulating factors, or transforming growth factor-β (TGF-β) and heparin as inhibiting factors. Furthermore, the endothelium synthesizes matrix components such as collagen IV, proteoglycane, and laminin. ECs are also responsible for the oxidation of low-density lipoprotein (LDL) and they express receptors for hormones and vasoactive substances. Very importantly, ECs are also involved in the regulation of inflammation and immunity, which involves the cytokines IL-1, IL-6, IL-8, adhesion molecules, and major histocompatibility antigens.

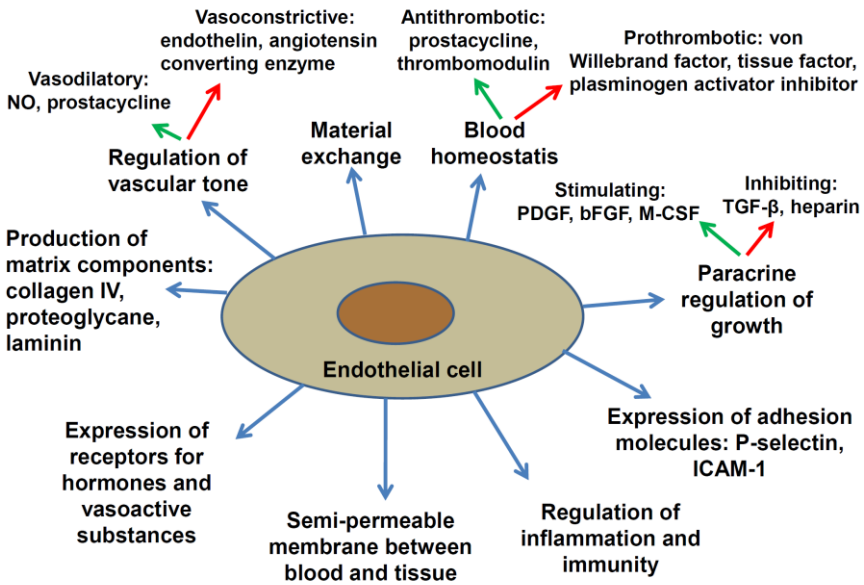

Figure 2: Major functions of endothelial cells (ECs).

The interaction of ECs and leukocytes, such as activated NK cells, involves attachment, rolling, and tethering. These functions are predominantly mediated by

selectins and carbohydrate-rich ligands, such as mucins (Springer 1994, Carlos et al 1994, Allavena et al 1996). Lymphocyte rolling might induce activation and facilitates the tight adhesion of leukocytes to ECs, which is enabled by the integrin family of cell adhesion molecules (Cordes et al 2007). According to their location in the inside of blood vessels, ECs have to tolerate haemodynamic forces such as shear stress. The shear stress in large arteries is enormous and ranges between 10 to 40 dynes/cm^2 (Resnick et al 2003). It has been demonstrated that cells elongate in shape and orient their major axis towards the flow direction in response to a steady state flow (Nerem 1991). Other studies have shown that ECs change their morphology, function, and gene expression in response to shear stress (Ando et al 2009). These responses to shear stress may play a crucial role in angiogenesis, vascular remodeling, and atherosclerosis (Ando et al 2009, Resnick et al 2003). Thus, shear stress and flow conditions are important to maintain normal functions of ECs. Due to chronic stress stimuli, the endothelium can lose its flexibility. Endothelial dysfunction can cause severe diseases such as atherosclerosis or thrombosis. The EU Framework Program CARDIORISK (2007-2011) was initialized to study clinicopathological effects on coronary microcirculation and endothelial cells following exposure of the heart to low dose irradiation. Epidemiological studies show an increased risk for cardiac diseases several decades after exposure of the heart to low dose radiation, e.g. after radiotherapy of breast cancer (Schultz-Hector et al, 2007).

1.2 Immune system and natural killer (NK) cells

Immune responses are mediated by two complementary systems: the innate immunity which is antigen independent and the adaptive immunity which is antigen dependent. Adaptive immune responses are mediated either by antigen specific antibodies (humoral immune response) or by lymphocytes such as T cells (cellular immune response). The innate immunity provides the first line of defense against bacterial and viral invasion and against tumor cells. Unspecific humoral factors are complement, acute phase proteins, and cytokines. Unspecific cellular components are macrophages, monocytes, mast cells, and granulocytes. Traditionally, natural killer (NK) cells are classified as effector cells of the innate immune system. Recent studies, however, have proposed that NK cells can be seen as an “evolutionary bridge” between the innate and adaptive immunity since they contain nearly all features of adaptive immunity including their memory status (Sun et al 2009). NK cells arise from lymphoid stem cells and account for 5-20% of peripheral blood mononuclear cells (PBMC). They recognize their target cells by “altered self” or by a reduced or missing expression of HLA-class-I-molecules and hence play a pivotal role in the early defense against viral infections and malignant transformations (Trinchieri 1989, Bielawska-Pohl et al 2005, Biron 1997). This “altered self” or “missing self” is a signal for NK cells to kill modified target cells by inducing cell death mechanisms (Lanier 2005). A typical feature of NK cells is that they neither express clonal T-cell receptors (TCR) complexed to CD3 like T cells nor antigen specific receptors/antibodies like B cells. The majority of NK cells express the low-affinity IgG receptor CD16 (Fc RIII), the neuronal adhesion molecule CD56, and the C-type lectin receptor CD94 (Gross, Schmidt-Wolf et al 2003). The functionality of NK cells is regulated by a fine balance mediated by a number of different inhibitory and activating NK cell receptors (NKR) (Biassoni et al 2003, Westgaard et al 2003). The following major human NKR families can be distinguished: C-type lectin superfamily receptors (e.g. CD94/NKG2), Ig superfamily receptors called the killer cell inhibitory receptor (KIR), immunoglobulin-like transcripts (ILT) or leukocyte Ig-like receptors (LIRs), and natural cytotoxicity receptors (NCR) (Moretta et al 2001, Lanier 1998 a, Biassoni et al 2000). These NKR can transduce activating or inhibitory signals to NK cells. Inhibitory receptors with specificity for classical and non-classical MHC class I

molecules protect host target cells against the cytolytic attack mediated by NK cells. Immunoreceptor tyrosine-based inhibitory motifs (ITIMs) in the cytoplasm mediate inhibitory signals (Bolland et al 1999). Via binding of ligands and activation, the inhibitory NKRs become tyrosine phosphorylated and recruit tyrosine phosphatases. Thus, NK cell-mediated cytotoxicity and cytokine expression is inhibited (Lanier 1998 b). Depending on its co-receptor, the C-type lectin receptor CD94 can mediate inhibitory and activating functions. Members of the NKG2 family, consisting of at least six members (NKG2 A–F), act as co-receptors for CD94 or as homomeric receptors. CD94/NKG2A and NKG2B are inhibitory receptors, whereas CD94/NKG2C, NKG2D, NKG2E, and NKG2F represent activating receptors (Brooks et al 1997, Houchins et al 1997, McQueen et al 2002). The NKG2D receptor is expressed by NK cells, γδ T cells, and a minority of $CD8^+$ T cells and interacts with the stress-inducible MHC class I chain-related (MIC) antigens, MICA and MICB, and the UL16-binding proteins (ULBP) (Borrego et al 2002, López-Botet et al 2000, Vivier et al 2002). Binding of antigens to the NKRs activates different signaling pathways (Vivier et al 2004). Thus, NK cell function seems to be determined by a balance between activating and inhibitory signals which initiate or suppress NK cell function (Valés-Gómez et al 1999, Lanier 1998 b and 2005). Figure 3 demonstrates a simplified scheme of the interaction of NK cells and target cells.

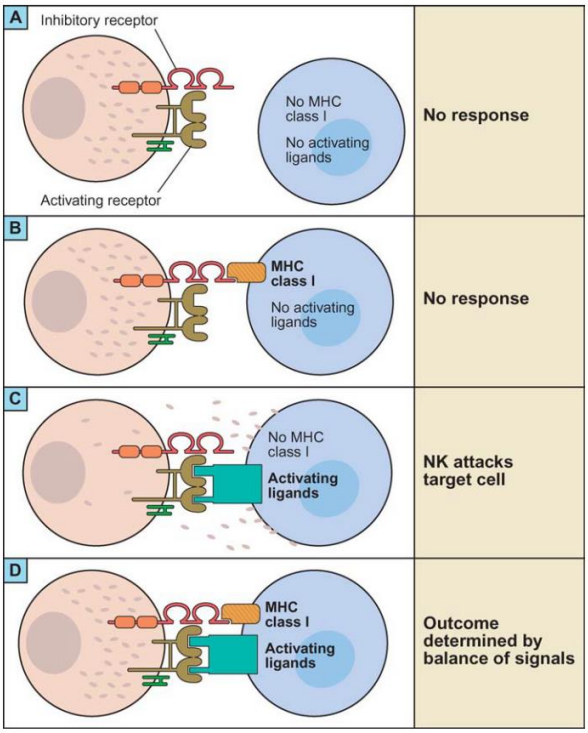

Figure 3 (Lanier 2005): Schematic representation of the interaction of NK cells and target cells.

One mechanism how NK cells kill their target cells is the induction of death receptor-mediated apoptosis. Death ligands on effector cells, such as Fas ligand or tumor necrosis factor (TNF), bind to death receptors expressed on target cells. After binding, intracellular adapter molecules are recruited that activate the caspase cascade that causes cell death (Screpanti et al 2001). Another mechanism involves the release of granules containing perforin and granzyme B. Granzyme B is a member of serine protease family that enters target cells by the assistance of perforin (Shafer-Weaver et al 2003). Inside the target cells, granzyme B plays an essential role in the granule-mediated apoptosis by triggering both caspase-dependent and caspase-independent apoptotic pathways (Trapani et al 2000).

1.3 Activating and inhibitory ligands for NK cells

Target cells express a number of inhibitory and activating cell surface ligands that impact the function of NK cells. Among them there are the highly polymorphic classical major histocompatibility complex (MHC) class I and II molecules and the less polymorphic non-classical (also termed class Ib) MHC gene products. Some of the MHC class Ib or MHC class I-related genes are called the MIC gene family, first described by Bahram and co-workers (1994). Only two of seven existing MIC genes are expressed, namely as MICA and MICB glycoproteins, the others are the pseudogenes MICC, D, E, F, and G (Zwirner et al 1999, Stephens 2001). MICB has structural and functional attributes similar to those of MICA (Steinle et al 2001). MICA and MICB are expressed in fibroblasts, epithelial and endothelial cells. They are stress-inducible and bind to NKG2D which, in turn, activate the cytolytic activity of NK cells (Bauer et al 1999). The recognition of MIC proteins is involved in anti-tumor immune responses, auto-immunity, and immune surveillance (Schrambach et al 2007). The promoter of MICA and MICB genes contains sequences that are similar to the heat shock elements of heat shock protein (HSP) 70 genes (Groh et al 1996). Among the activating NKG2D ligands there are also the glycosylphosphatidylinositol (GPI)-linked, MHC class I-related molecules ULBP 1-3, which are able to bind to the human cytomegalovirus glycoprotein UL16 (Sutherland et al 2002). The human cytomegalovirus (hCMV) contains open reading frames encoding for several proteins to protect cells against immune responses. Interestingly, one glycoprotein, UL16, was only found on surfaces of hCMV-infected cells but not on the virion itself. UL16 is able to block interaction of NK cells by activating ULBP molecules (Kubin et al 2001) and also binds to MICB (Sutherland et al 2001). The ULBPs are homologous to each other and they share 55-60% of the same amino acid sequence. ULBPs, however, are represented in a larger range of cells and tissues, e.g. on normal human epithelial and endothelial cells, than MICs, which are up-regulated on some epithelial tumors and on hCMV-infected endothelial and fibroblast cells in vitro (Kubin et al 2001, Sutherland et al 2002). For this reason, the MICs seem to have different functions in comparison to the ULBPs. In addition, MICs may be important for marking tumor and virus-infected cells for immune rejection (Sutherland et al 2001). In 1997, Multhoff et al identified membrane-bound heat shock protein 70 (Hsp70) on

tumor cells as another recognition structure for NK cells. Stress or heat shock proteins (HSPs) are highly conserved proteins that are expressed in prokaryotic and eukaryotic cells. Their expression is induced by a variety of stress stimuli such as heat, UV radiation, oxygen radicals, and viral or bacterial infections as well as by many chemicals including heavy metals and cytostatic drugs (Multhoff 2007). Intracellularly, HSPs act as molecular chaperons. They maintain protein homeostasis by assisting protein folding and unfolding, transport, maturation, and degradation. HSPs recognize and bind to nascent polypeptide chains or partially folded intermediates of proteins to prevent them from aggregation and misfolding. According to their molecular weights, HSPs in mammalians are subdivided into the HSP100, HSP90, HSP70, HSP60, and HSP20 major families. Depending on its subcellular localization, Hsp70 fulfills different functions. Cytosolic Hsp70 mediates protective functions, whereas extracellular or membrane-bound Hsp70 can induce immune responses. Most tumor cells exhibit elevated Hsp70 levels (Multhoff et al 1995). Furthermore, NK cells can be stimulated against membrane Hsp70 positive tumor cells by incubating them with the C-terminal domain of Hsp70 or a 14-mer peptide TKD in combination with interleukin 2 (IL-2) (Multhoff et al 1999). NK cells interact with Hsp70 via CD94 (Gross, Hansch et al 2003). Recently, the stress-inducible danger signals, MICA/B and Hsp70 have been described to act synergistically in order to enhance the cytolytic activity of human NK cells (Elsner et al 2010). The anchorage of Hsp70 in the membrane is enabled by the glycosphingolipid globoyltriaosylceramide Gb3, also termed CD77 (Gehrmann et al 2008). HLAE, a prominent member of the non-classical MHC (MHC class Ib), which is recognized by CD94/NKG2A (inhibitory) and CD94/NKG2C (activating) expressing NK cells, is characterized by a limited polymorphism and a tissue-specific and stress-inducible expression pattern (Ulbrecht et al 1992, Braud et al 1997). Although HLAE transcripts are always present in ECs (Ulbrecht et al 1992), the HLAE surface expression is highly variable. HLAE is known to act as a negative regulatory signal for NK cells expressing the inhibitory receptor CD94/NKG2A, and, therefore, might confer immune regulatory functions (Braud et al 1998, Lee et al 1998). Trophoblasts and tumor cells protect themselves against the attack by the innate immune system via an up-regulated expression of HLAE (Marin et al 2003). Stangl et al (2008) have previously shown that transfection of HLAE in Hsp70 membrane-positive tumor cells down-regulates the cytolytic activity of TKD/IL-2-activated NK cells in vitro and in

xenotransplantation. HLAE transgenic pigs expressing human HLAE on PBMCs and ECs, for example, were found to be protected against NK cell-mediated killing (Weiss et al 2009). Binding of HLAE to the CD94/NKG2C heterodimeric complex, however, induces activating signals via Syk family tyrosine kinases (Radons et al 2006).

Cell adhesion molecules (CAMs) are involved in cellular interactions such as cell-cell junctions, cell recognition, and signaling. Cadherins, integrins, selectins, and immunoglobulins are the four main mediators of cell interactions. The intercellular adhesion molecule (ICAM)-1 (also known as CD54) with a molecular weight of 75-115 kDa (Verdier et al 2009) is expressed on a variety of different cell types including leukocytes and endothelial cells. Due to the binding to its ligands, ICAM-1 plays an important role in the cross-talk of cells, e.g. in neutrophil and monocyte-endothelial cell adhesion that result in immune responses (Maio et al 1992). ICAM-1 is constitutively expressed on ECs and its expression can be further increased by pro-inflammatory cytokines (Lawson et al 2009). Interaction of circulating cells under flow conditions and the endothelium, however, is only possible under certain circumstances, e.g. in the presence of inflammatory processes or cancer metastasis (Verdier et al 2009).

1.4 Aims

The major goal of this study was to examine the cross-talk of either non-irradiated or irradiated human micro- or macrovascular endothelial cells (ECs) with natural killer cells (NK cells). By utilizing a newly established method that allows the cultivation of ECs under continuous flow conditions using a pump system coupled to a microscopical imaging unit (ibidi, Martinsried, Germany), growth behavior, morphology, and phenotype of primary and immortalized micro- and macrovascular human ECs were compared under static and flow conditions. Apart from morphology and phenotype, inhibitory and activating cell surface markers were comparatively studied on non-irradiated and irradiated ECs. The interaction of differently treated ECs and NK cells was tested by using different functional assays and microscopical imaging.

2 Material and methods

2.1 Cell culture

ECs can be divided into two major groups: the micro- and macrovascular ECs. In this work, members of both subtypes were investigated. Due to the limited availability and the short lifespan of primary ECs, also immortalized and transformed ECs were used.

2.1.1 Macrovascular human umbilical vein endothelial cells (HUVECs)

Human umbilical vein endothelial cells (HUVECs) represent the macrovasculature. Generally, they are recovered from umbilical vein vascular wall by a collagenase treatment (Baudin et al 2007). The HUVECs, which were used in this work, were purchased from PromoCell (HUVEC-c pooled Cat. No.: C-12203) and delivered as cryopreserved cells in passage 1. Cheung (2007) described that many studies were possible with cryopreserved HUVECs after retrieval. The cells were stored in a liquid nitrogen container at -180°C. After thawing, they were transferred in cell culture dishes or cell culture flasks at a density of 5000 – 10000 cells/cm^2. Cells were grown in HUVEC medium (Table 1) in an incubator (37°C, 5% CO_2, 80-100% humidity). The medium was exchanged 24 h after seeding of the cells. The cells were cultured up to 60-90% confluency. For splitting, the cells were washed twice with sterile phosphate-buffered saline (PBS), and 25 µl/cm^2 trypsin (PromoCell, C-41210) was added for 1-2 min at room temperature. When 50% of the cells were loose, they were detached by gentle tapping. Trypsin was neutralized by adding Trypsin Neutralizing Solution (PromoCell, C-41100) in equal volume. The cells were centrifuged for 4 min at 220 g and resuspended in pre-warmed (37°C) medium. Finally, they were re-seeded at a concentration of 5000 – 10000 cells/cm^2. The medium was replaced every 2-3 days. The doubling time was about 72 h. The cells were splitted twice a week and subcultured until passage 15.

Table 1: Ingredients of the HUVEC medium.

Ingredients	Company/Cat. No.
endothelial cell growth medium	PromoCell/C-22010
supplemented with:	
	SupplementMix PromoCell/C-39215
basic fibroblast factor 1 ng/ml	
endothelial cell growth supplement 0.4%	
epidermal growth factor 0.1 ng/ml	
fetal calf serum (FCS) 2%	
heparin 22.5 µg/ml	
hydrocortisone 1 µg/ml	
penicillin 100 IU/ml	Gibco/15140
streptomycin 100 µg/ml	Gibco/15140

2.1.2 EA.hy 926 cells

EA.hy 926 is a cell line which was derived from the fusion of HUVECs (primary macrovascular endothelial cells) with the epithelial lung tumor cell line A549-8 (Edgell et al 1983). The EA.hy 926 cells were kindly provided by the group of Prof. Dr. Günther Eißner (LMU Großhadern, Munich). Table 2 shows the ingredients of the specific EA.hy 926 medium.

Table 2: Ingredients of the EA.hy 926 medium.

Ingredients	Company/Cat. No.
RPMI 1640 medium	Gibco/21875
supplemented with:	
heat-inactivated FCS 10%	PAA/A15-101
penicillin 100 IU/ml	Gibco/15140
streptomycin 100 µg/ml	Gibco/15140

The cells were splitted twice a week, once they became confluent. After washing with sterile PBS, 25 µl/cm^2 trypsin (PromoCell, C-41210) was added and the cells were incubated for about 1 min at 37°C. When approximately 50% of the cells were loose, they were detached by gentle tapping. For stopping the effect of trypsin, the fivefold volume of medium was added. Then the cells were seeded at a density of 12500 cells/cm^2. The doubling time was about 48 h and EA.hy 926 cells could be used for research up to passage 45.

2.1.3 Human microvascular dermal endothelial cells (HMECs)

The microvascular system is represented by human dermal microvascular endothelial cells (HMECs). Dermal microvascular endothelial cells are recovered from foreskins and transfected with a PBR-322-based plasmid containing the coding region for the simian virus 40 A gene product, large T antigen, for immortalization (Ades et al 1992). The HMECs were kindly provided by the group of Prof. Dr. Günther Eißner (LMU Großhadern, Munich). Table 3 shows the ingredients of the specific HMEC medium.

Table 3: Ingredients of the HMEC medium.

Ingredients	Company/Cat. No.
MCDB 131 medium	Gibco/10372
supplemented with:	
endothelial growth factor 10 ng/ml	PromoCell/C-60170
L-glutamin 2 mM	PAN/P04-80100
hydrocortisone 1 µg/ml	PromoCell/C-31062
heat-inactivated FCS 15%	PAA/A15-101
penicillin 100 IU/ml	Gibco/15140
streptomycin 100 µg/ml	Gibco/15140

For splitting, the cells were washed with sterile PBS and incubated with 25 µl/cm^2 trypsin (PromoCell, C-41210) for 1 min in the incubator at 37°C. To detach the cells from the plastic surface of the cell culture flasks, strong tapping and some scrapping with cell scrapers (TPP, 99002) were necessary. Finally, the fivefold volume of

medium was added to stop the activity of trypsin. 12500 cells/cm^2 were seeded. The cells were splitted twice a week, the doubling time was about 48 h and HMECs were subcultured up to passage 25. Table 4 summarizes the most important characteristics of the ECs which were used.

Table 4: The most important characteristics of the ECs.

Cells	Type	Origin
HUVECs	primary	macro-
EA.hy 926	immortalized (HUVECs + carcinoma cell line A549)	macro-
HMECs	immortalized (PBR-322-based plasmid containing the coding region for the simian virus 40 A gene product, large T antigen)	micro-vascular

2.1.4 K562

The non-adherent growing myelogenous leukemia cell line K562 (American Type Culture Collection/ATCC, CCL-243) was used as a target to measure NK cell-mediated lysis. The cells were cultured in supplemented RPMI 1640 medium as indicated in Table 5.

Table 5: Ingredients of the supplemented RPMI 1640 medium.

Ingredients	Company/Cat. No.
RPMI 1640 medium	Gibco/21875
supplemented with:	
L-glutamin 2 mM	PAN/P04-80100
sodium-pyruvate 1 mM	PAN/P04-43100
heat-inactivated FCS 10%	PAA/A15-101
penicillin 100 IU/ml	Gibco/15140
streptomycin 100 µg/ml	Gibco/15140

2.1.5 Stimulation of NK cells

NK cells had been collected from healthy human donors by leukapheresis and a negative selection using magnetic bead separation (CD3/CD19 depletion) and then stored in a liquid nitrogen container (kindly provided by Stefan Stangl and Dr. Mathias Gehrmann, Dpt. of Radiation Oncology, Klinikum rechts der Isar, TUM). After thawing, NK cells were cultured at a cell density of 5 x 10^6 cells/ml. One part of the NK cells was stimulated whereas the other part remained un-stimulated as a control. NK cells were stimulated with the Hsp70 peptide TKD (2 µg/ml, multimmune GmbH) and IL-2 (100 IU/ml) for 4 days in an incubator (37°C, 5% CO_2). TKD is the N-terminal-extended 14-mer peptide TKDNNLLGRFELSG (TKD, aa 450-463) of the Hsp70 protein and stimulates NK cell activity (Multhoff et al 2001). IL-2 stimulates human lymphoid cells to proliferate and to become cytotoxic effector cells (Damle et al 1987). The cells were cultured in supplemented RPMI 1640 medium. The ingredients are specified in Table 5. The purity of the NK cells after recovery was tested by flow cytometry with respect to CD56 as an NK cell marker. Figure 4 shows that nearly 50% of the peripheral blood lymphocytes, which were used in these experiments, were NK cells.

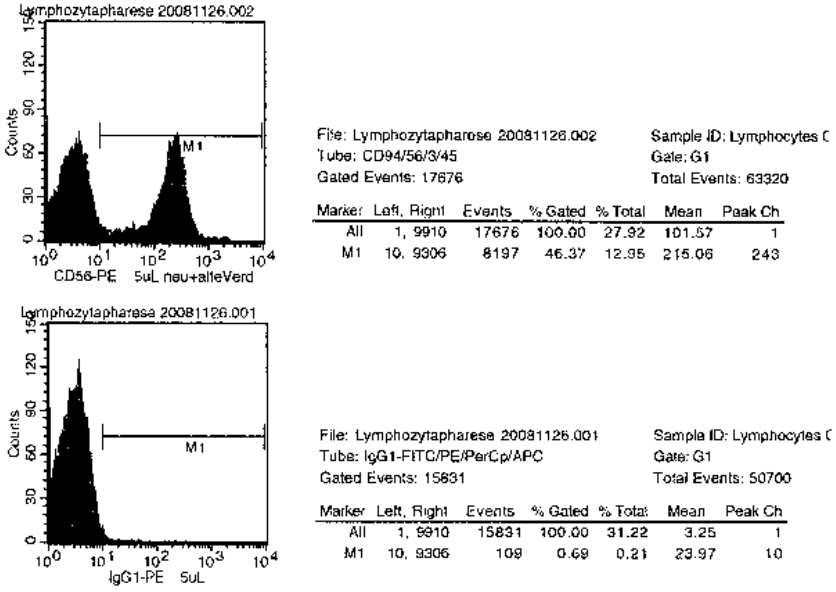

Figure 4: Flow cytometry analysis of the NK cells after recovery with respect to CD56 and its isotype control IgG1.

2.1.6 Freezing and thawing cells

For freezing, the cells were washed with ice-cold sterile PBS and centrifuged at 500 g and 4°C. The cells were resuspended in 0.9 ml/vial FCS. After adding the same volume of freezing medium (RPMI 1640 medium containing 20% DMSO, Sigma 2650) the cells were stored in a liquid nitrogen container.

For thawing, the frozen cells were transported in liquid nitrogen to the laminar flow bench and then rapidly thawed in a water bath (37°C). The resulting cell suspension was transferred into a 15 ml tube with pre-cooled medium, washed, and centrifuged twice at 350 g and 4°C for 5 min. Then the cells were transferred to cell culture flasks and put in an incubator.

2.1.7 Additional cell culture equipment

Table 6 summarizes the additional tools and equipment used for cell culture.

Table 6: Additional tools and equipment for cell culture.

Tools and equipment	Company/Cat. No.
cell culture flask T_{75}/T_{25}	Corning/430720/3056
centrifuge Fresco 17	Heraeus
centrifuge Multifuge 3S-R	Heraeus
centrifuge tubes PP 15 ml/50 ml	TPP/Sarstedt
incubator BBD 6220	Hereaus
laminar flow bench BSB 3A	Gelaire
pipettes	Eppendorf
sterile pipettes (10 ml, 25 ml, 50 ml)	Sarstedt

2.2 Immunofluorescence staining

2.2.1 Staining of ECs for CD31 and cmHsp70.1

The cells were seeded on two-well chamber slides (Lab-Tek Nunc, 177380) and kept overnight in a humidified atmosphere at 37°C and 5% CO_2. After washing with ice-cold PBS supplemented with 10% bovine serum albumine (BSA), the cells were incubated with anti-CD31 (PE, BD Pharmingen, 555446) and anti-cmHsp70.1 (FITC, multimmune GmbH, Munich) antibodies for 1 h at 37°C. Three washing steps of 5 min with PBS containing 1% BSA were performed before another staining with DAPI.

2.2.2 Factor VIII-related antigen-(von Willebrand factor) staining of ECs

The cells were seeded on two-well chamber slides (Lab-Tek Nunc, 177380) and kept overnight in a humidified atmosphere at 37°C and 5% CO_2. For fixation, the cells were washed with ice-cold PBS and then incubated with an acetone/methanol-mixture (1:1) for 2 min. After washing with PBS, the cells were incubated with anti-von Willebrand factor antibodies (Sigma, F3520) for 1 h at 4°C. After another washing step, cells were incubated with the second antibody IgG-FITC (BD Biosciences, 345815) for 1 h at 4°C. Then the cells were washed and stained with DAPI.

2.2.3 DAPI staining

For counterstaining DNA adherent cells were incubated with one drop of 4´,6-diamidino-2-phenylindole (Vector, Vectashield Mounting Medium for fluorescence with DAPI, H-1200) diluted 1:1 with PBS containing 1% BSA and then covered with a cover glass slide.

2.2.4 PKH staining

After harvesting, the cells were washed once with 10 ml RPMI 1640 medium and centrifuged at 400 g for 5 min at room temperature. The supernatant was discarded and the cells were resuspended with Diluent C (Sigma, CGLDIL) at a concentration of 10^6 cells/200 µl. PKH26 (Sigma, PKH26-GL) and PKH67 (Sigma, PKH67-GL) from PKH Linker Kit (Sigma – Aldrich) were used for staining. PKH staining dyes were diluted 1:250 with Diluent C to prepare the staining solutions. Then the cell

suspension was added, mixed, and incubated at room temperature for 5 min by turning over the tube every 30 sec. Finally the cells were washed with the equal volume of PBS containing 10% FCS and supplemented RPMI 1640 medium (Table 5), centrifuged at 400 g at room temperature for 10 min and then washed three times with 10 ml of supplemented RPMI 1640 medium (Table 5).

All fluorescence staining experiments were analyzed on a Zeiss fluorescence microscope Axioskop 2 plus with appropriate filters.

2.3 Flow experiments

A pump system (ibidi, Martinsried, Germany) was used to create unidirectional continuous flow. The system is shown in Figure 5 and consists of an air pressure pump with integrated valve control (A), a fluidic unit (B) with a perfusion set (H) (containing two reservoirs with medium), and a µ-slide (I). The unit is complemented by a set of valves which generate unidirectional flow. Air pressure tubings (C, D) connect the pump (A) with the fluidic unit (B) over a drying bottle filled with silica beads (E). The valve control is connected to the fluidic unit by an electric cable (F). The pump is linked with a notebook via a USB cable (G).

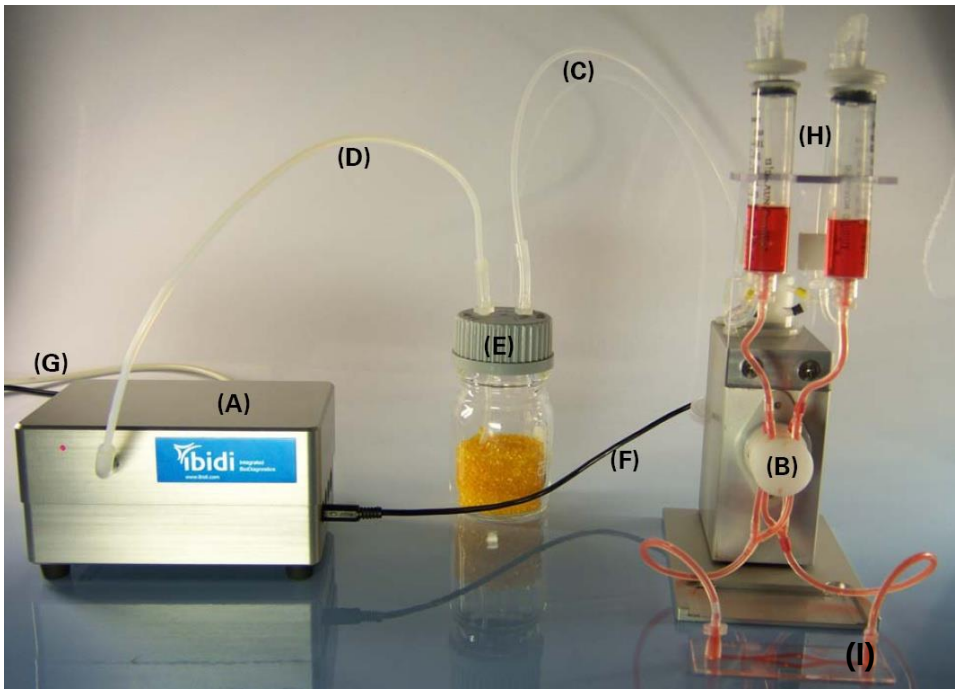

Figure 5 (origin: ibidi, Martinsried, Germany): The ibidi pump system with its elements. (A) air pressure pump, (B) fluidic unit, (C, D) air pressure tubings, (E) drying bottle filled with silica beads, (F) electric cable, (G) USB cable, (H) perfusion set, and (I) µ-slide.

The principle of flow generation is demonstrated in Figure 6, which shows a schema of the fluidic unit with the perfusion set. The pump system applies negative or positive pressure to the reservoirs to move the medium from one reservoir to the other one through the µ-slide. Regular valve switching effects that the flow direction through the µ-slide is continuously unidirectional. In Figure 6 the mechanism with negative pressure is demonstrated. At state “1” pressure is provided at the reservoir on the left. So medium is sucked from the right reservoir to the left one. After an

adjustable time (ca. 30-60 sec) the valves switch their position (state “2”) and the medium flows now from the left to the right reservoir. Through the slide, however, the flow doesn´t change its direction. With positive pressure the medium is not sucked but pressed from one reservoir to the other one.

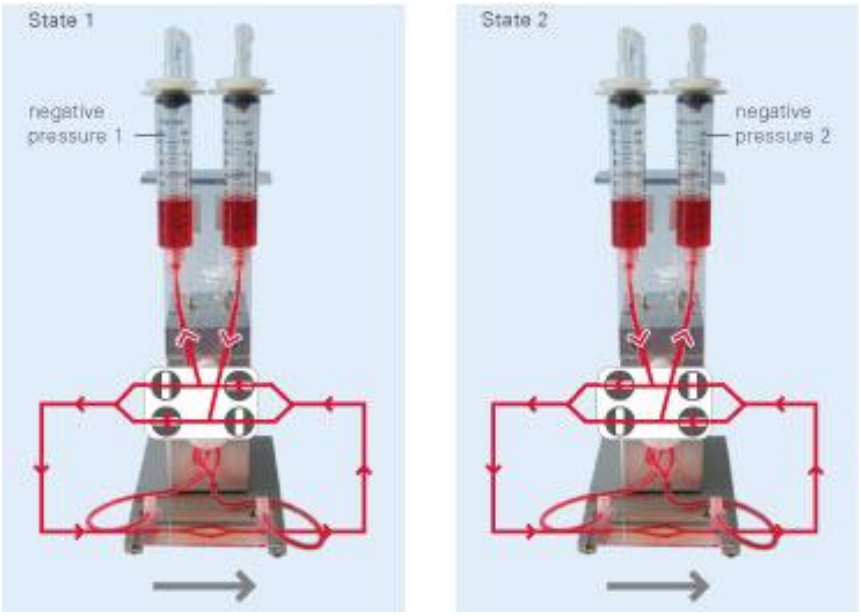

Figure 6 (origin: ibidi, Martinsried, Germany): The principle of flow generation. Provided pressure moves the medium from one reservoir to the other one through a µ-slide. By regular valve switching continuous unidirectional flow is assured.

The advantage of positive pressure is that less air bubbles are sucked into the tubes from the outside. The disadvantage is that the air for the pump has to be sucked from the inside of the incubator to attain air containing 5% CO_2. However, the air inside of the incubator has an atmosphere of nearly 100% humidity so it has to be dehydrated to avoid erosion of the ibidi pump system. The cells were seeded on a µ-slide, which is shown in Figure 7. The material of the µ-slides is a plastic of high optical quality and is in general coated with protein to promote cell adhesion.

Figure 7 (origin: ibidi, Martinsried, Germany): A µ-slide to observe the cells under flow.

Mostly the whole system stood in the incubator in a humidified atmosphere at 37°C and 5% CO_2. For microscopic analysis only the reservoir remained in the incubator, the tubes and the µ-slides containing the viable cells were located outside the incubator. Therefore, the connecting tubular system had to be isolated with thermoplastic foam plastic and a heated cover sheet. The µ-slides with the cells were placed under the microscope in a transparent, heated chamber at 37°C, 5% CO_2, and 80-100% humidity. The temperature of the chamber was adjusted by the lid and the plate heating system. For flow and static conditions different temperatures had to be chosen (lid and plate: 49°C for flow conditions or lid: 40°C and plate: 40.5°C for static conditions). For calibration, a temperature sensor was introduced into the interior of the tubes in close proximity to the cells. A temperature of nearly 37°C was reached over a constant time. All materials and the medium had to be pre-warmed to avoid the temperature-induced generation of air bubbles, which are visible under the microscope.

For starting a flow experiment, cells were seeded on pre-warmed µ-slides. Table 7 shows the characteristics of two different µ-slides, which were used. After incubation overnight the flow system was started by stepwise increasing the flow rate to adapt the cells to the shear stress. With the provided software (Figure 8, pump control v 1.4.0, ibidi, Martinsried, Germany) different parameters could be adjusted to control the pressure and the shear stress. Adjustable parameters (Table 8) were for example cycle duration, shear stress, flow rate, and the next continuous switching operation time (here 30 sec). According to the literature (Young et al 2010), HUVECs can be treated with shear stress up to 25 dyne/cm^2.

Table 7: Characteristics of µ-slides.

Type	Cell concentration	Growth area	Channel volume/height
µ-Slides $I^{0.4}$	1 x 10^6 cells/ml	2.5 cm^2	100 µl/400 µm
µ-Slide VI	2.5 x 10^5 cells/ml	0.6 cm^2	30 µl/400 µm

Table 8: Defined parameters for the flow system.

Cycle duration	Shear stress	Flow rate
5 h	1 dyne/cm^2	0.8 ml/min
5 h	2.5 dyne/cm^2	2 ml/min
Infinite	5 dyne/cm^2	4 ml/min

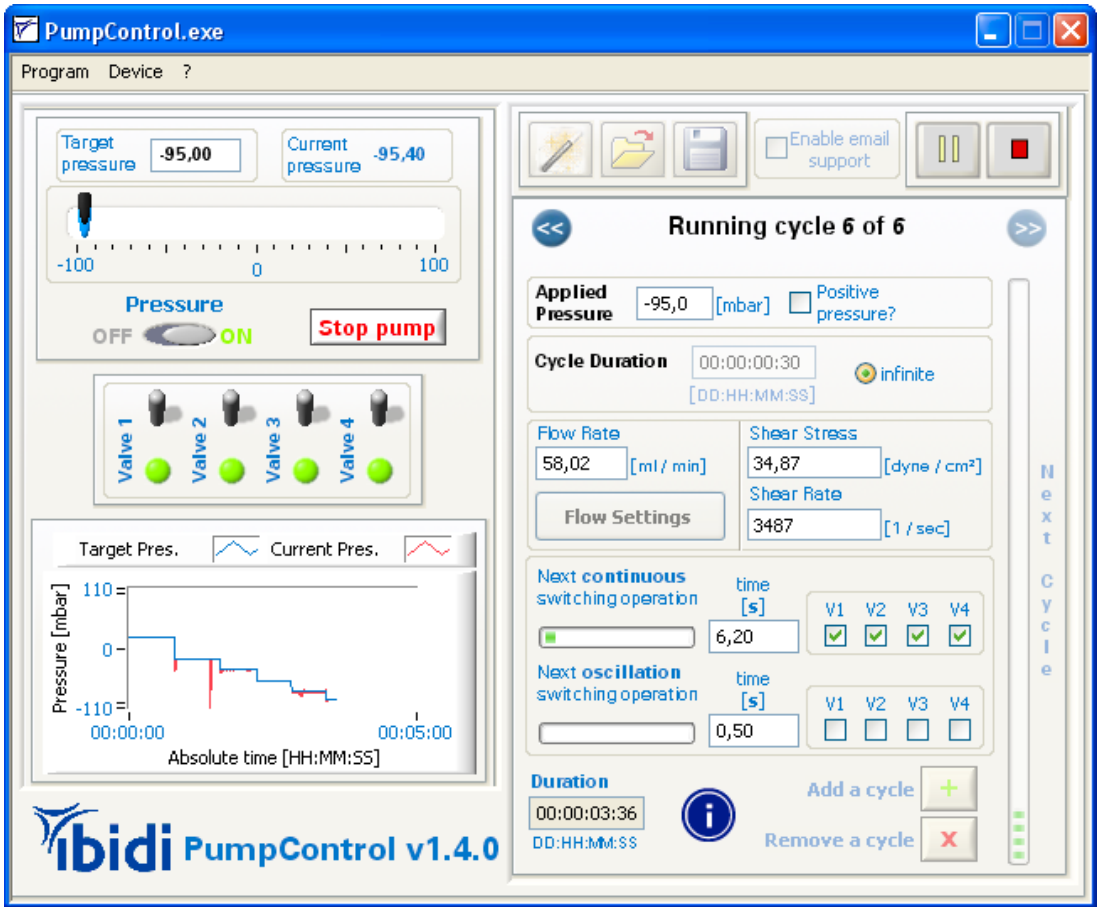

Figure 8 (origin ibidi, Martinsried, Germany): Input mask of the software “PumpControl v. 1.4.0” from ibidi for adjustment of specific parameters, such as cycle duration, shear stress, and flow rate.

After flow, cell suspensions were generated by trypsinization of the µ-slides for flow cytometry analysis. The medium was removed and the channels were washed with 2 x 500 µl PBS. The entire PBS was aspirated and 100 µl trypsin (PromoCell, C-41210) was added and incubated for 3 min at 37°C. After tapping the slides the channel was flushed five times with 200 µl medium and the cell suspension was recovered from the opposite end of the channel.

The entire equipment of ibidi (Martinsried, Germany) which was used is listed in Table 9.

Table 9: Equipment of ibidi (Martinsried, Germany).

Equipment of ibidi	Cat. No.
µ-Slides $I^{0.4}$, ibiTreat	80176
µ-Slide VI, ibiTreat	80626
air pressure pump	10905
fluidic unit	10903
perfusion set (50 cm, ID (inner diameter) 0.8 mm, white)	10963
valve connection cable	10981
notebook Lenovo	10908
heating system	10918
heating insert	10930
temperature controllers	HT 200
gas incubation system with humidifying column	10922

2.4 Photography

Morphology studies were performed with an Axiovert 40 c microscope from Zeiss, images were taken with a camera from Imaging source (DFK 41AU02), and a software from ibidi (CamControl v0.1, Martinsried, Germany). The images were converted into films with the software TMPGEnc 4.0 Xpress.

2.5 Flow cytometry

Table 10 summarizes all conjugated and un-conjugated antibodies which were used for flow cytometry. Briefly, 1 x 10^5 cells were washed with PBS supplemented with 10% heat-inactivated FCS, incubated with un-conjugated or conjugated monoclonal antibodies for 30 min at 4°C, and washed again. A secondary antibody incubation step (30 min at 4°C) was necessary for those cells which were treated with un-conjugated primary antibodies. After adding 1 µl/100 µl propidium iodide (Calbiochem, 537059) to determine viability of cells, cells were analyzed on a FACSCalibur™ flow cytometer (Becton Dickinson). Isotype-matched control antibodies were used for each antibody.

Table 10: Antibodies for flow cytometry.

Antibody	Isotype	Company/Cat. No.
primary antibody:		
CD3-FITC/16/56-PE	mouse IgG1	BD Bioscience Becton Dickinson/342403
CD54-FITC	mouse IgG1	Beckman Coulter/PN IM0726U Clone84H10
CD77-FITC	mouse IgM_{κ}	BD Pharmingen/551353
CD94-FITC	mouse $IgG1_{\kappa}$	BD Pharmingen/555888
mouse IgG		Jackson ImmunoResearch/015-000-003
Hsp70(cmHsp70.1)FITC	mouse IgG1	multimmune GmbH
Hsp70(SPA810)-FITC	mouse IgG1	assay designs/SPA-810Fl
HLA-E	mouse IgG1	ExbioPraha/11-393-C100 CloneMEM-E/06
MICA-APC	mouse IgG_{2B}	R&D Systems/FAB 1300A Clone 159227
MICB-APC	mouse IgG_{2B}	R&D Systems/FAB 1599A Clone 236511
ULBP-1	mouse IgG_{2A}	R&D Systems/MAB 1380 Clone 170818
ULBP-2-APC	mouse IgG_{2A}	R&D Systems/FAB 1298A Clone 165903
ULBP-3	mouse IgG_{2A}	R&D Systems/MAB 1517 Clone 166510
secondary antibody:		
Goat- anti-mouse-FITC		DAKO/F 0479
isotype control:		
mouse IgG1-APC		CALTAG Laboratories/MG105
mouse IgG1-FITC		BD Biosciences/345815
mouse IgG1-PE		BD Biosciences/345816
mouse IgG_{2A}-APC		R&D Systems/IC003A
mouse IgG_{2A}-PE		Becton Dickinson/349053
mouse IgG_{2A}-Pure		Becton Dickinson/349050
mouse IgG_{2B}-APC		R&D Systems/IC0041A
mouse IgMκ-FITC		BD Pharmingen/555583

2.6 Irradiation

The energy dose of irradiation has the unit Gray [Gy] and can be calculated applying following formula:
D = E/M [Gray = Joule/Kilogram], with D = dose, E = energy and M = mass.
According to the literature (Ahmad et al 2007), HUVECs were irradiated with X-rays up to 8 Gy, whereby the dose of 8 Gy was highly lethal for HUVECs and a dose ≥ 4 Gy significantly reduced the number of capillary-like structures formation of HUVECs. EA.hy 926 cells were irradiated with a low dose irradiation in the range of 0.3 to 3 Gy (Rödel et al 2010). Regarding these results, in this work all cells were irradiated with an irradiation dose of 4 Gy. The HMECs were additionally treated with a dose of 0.2 Gy and 2 Gy.
For an experiment, ECs were seeded in cell culture flasks, incubated overnight and then irradiated with the irradiation unit (Gulmay Isodose Control, Solingen, Germany) generating X-rays at 70 kV, 10 mA, and a dose of 1 Gy/min. After a recovery of 12 h, supernatants were centrifuged to remove the detached cells. The fraction of surviving cells was used for flow cytometry measurements and further experiments.

2.7 Cytotoxicity assays

2.7.1 Granzyme B ELISPOT assay

Two different cytotoxicity assays were performed to measure the NK cell-mediated lysis. One method was the Granzyme B Elispot assay. Granzyme B is secreted by NK cells during their cytolytic attack on target cells and can be captured and detected by antibodies. The principle of this assay is shown in Figure 9. Specific antibodies are bound to the surface of a well. Effector and target cells are added and co-incubated for 4 h at 37°C. Thereby cytokines are secreted and captured by the antibodies. With a second antibody which is coupled to an enzyme the captured cytokine is visualized by color and the so developed spots can be counted.

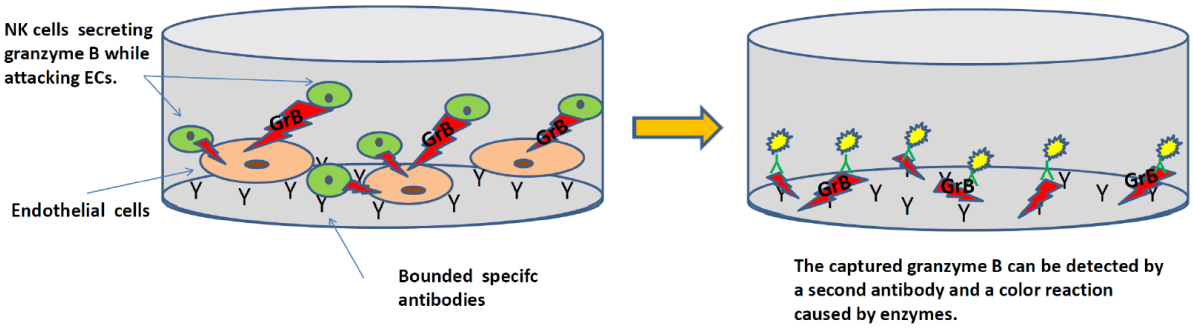

Figure 9: Scheme of the ELISPOT assay.

To quantify granzyme B secretion, the Granzyme B Elispot Set (BD Bioscience, 552572) was used. Multiscreen TM-IP plates (MAIPN4510, Millipore GmbH, Schwalbach, Germany) were coated overnight at 4°C with 100 µl/well capture antibody (Purified anti-human Granzyme B, 5 µg/ml, BD Biosciences). Then the plates were blocked for 1 h at room temperature with supplemented RPMI 1640 medium (Table 5). 3 x 10^3 target cells per well were added to duplicates of NK cells in different ratios (from 10:1 to 0.15625:1 effector to target (E:T) ratios) at a final volume of 200 µl of RPMI 1640 medium supplemented with 10% FCS and incubated for 4 h in a humidified atmosphere at 37°C and 5% CO_2. Negative controls were performed by effector cell duplicates in absence of target cell. The plates were washed twice with deionized water and three times with PBS containing 0.05% Tween-20 (TPBS). Detection antibody (100 µl/well, biotinylated anti-human

granzyme B antibody, 2 µg/ml, BD Biosciences) was added and incubated for 2 h at room temperature. After washing three times with TPBS, Avidin-HRP (1:100, BD Biosciences) was added and incubated for 1 h at room temperature. Further washing steps were performed with TPBS (four times) and PBS (twice). Granzyme B was visualized by the addition of 100 µl/well freshly made substrate solution. To make the substrate solution, 333 µl of AEC stock solution (100 mg 3-amino-9-ethyl-carbazole, Sigma A-5754, in 10 ml N,N-dimethylformamide, Sigma D-4551) and 5 µl H_2O_2 (30%) were added to 10 ml of 0.1 M acetate puffer (pH 5.0). Plates were incubated for 25 min in the dark at room temperature. Substrate reaction was stopped by washing three times with deionized water. After drying overnight, the red spots were counted automatically using the Bioreader 3000 (BioSys GmbH).

2.7.2 ^{51}Cr release assay

In addition to the Granzyme B ELISPOT assay, cytolytic activity of NK cells was determined in a standard ^{51}Chromium-release assay (Brunner et al 1968). Here the target cells are labeled with radioactive ^{51}Chromium. When these cells are attacked, the radioactive Chromium is released into the medium and can be detected by a γ-Counter. A scheme of this assay is shown in Figure 10.

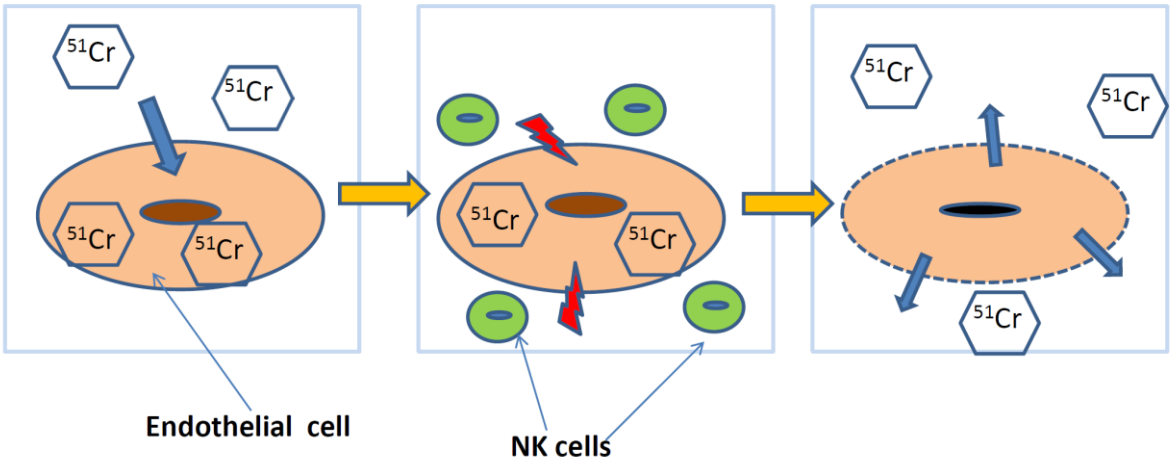

Figure 10: Scheme of the ^{51}Cr release assay.

3 x 10^5 target cells were labeled with 100 µCi of $Na_2{}^{51}CrO_4$ (CrRA415, Hartmann Analytic GmbH, Braunschweig, Germany) in 12 ml tubes (Greiner Bio-One, 164160) at 37°C and 5% CO_2 for 1.5 h. Effector cells were seeded in duplicates at different

E:T ratios from 10:1 to 0.3125:1 on 96 well U-bottom plates. After two washing steps, target cells were resuspended with RPMI 1640 medium containing 10% heat-inactivated FCS and distributed in duplicates to NK cells in an amount of 3 x 10^3 cells/well at a final volume of 200 µl medium. Duplicates of radioactive labeled target cells were disposed without NK cells in a concentration of 3 x 10^3/well in 200 µl medium to determine spontaneous release. Maximal release was quantified by adding 0.5% Triton X to the target cells. After incubation for 4 h at 37°C and 5% CO_2, cell-free supernatants (50 µl/well) were transferred into a LumaPlate™-96 (Packard, 6006633) and dried overnight. Radioactivity was measured with a γ-Counter (Top Count NXT ™ Packard Instruments) in counts per minute (cpm). The specific lysis (%) was calculated applying following equation:

Specific lysis (%) = ([experimental release – spontaneous release]/[maximum release - spontaneous release]) x 100

Definitions:
Experimental release = cpm released from target cells after an incubation with effector cells (NK cells) within 4 h.
Spontaneous release = cpm released from target cells in the absence of NK cells within 4 h.
Maximum release = cpm released by target cells after treatment with detergents.

2.8 Other materials

All other materials were purchased from Sigma, Merck, and Carl Roth GmbH.

3 Results

3.1 Characterization of ECs

3.1.1 Morphology

3.1.1.1 Immunofluorescence staining

Characteristic markers of ECs are factor VIII-related antigen (von Willebrand factor) and CD31. The factor VIII-related antigen stabilizes the coagulation factor VIII. Furthermore, platelets can adhere to injured vessel walls by using factor VIII-related antigen. It is localized in vesicles of the cytosol and is therefore visible in immunofluorescence staining as small vesicular spots. The immunoglobulin CD31, also known as platelet endothelial cell adhesion molecule PECAM-1, is an adhesion molecule, which mediates both, leukocyte-endothelial and endothelial-endothelial interactions. CD31 is localized in the cell membrane. Figure 11 shows the immunofluorescence staining for factor VIII-related antigen (green, Figure 11 a, b, and c) and for CD31 (red, Figure 11 d, e, and f). All examined human ECs, namely the HUVECs, EA.hy 926 cells, and HMECs, were positively stained for these markers. In addition, the nuclei were colored with DAPI (blue).

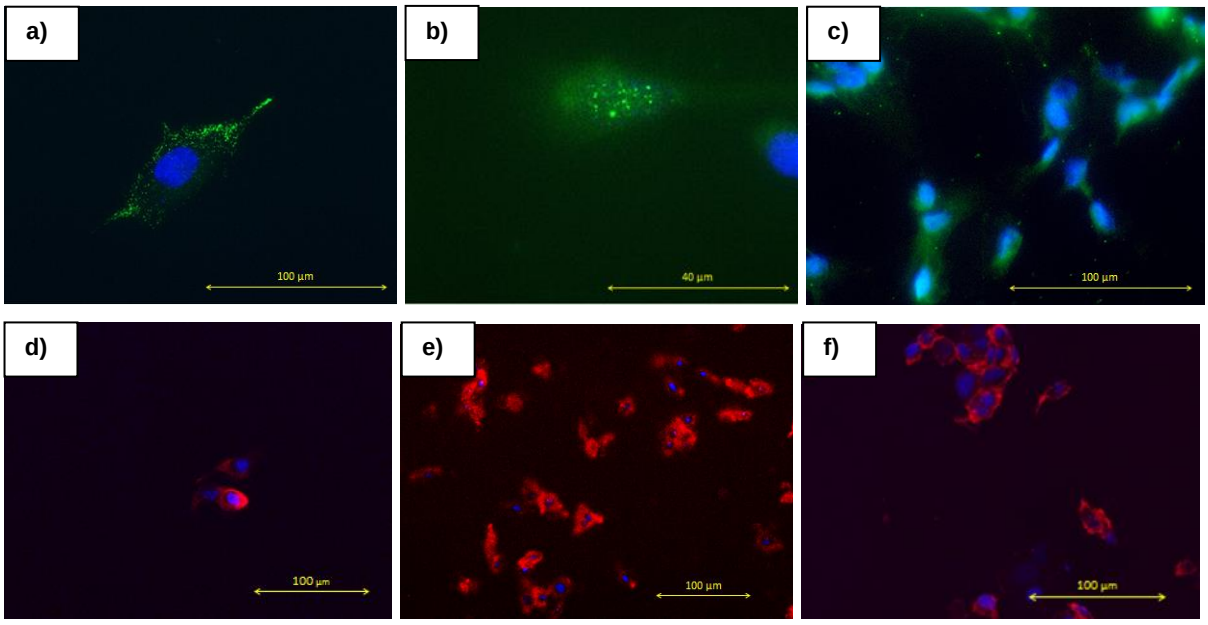

Figure 11: Immunofluorescence images of HUVECs (a, d), EA.hy 926 cells (b, e), and HMECs (c, f) stained for factor VIII-related antigen (green, a-c) and CD31 (red, d-f). The nuclei were stained with DAPI (blue). All cells are positive for these markers.

3.1.1.2 Morphology of adherence

ECs are characterized by their typical cobblestone morphology in cell culture. The cells imaged by light microscopy directly after seeding on slides and the process of adherence was recorded using a Zeiss camera system. Few hours after seeding, the cells changed their shape from round to rhombic and these morphological changes were associated with the adherence of the ECs to the surface of the slides. Figure 12 depicts differences in cell morphology directly after seeding (Figure 12 a, c, and e) and after a culture period of 5 h at 37°C (Figure 12 b, d, and f). Compared to HUVECs and HMECs, it takes longer for EA.hy 926 cells to become adherent.

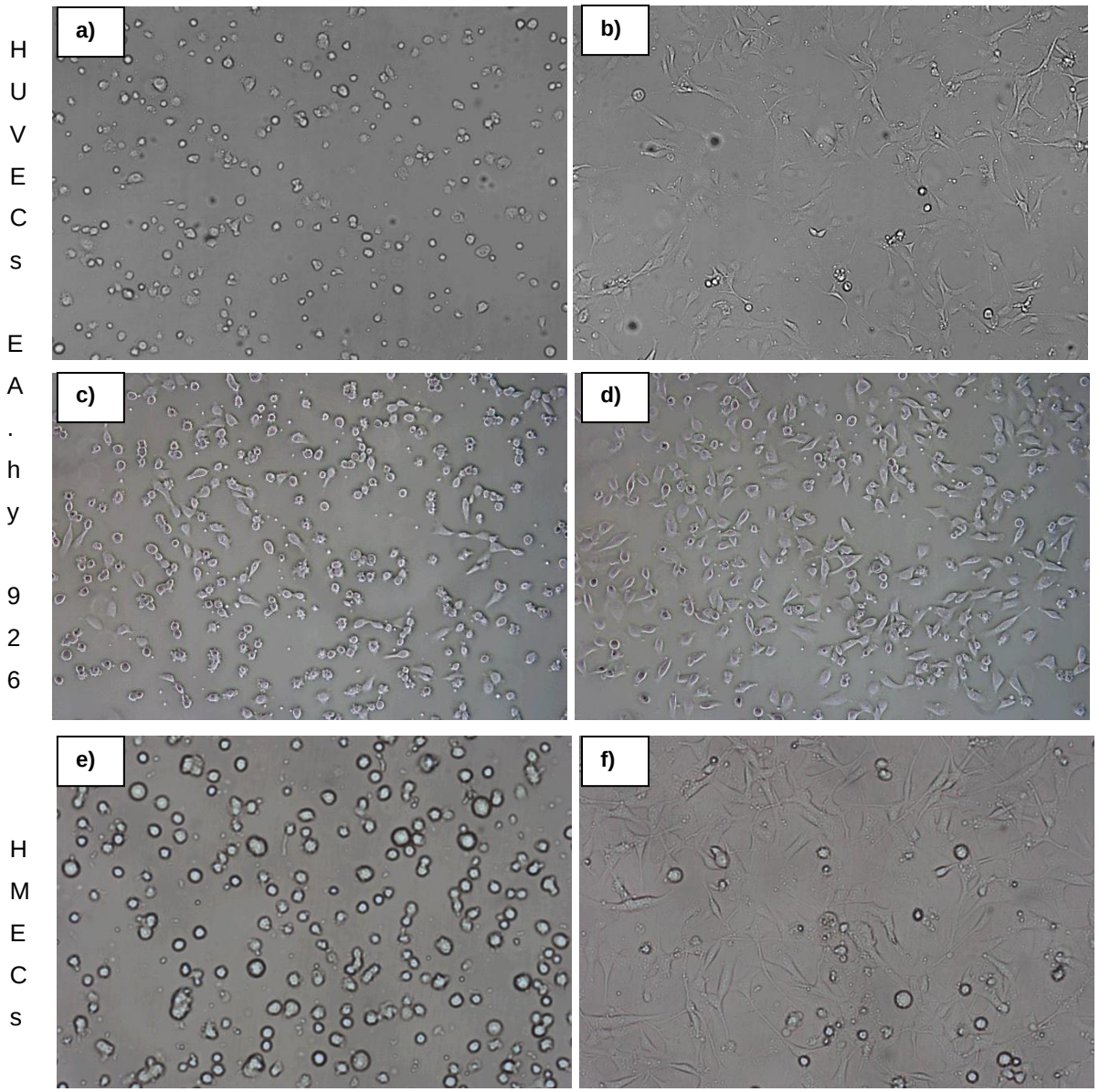

Figure 12: HUVECs (10 x; a, b), EA.hy 926 cells (10 x; c, d), and HMECs (20 x; e, f) immediately after seeding (a, c, e) and after a culture period of 5 h at 37°C (b, d, f).

3.1.1.3 Morphology under flow

In vivo ECs are exposed to the blood flow. To simulate physiological flow conditions, a commercial pump system (ibidi, Martinsried, Germany) was used and images were taken of ECs under flow and under static culture conditions (control cells). Figure 13 represents differences in the morphology of ECs under static (Figure 13 a, c, and e) and flow (Figure 13 b, d, and f) conditions. The cells were seeded 24 h before starting the flow. In Figure 13 b, d, and f the flow direction is marked with an arrow and the flow duration is listed.

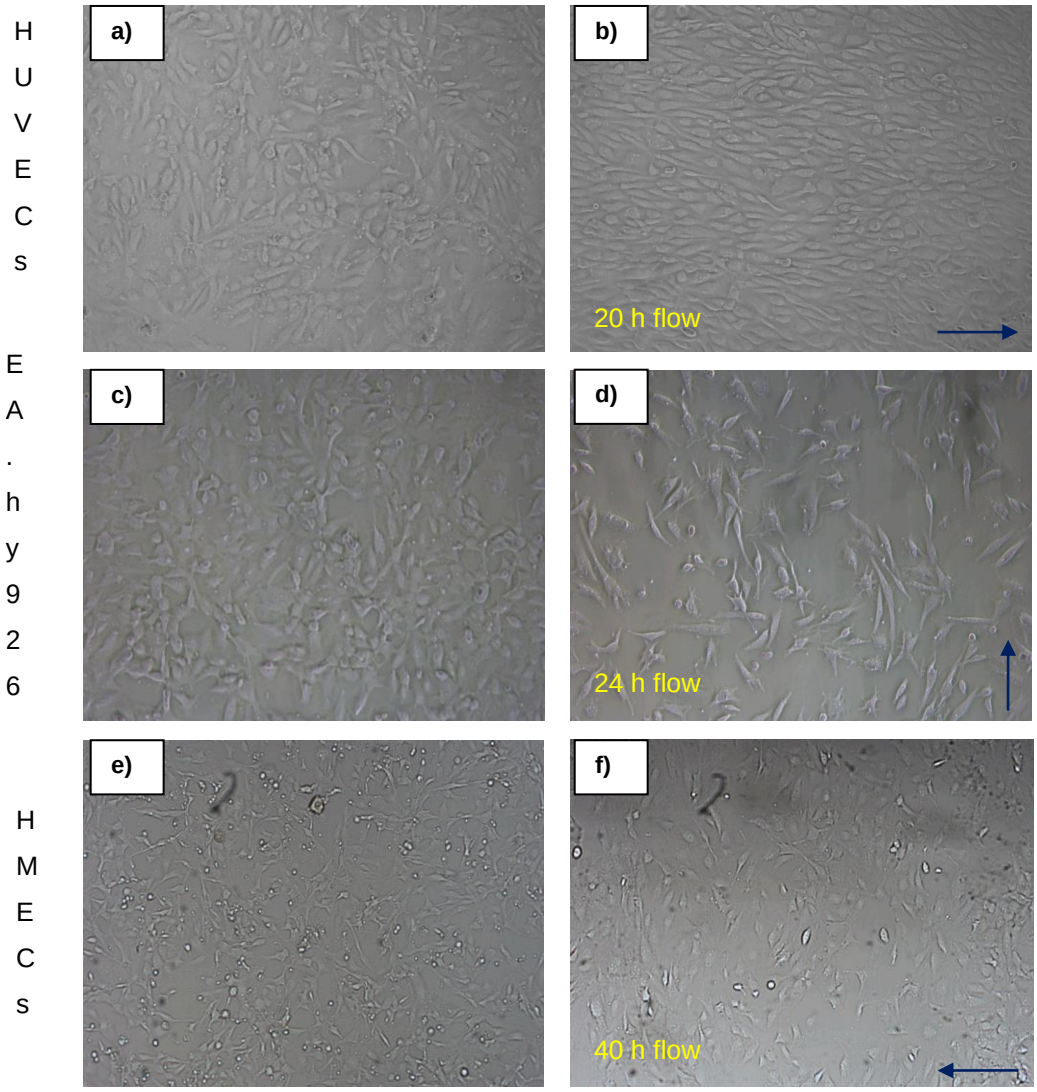

Figure 13: HUVECs (10 x; a, b), EA.hy 926 cells (10 x; c, d), and HMECs(10 x; e, f) under static (a, c, e) or flow (b, d, f) conditions. The flow direction is marked with an arrow. The cells were seeded 24 h before starting the flow.

The primary ECs, namely the HUVECs, oriented towards the flow direction within few hours and showed an aligned growth pattern. The other ECs, however, didn´t show any alignment under flow. Nevertheless, with respect to viability HMECs seemed to survive better under flow conditions than under static culture conditions. The majority of EA.hy 926 cells, however, died after 2 days under flow conditions. Interestingly, the HUVECs were very sensitive to shear stress. They lost their aligned growth orientation already a few hours after stopping the flow. Figure 14 shows the different morphologies of HUVECs before starting the flow (Figure 14 a), after 24 h under flow (Figure 14 b), and few hours after stopping the flow (Figure 14 c).

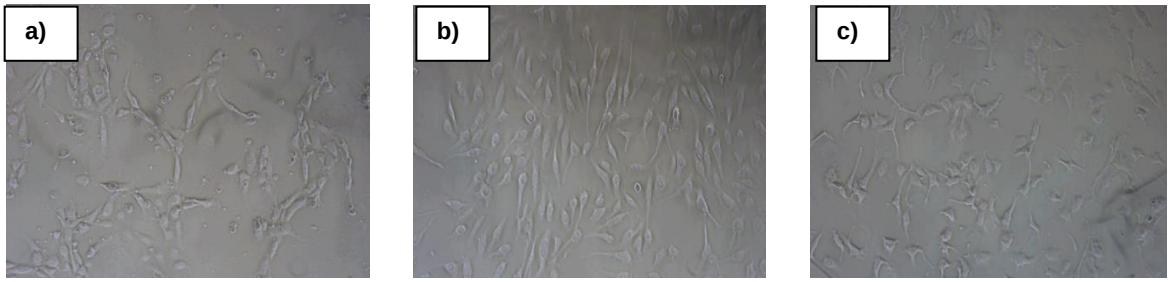

Figure 14: The morphology of HUVECs (10 x) before starting the flow (a), after 24 h under flow (b), and few hours after stopping the flow (c).

Under flow, HUVECs showed migratory capacity even against the flow direction and a continuous proliferation (Figure 15). The shape of the cells changed from rhombic (Figure 15 a) to round (Figure 15 b), one cell divided (Figure 15 c-e), and then became adherent (Figure 15 f). The time scale marks the duration of the flow.

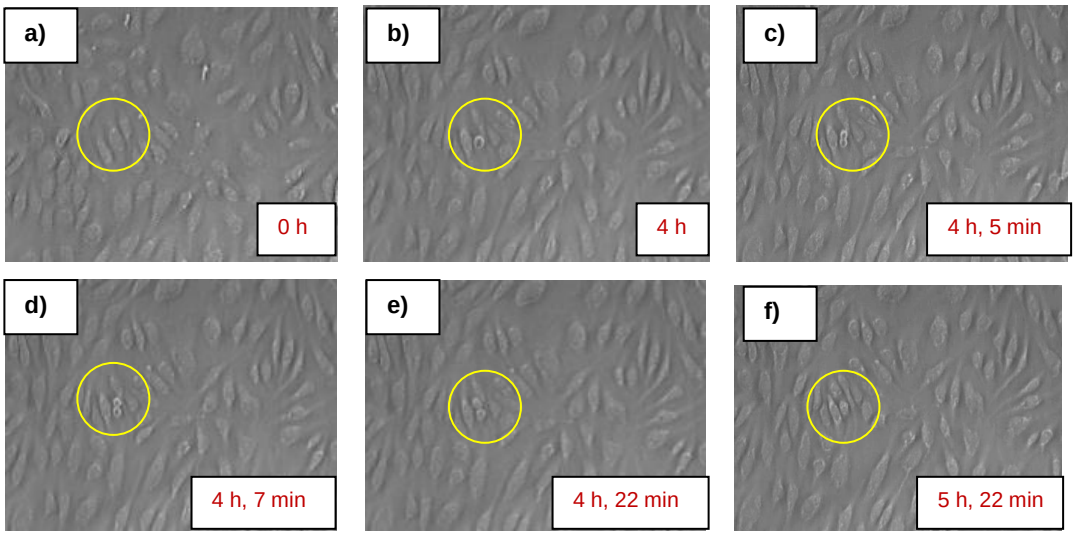

Figure 15 a-f: Details of the proliferative capacity of HUVECs under flow conditions (10 x). The time scale marks the duration of flow.

3.1.2 Phenotype

3.1.2.1 Phenotype at rest

The expression of different cell surface markers (ULBP1-3, MICA/B, Hsp70, CD77, CD54, and HLAE) on the ECs, which are known to play a role for the interaction with NK cells, were analyzed by flow cytometry. In Table 11 the expression of these cell surface markers on HUVECs, EA.hy 926 cells, and HMECs under static conditions and without any treatment is summarized. There are some similarities but also striking differences in the expression of the different cell surface markers. None of the ECs did express ULBP1. In contrast to the immortalized ECs, the primary macrovascular HUVECs only present ULBP2 and MICA on its cell surface. In comparison to the HUVECs, the immortalized EA.hy 926 cell line expressed additional markers, such as ULBP3 and HLAE, on their cell membrane. The microvascular cell line HMEC resembled the phenotype of EA.hy 926 cells with the exception that the MICA expression was substituted by MICB in HMECs. In contrast to the other ECs, HMECs express CD54. Furthermore, the expression of Hsp70, as determined by cmHsp70.1 but not by SPA810 Hsp70-specific antibodies, was detectable only on the immortalized ECs. Interestingly, the HMECs were positive for CD77, which might indicate that similar to tumor cells, Hsp70 is anchored via the lipid component globoyltriaosylceramide in the plasma membrane.

Table 11: The expression of different cell surface markers on HUVECs, EA.hy 926 cells, and HMECs is listed in percentage of positive cells (%), +/- standard error of mean (SEM), and mean fluorescence intensity (mfi).

	HUVECs	**EA.hy 926**	**HMECs**	**Expression pattern**
Marker	% +/- SEM (mean fluorescence intensity)			HUVECs/EA.hy926/HMECs ++ >70%, + >20%, - <20%
ULBP1	0 +/- 1 (66)	0 +/- 0 (46)	4 +/- 1 (43)	-/-/-
ULBP2	48 +/- 7 (59)	96 +/- 2 (63)	98 +/- 1 (131)	+/++/++
ULBP3	6 +/- 3 (52)	58 +/- 11 (52)	51 +/- 11 (62)	-/+/+
MICA	73 +/- 6 (107)	21 +/- 4 (46)	8 +/- 3 (116)	++/+/-
MICB	3 +/- 1 (47)	2 +/- 1 (25)	36 +/- 10 (37)	-/-/+
cmHsp70.1	16 +/- 4 (112)	58 +/- 5 (69)	48 +/- 6 (54)	-/+/+
SPA810	1 +/- 1 (91)	2 +/- 0 (51)	2 +/- 0 (44)	-/-/-
CD77	0 +/- 0 (77)	0 +/- 0 (57)	50 +/- 4 (106)	-/-/+
CD54	5 +/- 2 (88)	13 +/- 2 (46)	21 +/- 3 (49)	-/-/+
HLAE	1 +/- 0 (110)	86 +/- 3 (162)	83 +/- 4 (201)	-/++/++

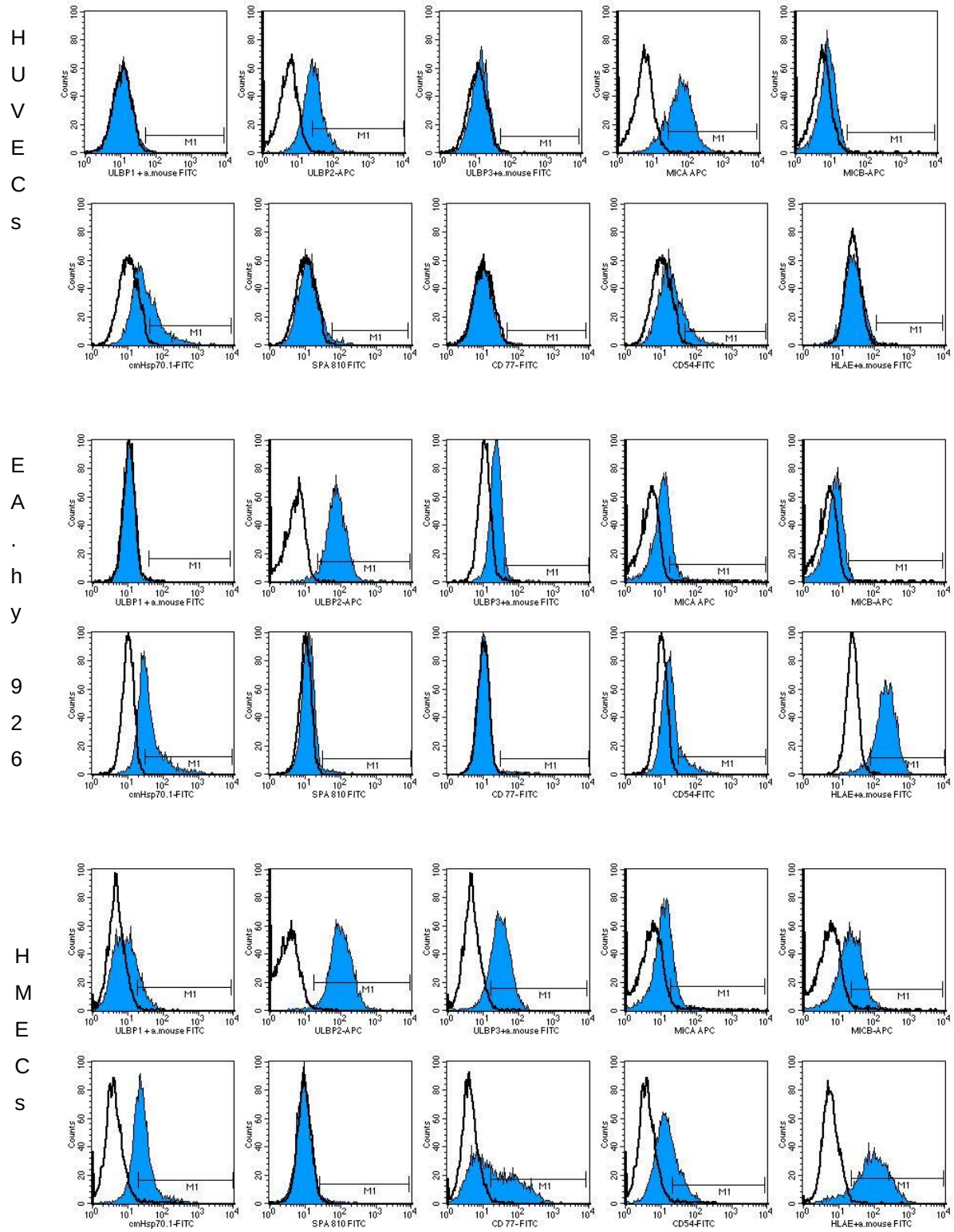

Figure 16: The overlays of the phenotype of HUVECs, EA.hy 926 cells, and HMECs are illustrated. The examined markers are: ULBP1-3, MICA/B, Hsp70/cmHsp70.1 mAb, Hsp70/SPA810, CD77, CD54, and HLAE. The blue graphs represent the staining with the specific antibodies and the white graphs the staining with the isotype-matched control antibodies.

The overlays of the examined cell surface markers (ULBP1-3, MICA/B, Hsp70/cmHsp70.1 mAb, Hsp70/SPA810, CD77, CD54, and HLAE) are shown in Figure 16. The blue graphs represent the staining with the specific antibodies and the white graphs represent the staining with the isotype-matched control antibody. Additionally to the flow cytometry analysis, fluorescence images of the HMECs were taken after staining with anti-Hsp70 (green) and anti-CD31 (red) immunofluorescence antibodies (Figure 17). Furthermore, the nuclei were counter-stained with DAPI (blue).

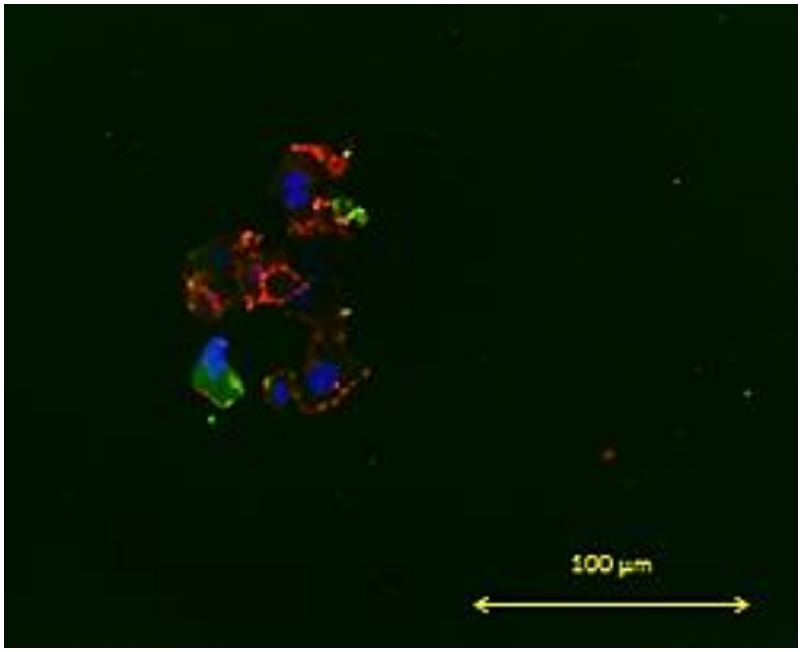

Figure 17: HMECs were stained with immunofluorescence dyes with anti-Hsp70 antibodies (green) and anti-CD31 antibodies (red), and the nuclei were stained with DAPI (blue).

3.1.2.2 Phenotype after flow conditions

Regarding the observations, that ECs seem to prefer flow conditions to static growth conditions, HUVECs have been comparatively analyzed by flow cytometry after growing under static or flow conditions with respect to the expression of MICA, CD54, and HLAE. The control group (without flow) was seeded under identical conditions. The flow lasted for 22 h. Figure 18 shows the results of the flow cytometry analysis. The bars on the left panel represent the percentage of positively stained cells and the bars on the right panel the mean fluorescence intensity (mfi). Changes in the expression pattern were visible only in the mfi but not in the percentage of positively stained cells. The cells under flow (blue) express slightly more CD54 and HLAE than the cells under static conditions (yellow).

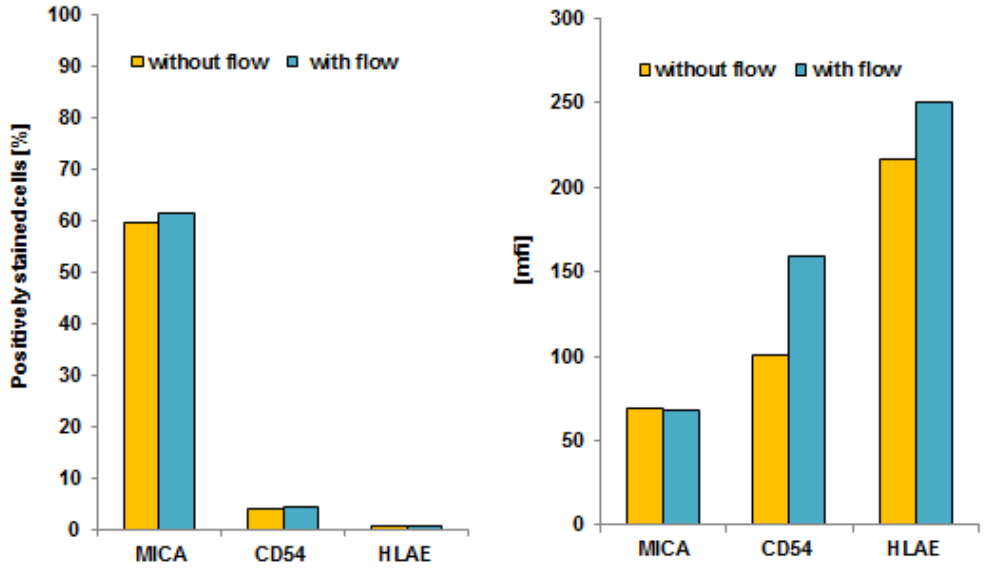

Figure 18: HUVECs were analyzed by flow cytometry after growing under static (yellow) or flow conditions (blue) regarding the expression of MICA, CD54, and HLAE. The bars on the left panel present the percentage of positively stained cells and the bars on the right panel the mean fluorescence intensity (mfi).

3.1.2.3 Phenotype after irradiation

In order to evaluate whether ionizing irradiation has an effect on the expression of the examined cell surface markers, the ECs were irradiated and then examined by flow cytometry. The results of the flow cytometry analysis are summarized in Figures 19/20. The bars on the left (Figure 19)/upper (Figure 20) panel represent the percentage of positively stained cells and the bars on the right (Figure 19)/lower (Figure 20) panel the mfi. All cells were irradiated with a dose of 4 Gy (Figure 19, a-c, blue) and the HMECs additionally with 0.2 Gy (red) and 2 Gy (green) (Figure 20). Yellow bars represent the results of non-irradiated cells. All cells were stained and analyzed 12 h after irradiation. Significant changes were found in the expression pattern of HLAE. HLAE was up-regulated after irradiation with 4 Gy on HUVECs and EA.hy 926 cells, whereas HLAE was slightly down-regulated on HMECs, in a dose dependent manner. Slight changes could be seen in the expression of following markers: ULBP2 was up-regulated on HUVECs and EA.hy 926 cells after irradiation with 4 Gy and on HMECs concomitant with the increase of the radiation dose. ULBP3 was down-regulated on EA.hy 926 cells and HMECs, whereas ULBP3 was slightly up-regulated on HUVECs. MICA was up-regulated on HUVECs and down-regulated on HMECs. Hsp70 was up-regulated on HUVECs and EA.hy 926 cells.

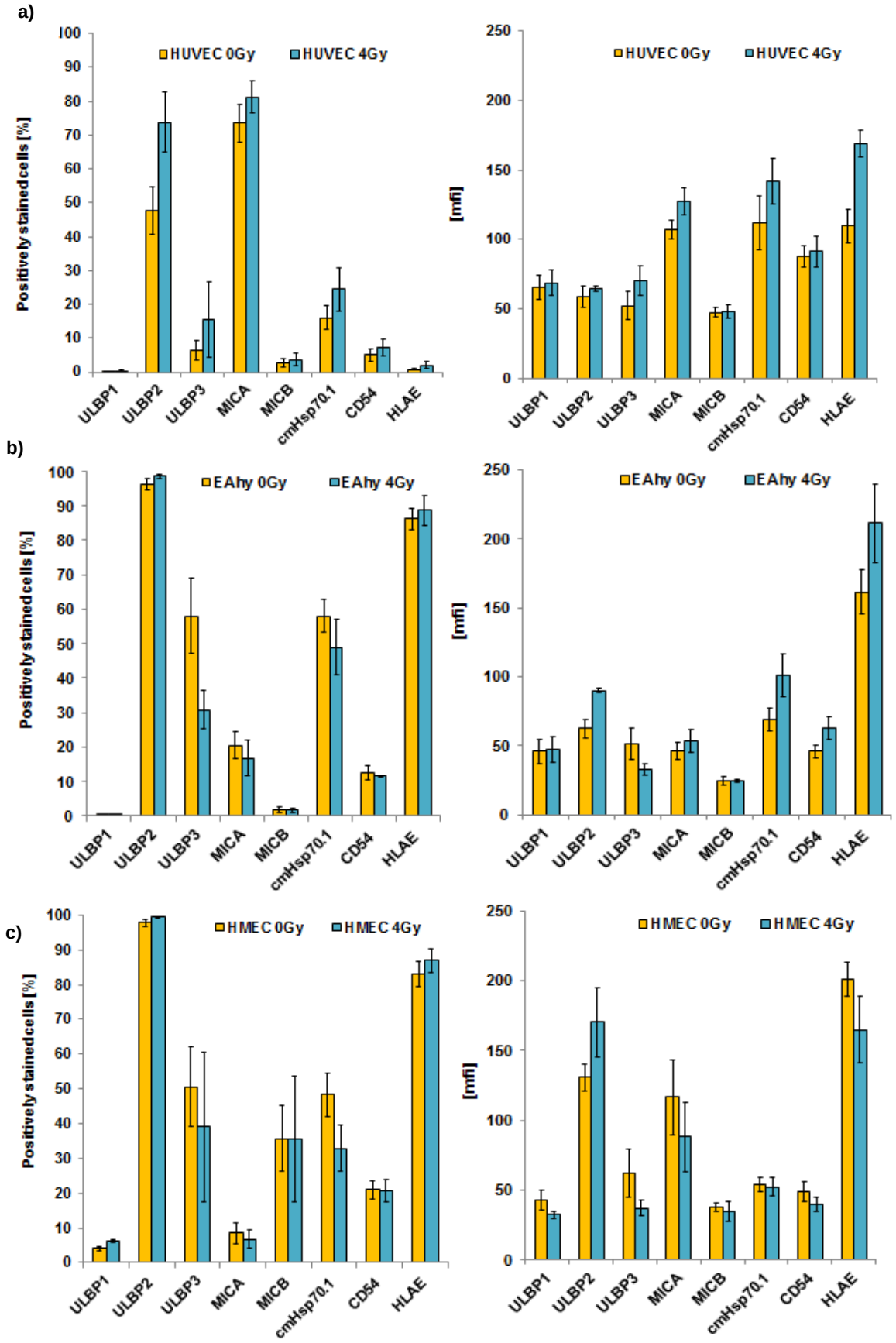

Figure 19: The phenotype of HUVECs (a), EA.hy 926 cells (b), and HMECs (c) after (blue) or without (yellow) irradiation with 4 Gy was analyzed by flow cytometry. The bars on the left panel represent the percentage of positively stained cells and the bars on the right panel the mean fluorescence intensity (mfi). The results are shown as the mean +/- SEM of several independent experiments.

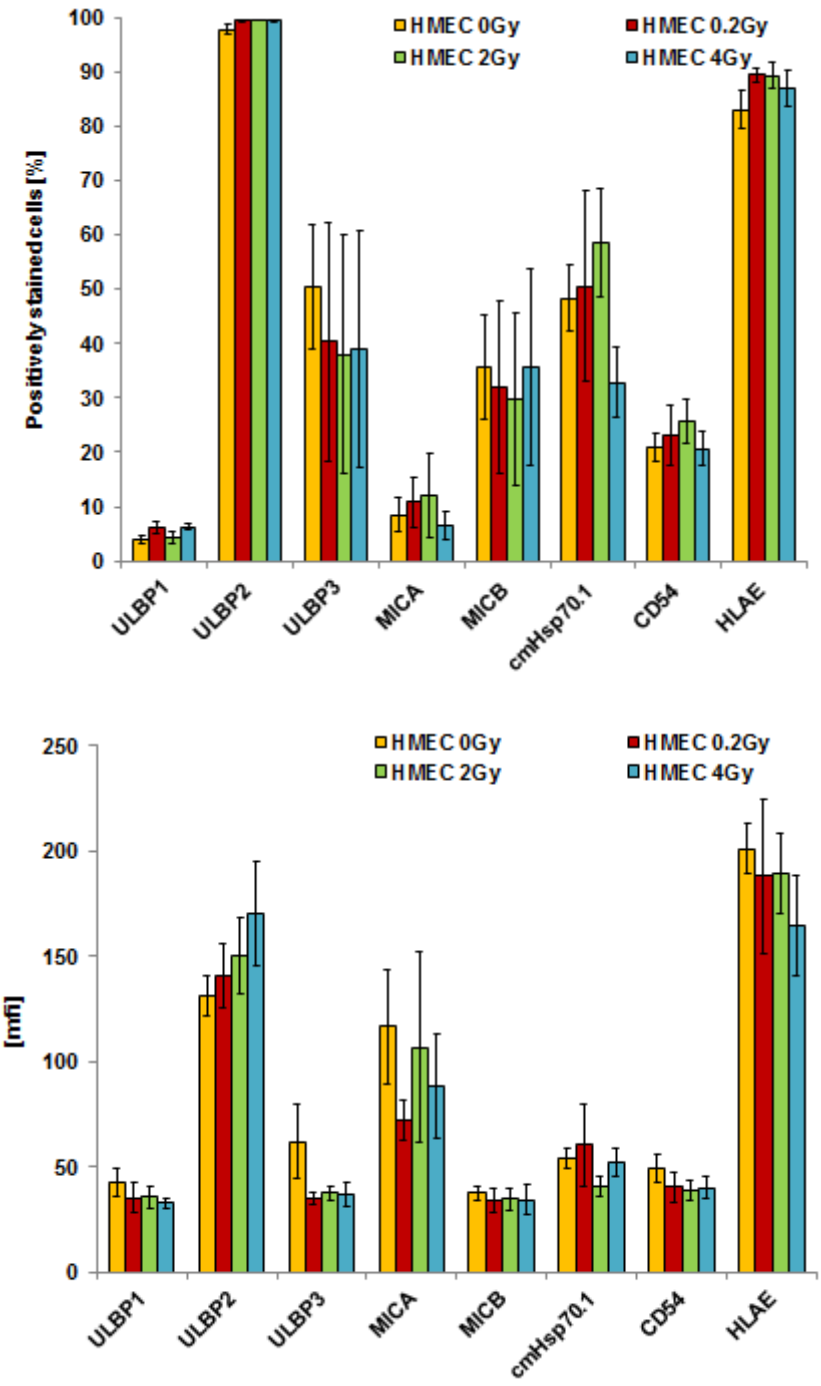

Figure 20: The phenotype of the HMECs was analyzed by flow cytometry after irradiation with 0.2 (red), 2 (green), and 4 (blue) Gy or without irradiation (yellow). The bars in the upper panel represent the percentage of positively stained cells and the bars in the lower panel the mean fluorescence intensity (mfi). The results are shown as the mean +/- SEM of several independent experiments.

3.2 Characterization of NK cells

Human NK cells were used as effector cells to study their interaction with the ECs. After recovery and purification of peripheral blood mononuclear cells (PBMCs), an enrichment of NK cells up to about 50% has been achieved in these experiments. The term “NK cell population” means that PBMCs were used which contain about 50% NK cells. For stimulation, these NK cells were incubated for four days with IL-2 and TKD, whereas un-stimulated NK cells were kept in culture in RPMI 1640 medium without any growth and stimulation factors. The expression of NK cell surface markers was analyzed by flow cytometry using antibodies directed against CD16/CD56 and CD94 as NK markers and CD3 as a T cell marker. Figure 21 shows the results of this analysis with un-stimulated resting (yellow) and TKD/IL-2 stimulated NK cells (blue). Apparently, the mfi of CD16/56 and CD94 is up-regulated after stimulation with TKD/IL-2.

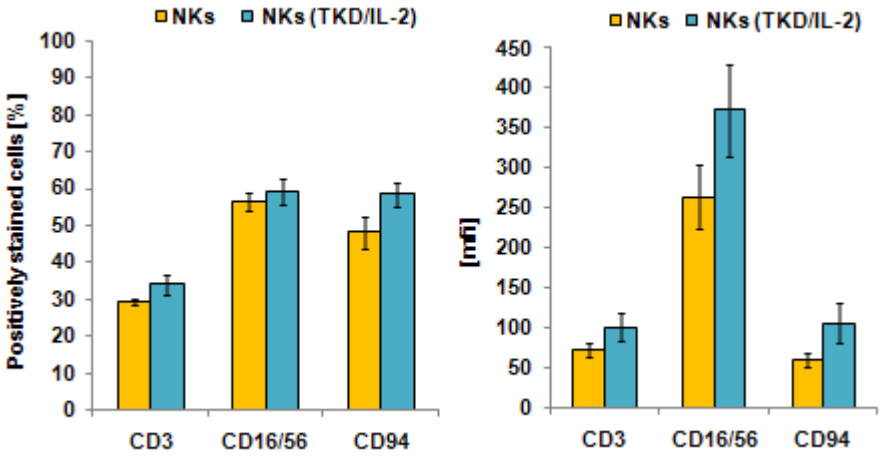

Figure 21: The expression of some cell surface markers was analyzed by flow cytometry. Resting (yellow) and stimulated (TKD/IL-2, blue) NK cells were compared. The results are shown as the mean +/- SEM of several independent experiments.

3.3 Interaction of ECs and NK cells

3.3.1 Morphology

3.3.1.1 Light microscopy

As described in the previous chapters, ECs express cell surface markers which have an influence on the interaction with NK cells. Therefore, some experiments focused on the interaction of ECs and NK cells. Microscopic images and films were taken using resting and stimulated (TKD/IL-2) NK cells and ECs in co-incubation assays. Figure 22 illustrates ECs in the absence (Figure 22 a) and in the presence (Figure 22 b) of NK cells. The effector to target (E:T) ratio in this experiment was 4:1. Directly after addition of NK cells, the effector cells were homogeneously distributed. Already few minutes later NK cells actively started to migrate towards the adherent ECs.

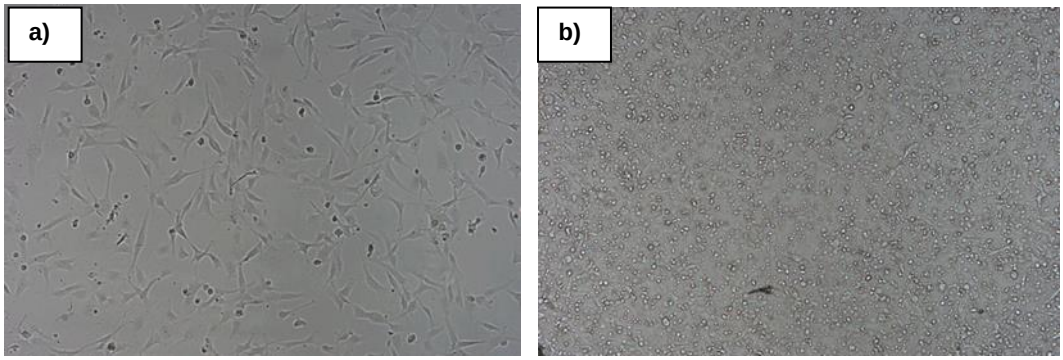

Figure 22: The process of the beginning of the co-incubation of ECs and NK cells is presented. The angled and big cells are the ECs (a). The round and small NK cells are shown directly after adding to the ECs (b). The E:T ratio was 4:1.

Figure 23 illustrates the ECs 20 h after co-incubation with resting (Figure 23 b, e, h) or stimulated NK cells (Figure 23 c, f, i) in comparison to equally treated ECs without any contact to NK cells for control reasons (Figure 23 a, d, g). The E:T ratios were 2:1 (HUVECs, a-c), 4:1 (EA.hy 926 cells, d-f), and 2:1 (HMECs, g-i). The small and round cells represent the NK cells and the large adherent cells are the ECs. Stimulated (TKD/IL-2) NK cells were attracted by the ECs and thus located in their close proximity. In the interspace between the ECs nearly no stimulated NK cells were found. In contrast, resting NK cells were distributed more homogeneously over the whole slide. Thus, the stimulation of NK cells enhanced the migratory and cytolytic activity of NK cells against ECs.

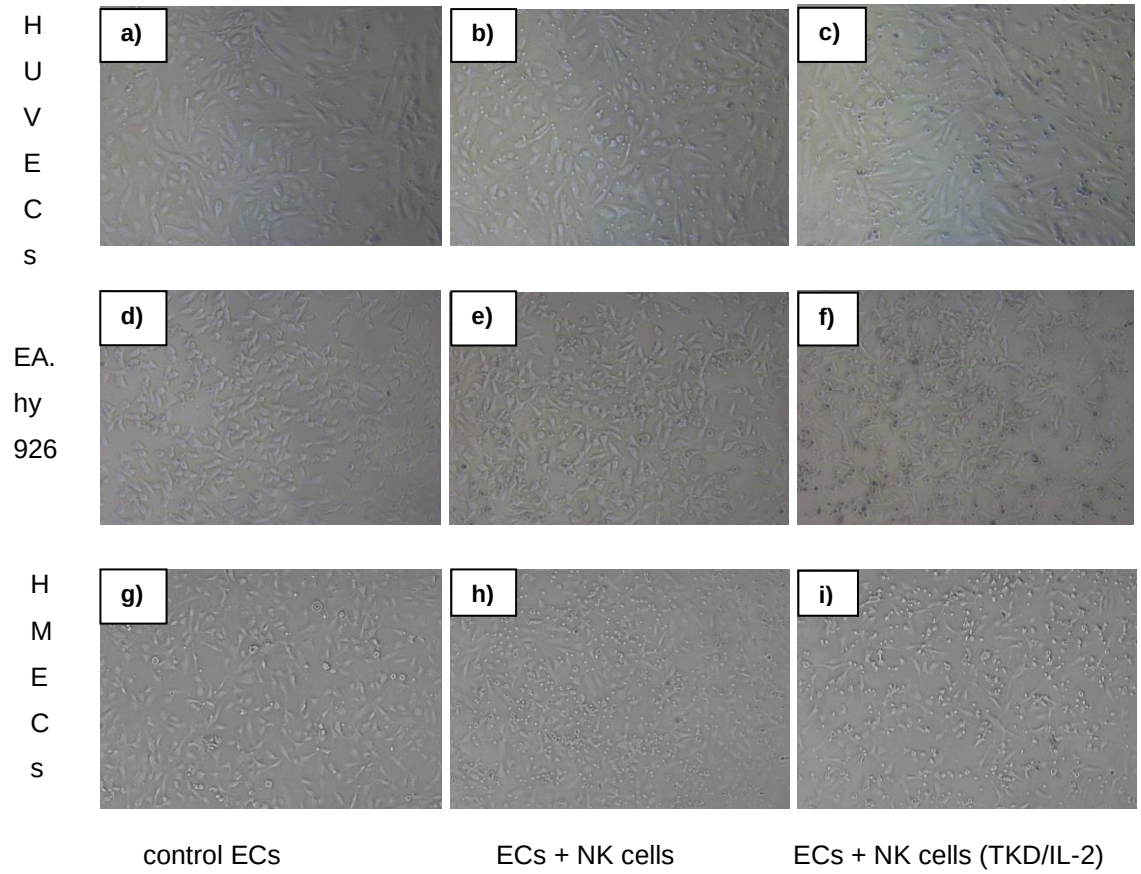

Figure 23: The status is shown of HUVECs (a-c), EA.hy 926 cells (d-f), and HMECs (g-i) 20 h after co-incubation with un-stimulated (b, e, h) or stimulated (c, f, i) NK cells (10 x). For control reasons ECs without any contact to NK cells are presented (a, d, g). The E:T ratios were 2:1 (HUVECs), 4:1 (EA.hy 926 cells), and 2:1 (HMECs). The small and round cells are the NK cells and the large and angled cells are the ECs.

Figure 24 presents images of the interaction of HMECs and NK cells at a higher magnification and under phase contrast to point out the difference between the attack of resting (Figure 24 a) and stimulated (Figure 24 b) NK cells. The E:T ratio was 4:1 and the co-incubation lasted for 25 h. The stimulated but not the resting NK cells formed cell aggregates with the ECs. The attack of NK cells on HMECs was filmed over a period of 8 h. Some images of this film (Figure 25) demonstrate in detail the difference in the behaviour of un-stimulated (Figure 25 a and b) and stimulated (Figure 25 c and d) NK cells using an E:T ratio of 10:1. Figures 25 a and c present the NK cells at the start of the co-incubation and Figures 25 b and d the status of the cells after 8 h. Only stimulated but not resting NK cells were efficient in the eradication of ECs. Furthermore, the photomicroscopic images indicate that one EC is attacked by a number of activated NK cells.

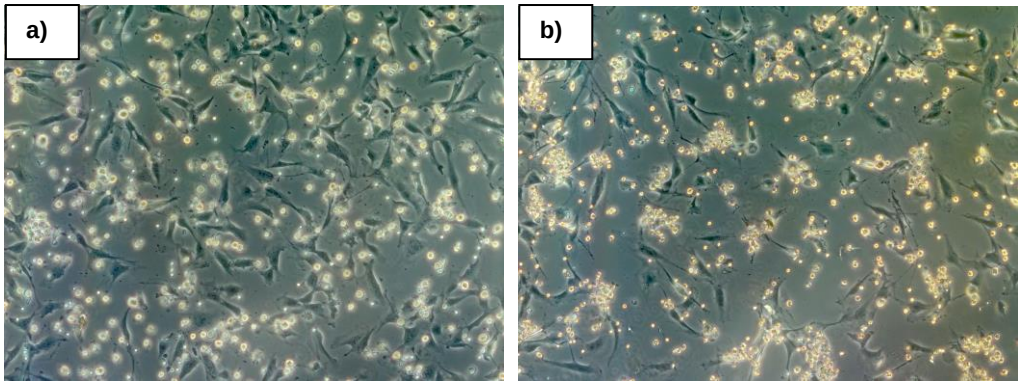

Figure 24: HMECs (big and angled cells) are presented 25 h after co-incubation with un-stimulated (a) or stimulated (b) NK cells (10 x, Ph 1). The E:T ratio was 4:1.

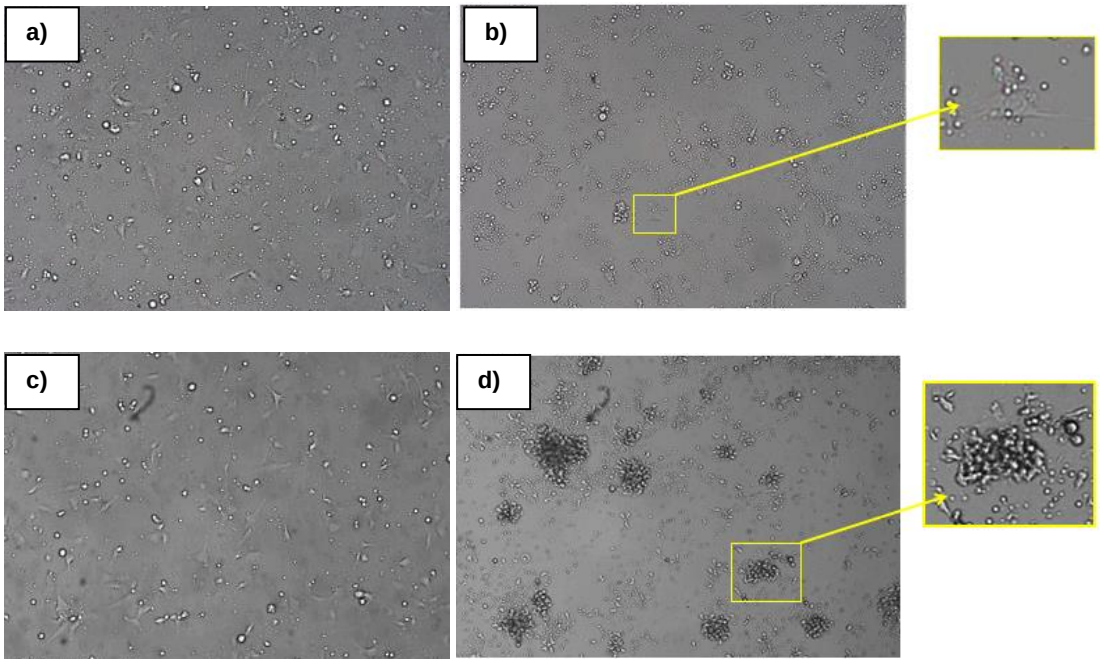

Figure 25: Some details of the co-incubation of HMECs with resting (a, b) or stimulated (c, d) NK cells (10 x) are illustrated. The E:T ratio was 10:1. Figures a and c present the beginning of the co-incubation and Figures b and d the cells 8 h after co-incubation.

Figure 26 shows some details of another film presenting the co-incubation of stimulated NK cells with HMECs. Already few minutes after addition, the stimulated NK cells started to kill the HMECs. Again, one HMEC (marked with a yellow circle) was attacked by several NK cells. The large and expanded surface of the cell got smaller and smaller until the cell was completely detached from the plastic surface of the slide. The pictures cover a period from 0 to 62 min.

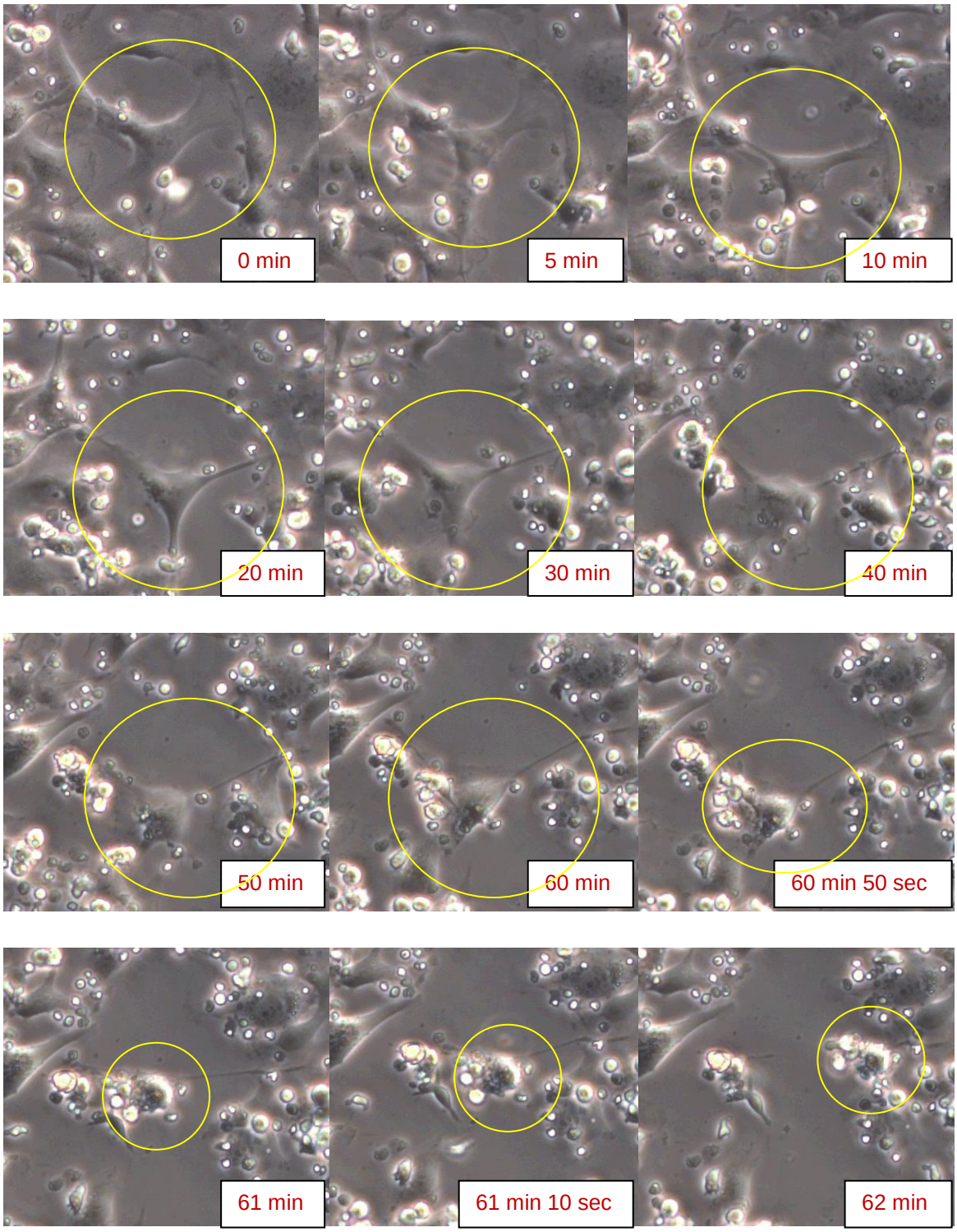

Figure 26: The detachment from the surface of a single HMEC (marked with a yellow circle) by stimulated NK cells is presented (E:T ratio: 4:1). The time scale presents the time passing after the first image.

In order to examine whether NK cells could attack ECs even under flow conditions, another co-incubation experiment was performed. Adherent HMECs were placed under flow and stimulated NK cells were added at an E:T ratio of 100:1 with a concentration of 3.3 x 10^6 NK cells/ml medium. Some images of the film are shown in Figure 27. Figure 27 demonstrates the interaction of stimulated (TKD/IL-2) NK cells with HMECs at a flow velocity of 3.0 ml/min (3.95 dyne/cm^2). At this flow rate NK cells were flushed over the adherent ECs, which is visualized by white marks on the images (circuited with yellow color). After reduction of the flow velocity to 1.0 ml/min (1.32 dyne/cm^2) some NK cells could attach onto HMECs (Figure 27 b, circuited with yellow circles). The flow direction is marked with a blue arrow.

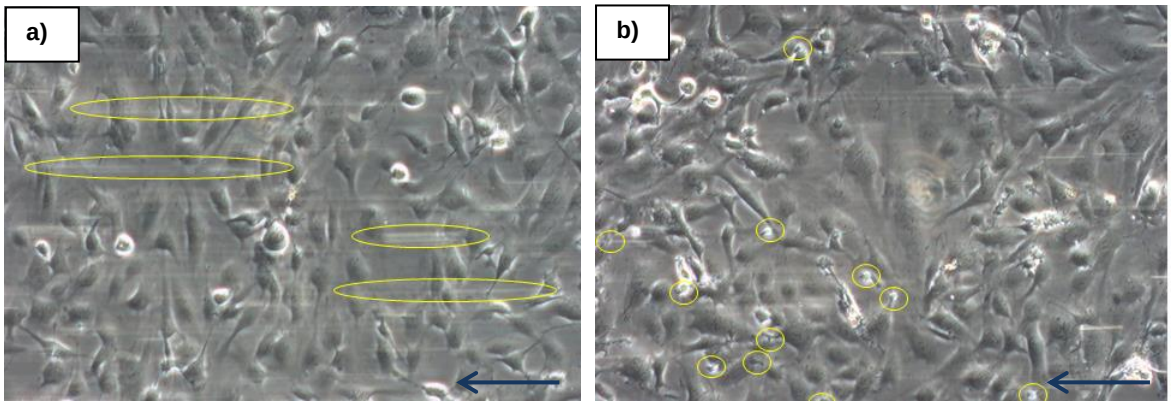

Figure 27: HMECs were co-incubated with stimulated NK cells under flow at two different flow velocities: 3.0 ml/min (a) and 1.0 ml/min (b) (20 x). The flow direction is marked with an arrow.

3.3.1.2 PKH staining

PKH immunofluorescence staining was used to illustrate the interaction of NK cells and HMECs. The cells were stained with PKH fluorescence dyes, which penetrate into the membrane lipid layers of viable cells. In Figure 28 the difference between the co-incubation with resting (Figure 28 a) and stimulated (Figure 28 b) NK cells (red) are illustrated at an E:T ratio of 4:1. The images were taken 20 h after co-incubation. As described above by means of light microscopic images, stimulated NK cells (red) were located in close proximity to the ECs (green). The adherence of activated NK cells to HMECs was visualized in an orange spectrum. In the interspace nearly no stimulated NK cells were found, whereas un-stimulated NK cells were detected more randomly. Thus, the expectation could be proven, that stimulation with TKD/IL-2 enhances the activity of NK cells to migrate towards ECs. In Figure 29 the strong attachment of a single stimulated NK cell (red) on a HMEC (green) is illustrated.

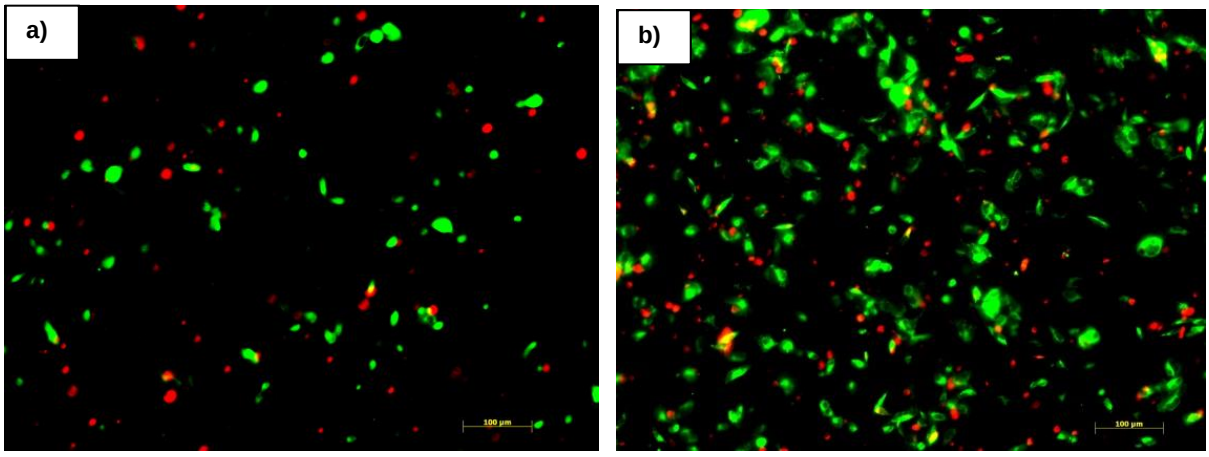

Figure 28: HMECs (green) were co-incubated with resting (a) or stimulated (b) NK cells (red) after staining with PKH fluorescence dyes. The E:T ratio was 4:1.

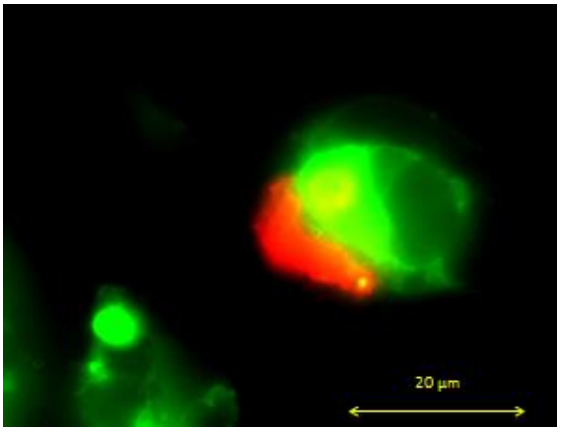

Figure 29: The attachment of one stimulated NK cell (red) at a HMEC (green) is illustrated with PKH fluorescence dyes.

3.3.2 Cytotoxicity assays

3.3.2.1 Resting versus stimulated NK cells

The light and immunofluorescence microscopical studies reveal that activated but not resting NK cells interact with ECs. Therefore, cytotoxicity assays, such as the Granzyme B ELISPOT assay and the ^{51}Cr release assay, were performed to quantify the amount of kill. The myelogenous leukemia cell line K562 was used as a positive control for measuring NK cell-mediated cytolysis (Gross, Schmidt-Wolf et al 2003). Figure 30 shows the results of the flow cytometry analysis of K562 cells with respect to Hsp70 (using cmHsp70.1 and SPA810 mAb) and to CD77. K562 cells were only positive for Hsp70 using cmHsp70.1 mAb and thus they provide a target for TKD/IL-2 activated NK cells.

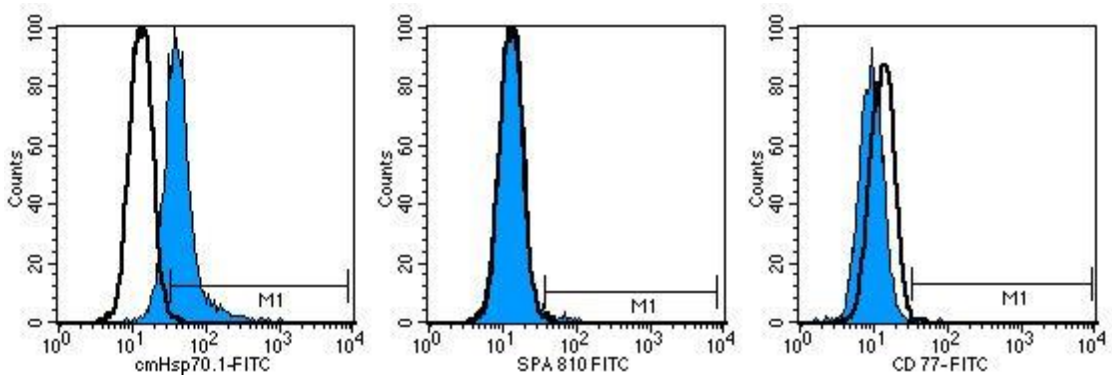

Figure 30: The myelogenous leukemia cell line K562 was analyzed by flow cytometry regarding the cell surface markers Hsp70 (using cmHsp70.1 mAb and SPA810 antibodies), and CD77. The blue graphs represent the staining with the specific antibodies and the white graphs the staining with the isotype-matched control antibodies.

First the lysability of HMECs and K562 cells were compared by using un-stimulated and stimulated NK cells (see Figure 31). The experiments were performed using Granzyme B ELISPOT assays (Figure 31 a) and ^{51}Cr release assays (Figure 31 b). Similar conclusions could be drawn by these two methods. Similar to K562 cells (represented by the green and blue lines), HMECs (represented by the red and yellow lines) provide a target cell line for NK cells. The cytolytic capacity of stimulated NK cells (represented by the blue and yellow lines) was significantly enhanced compared to the capacity of un-stimulated NK cells (represented by the green and red lines).

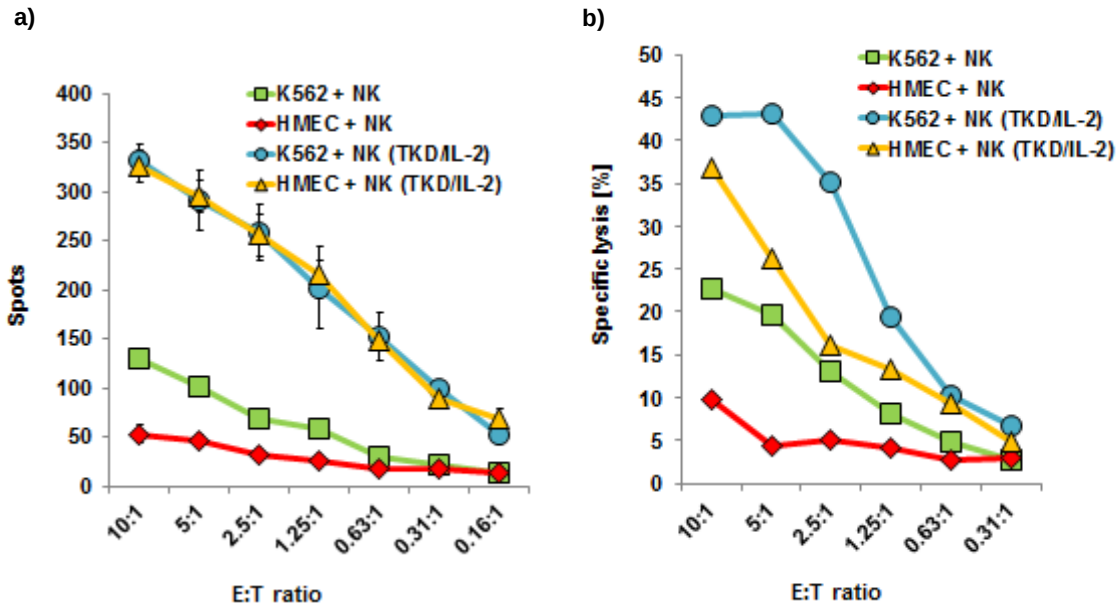

Figure 31: Granzyme B ELISPOT assays (a) and ^{51}Cr release assays (b) were performed with K562 cells (green and blue) and HMECs (red and yellow) as target cells, and with un-stimulated (green and red) and stimulated (blue and yellow) NK cells as effector cells. The results are shown as the mean +/- SEM of several independent experiments.

3.3.2.2 Comparison of the ECs

HUVECs, EA.hy 926 cells, and HMECs were used as target cells in a Granzyme B ELISPOT assay with stimulated NK cells. The results are shown in Figure 32 and Figure 33 a. Figure 32 shows an image of an ELISPOT plate. Already by visual inspection of the ELISPOT plate the difference in the cytolytic attack between the different ECs is apparent. The wells with the HUVECs contain much more red spots than the other wells. The red spots represent lysed ECs. According to the different E:T ratios the intensity of the spots decreased from the upper to the lower rows. Figure 33 a shows the summary of the results of several Granzyme B ELISPOT assays. Interestingly, primary HUVECs (represented by the yellow line) were attacked stronger than the immortalized HMECs (blue) and EA.hy 926 cells (red). Similar results could be determined in a comparative experiment (Figure 33 b) using HUVECs (yellow) and HMECs (blue) in a ^{51}Cr release assay. In conclusion, primary HUVECs were lysed better than the two immortalized endothelial cell lines.

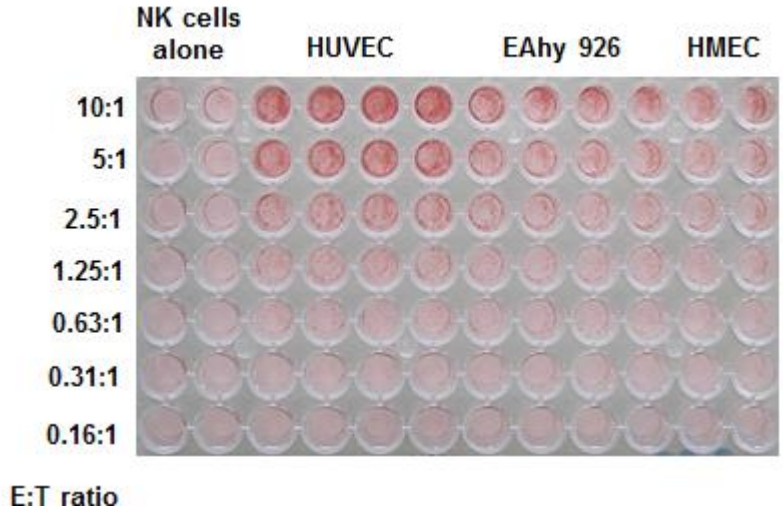

Figure 32: The image presents a plate after performing a Granzyme B ELISPOT assay with HUVECs, EA.hy 926 cells, and HMECs. The red spots represent lysed ECs. Different E:T ratios were performed from the upper to the lower rows.

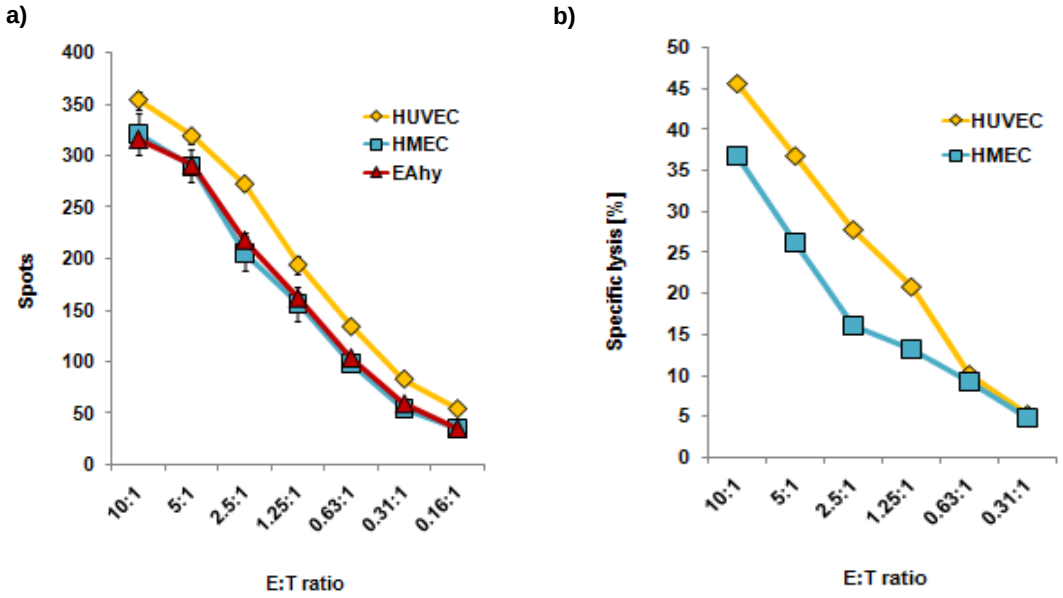

Figure 33: Cytotoxicity assays were performed with Granzyme B ELISPOT (a) and ^{51}Cr release (b) assays to compare the lysabilities of HUVECs (yellow), HMECs (blue), and EA.hy 926 cells (red). The results are shown as the mean +/- SEM of several independent experiments.

3.3.3 Phenotype

3.3.3.1 Phenotype of the ECs after contact with NK cells

The proportion of marker positive target cells and the cell surface density of the markers following co-incubation of the ECs with resting and activated NK cells for 12 h were analyzed by flow cytometry in separately gated cell populations. The results regarding all examined cell surface markers are shown in Figure 34, in which the HUVECs are presented by Figure 34 a, the EA.hy 926 cells by Figure 34 b, and the HMECs by Figure 34 c. The bars represent the control cells (yellow) without any contact to NK cells and the cells after co-incubation with resting (red) and stimulated (blue) NK cells. The graphs on the left side illustrate the percentage of positively stained cells and the graphs on the right side show the mfi.

Apart from MICA, Hsp70, CD54 (ICAM-1), and HLAE, none of the cell surface markers appeared to be affected by the contact with NK cells. The changes in the expression pattern are specified in Figure 35 with MICA (Figure 35 a), Hsp70 (Figure 35 b), CD54 (Figure 35 c), and HLAE (Figure 35 d). The HUVECs are represented by the left bars, the EA.hy 926 cells by the middle bars, and the HMECs by the right bars.

The percentage of $MICA^+$ primary HUVECs slightly dropped, as did the proportion of $MICA^+$ in its corresponding immortalized partner cell line EA.hy 926 (Figure 34 a and b, left panel). The cell surface density of MICA on the surviving cell fraction remained unaltered in HUVECs and EA.hy 926 cells (Figure 34 a and b, right panel). The microvascular cell line HMEC, which contains a very low proportion of $MICA^+$ cells, showed a decrease in the surface density of this marker (Figure 34 c, right panel), and there was also a small reduction in the proportion of $MICB^+$ cells (Figure 34 c, left panel).

The percentage of $cmHsp70.1^+$ cells increased at the HUVECs and the HMECs (Figure 35 b, left panel) and the mfi of cmHsp70.1 decreased at the HUVECs (Figure 35 b, right panel).

With respect to the intercellular adhesion molecule ICAM-1 (CD54), all three EC types reacted similarly by significantly up-regulation of the percentage of cells expressing this adhesion molecule and its cell surface density following contact with activated NK cells (Figure 35 c).

The most striking difference between the EC types was observed with respect to the expression of HLAE. After contact with activated NK cells, but not with resting NK

cells, the percentage of HLAE$^+$ HUVECs increased from below 5% up to nearly 100% within 12 h (Figure 35 d, left panel). Since the doubling time of HUVECs is slow (72 h), these results suggest that HLAE is actively up-regulated in primary macrovascular ECs. In contrast, almost all EA.hy 926 cells and HMECs initially showed a membrane HLAE$^+$ phenotype and contact with activated NK cells only enhanced the density of HLAE expression (Figure 35 d).

In contrast to TKD/IL-2-activated NK cells, resting NK cells had no influence on the viability of the ECs, nor did they alter significantly the expression of MICA, ICAM-1 (CD54), Hsp70, and HLAE.

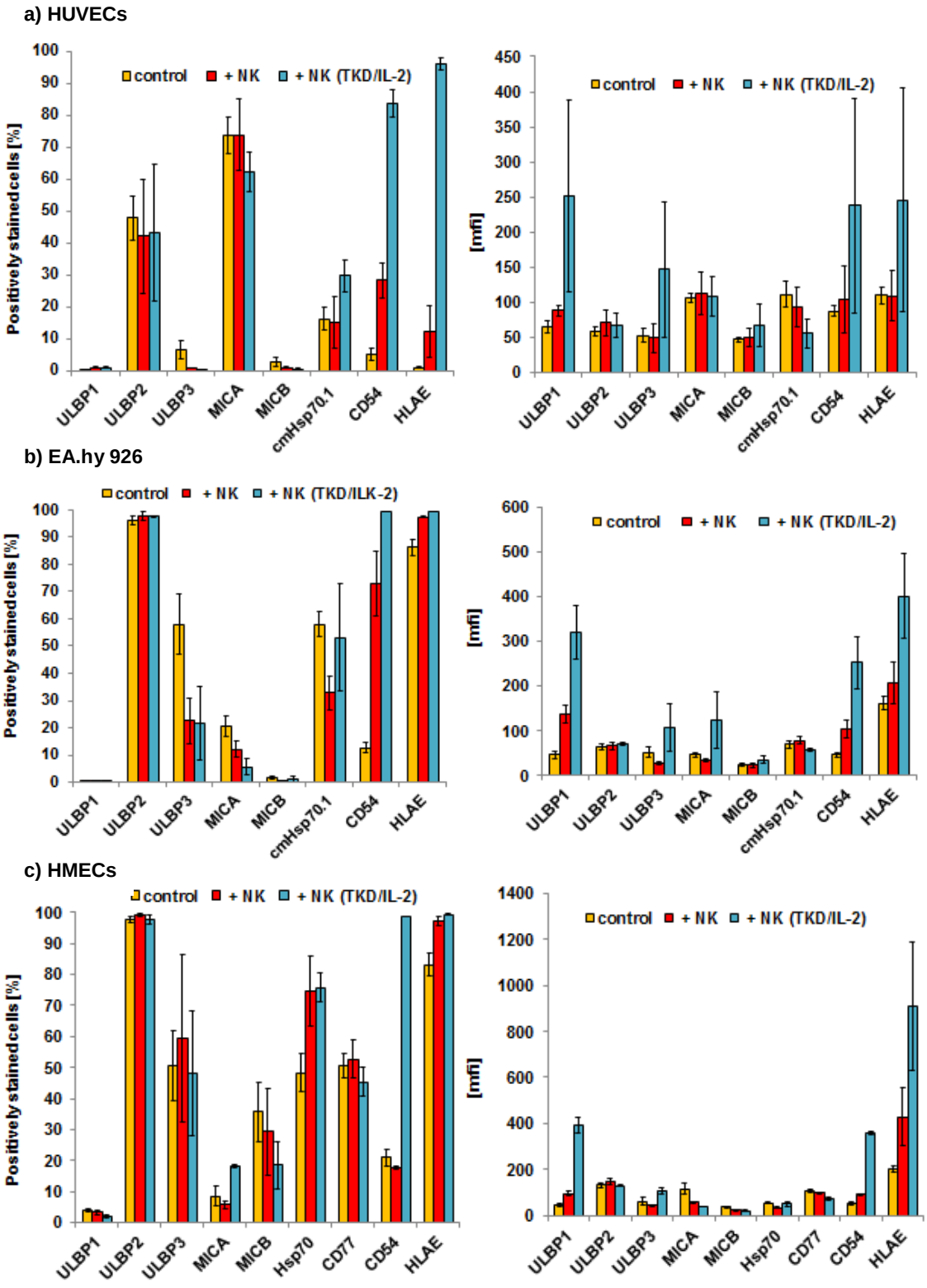

Figure 34: The phenotype of HUVECs (a), EA.hy 926 cells (b) and HMECs (c) was analyzed by flow cytometry after co-incubation with un-stimulated (red) and stimulated (blue) NK cells. For control reasons ECs without any contact to NK cells were also examined (yellow). The bars on the left panel represent the percentage of positively stained cells and the bars on the right panel the mean fluorescence intensity (mfi). The results are shown as the mean +/- SEM of several independent experiments.

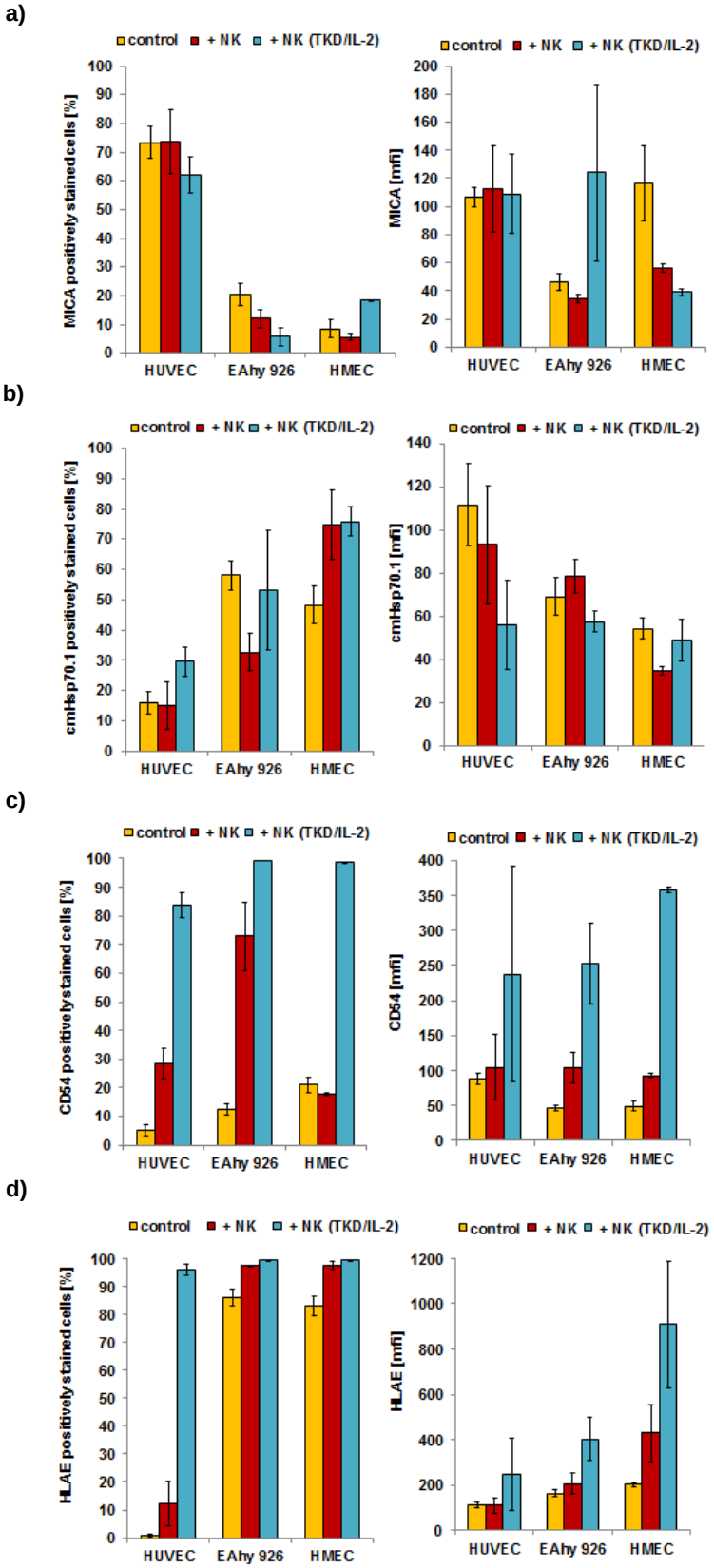

Figure 35: The expression of MICA (a), cmHsp70 (b), CD54 (c), and HLAE (d) of HUVECs (left bars), EA.hy 926 cells (middle bars) and HMECs (right bars) was analyzed by flow cytometry after co-incubation with unstimulated (red) and stimulated (blue) NK cells. For control reasons ECs without any contact to NK cells were also examined (yellow). The graphs on the left panel represent the percentage of positively stained cells and the graphs on the right panel the mean fluorescence intensity (mfi). The results are shown as the mean +/- SEM of several independent experiments.

3.3.3.2 Phenotype of HUVECs following the removal of activated NK cells

After co-incubation with activated NK cells surviving HUVECs were further cultivated without NK cells and analyzed by flow cytometry seven days later. The dramatic up-regulation of CD54 and HLAE on HUVECs was transient, since the levels of these proteins on the cell surface dropped to the very low baseline levels following the removal of activated NK cells (Figure 36). The blue bars represent the HUVECs immediately after co-incubation with NK cells, which occurred overnight, and the yellow bars represent the surviving HUVECs which were cultured for one week in normal HUVEC medium after the removal of NK cells. The graph on the left panel represents the percentage of positively stained cells and the graph on the right panel the mfi.

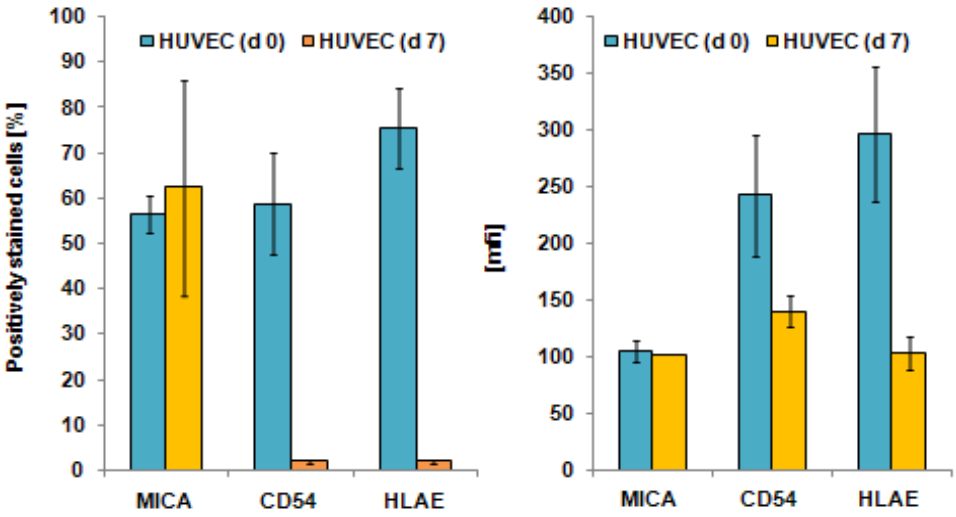

Figure 36: After co-incubation with stimulated NK cells, surviving HUVECs were cultured further without any contact to NK cells and the expression of MICA, CD54, and HLAE was analyzed again at day seven by flow cytometry. The graph on the left panel represents the percentage of positively stained cells and the graph on the right panel the mfi. The results are shown as the mean +/- SEM of several independent experiments.

Consequently, these cells showed the same attitude in the Granzyme B ELISPOT assay as not manipulated HUVECs. Figure 37 shows the result of the Granzyme B ELISPOT assay with stimulated NK cells and HUVECs which had no contact to NK cells (yellow) or HUVECS which were co-incubated with stimulated NK cells and then further cultivated after the removal of the NK cells (purple).

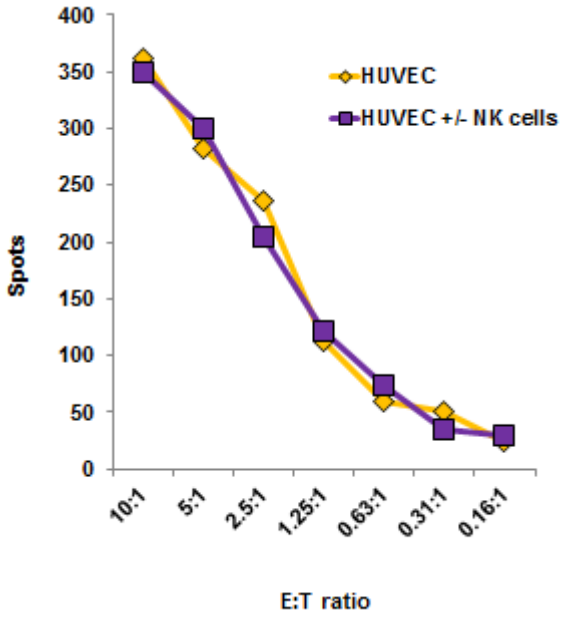

Figure 37: The Granzyme B ELISPOT assay was performed with stimulated NK cells and HUVECs which had no contact to NK cells (yellow) or HUVECS which were co-incubated with stimulated NK cells and then further cultivated after the removal of the NK cells (purple).

3.3.3.3 Phenotype of NK cells after contact with ECs

As proven above, the co-incubation of ECs with NK cells has effects on the phenotype of the ECs. In order to look for changes in the phenotype of the NK cells another flow cytometry analysis was made. The expression of CD3, CD16/56, and CD94 was analyzed on stimulated and un-stimulated NK cells after contact as well as without contact to HMECs and HUVECs (see Figure 38). The blue bars represent the NK cells without any contact to the ECs and the other bars represent the NK cells after co-incubation with HMECs (yellow, Figure 38 a and c) and HUVECs (green, Figure 38 b and d). Figures 38 a and b summarize the phenotype of the un-stimulated NK cells and Figures 38 c and d the phenotype of the stimulated NK cells. The graphs on the left panel represent the percentage of positively stained cells and the graphs on the right panel show the mfi. One significant change was remarkable. The mfi of CD16/56 decreased at the un-stimulated as well as at the stimulated NK cells after co-incubation with the ECs. Thus, the interaction of NK cells and ECs had also influence on the phenotype of the NK cells and not only on the phenotype of the ECs.

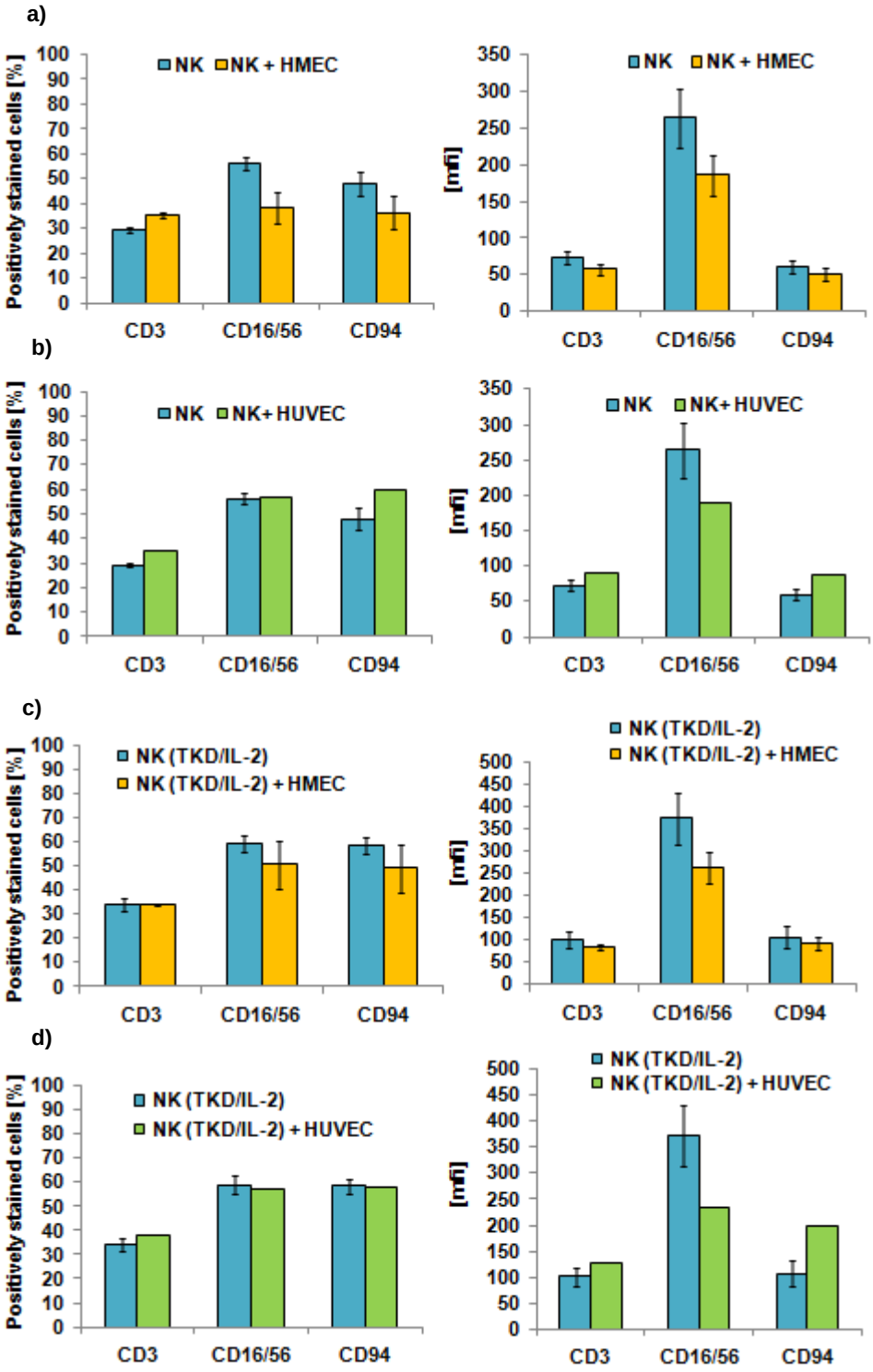

Figure 38: The expression of CD3, CD16/56 and CD94 by un-stimulated and stimulated NK cells was analyzed by flow cytometry and NK cells without contact to ECs (blue) were compared with NK cells after co-incubation with HMECs (yellow) and HUVECs (green). A) and b) summarize the phenotype of the un-stimulated NK cells and c) and d) the phenotype of the stimulated NK cells. The graphs on the left panel represent the percentage of positively stained cells and the graphs on the right panel show the mean fluorescence intensity (mfi). The results are shown as the mean +/- SEM of several independent experiments.

3.3.4 Effects of irradiation on the interaction of the ECs and NK cells

As described in chapter 3.1.2.3, exposure to ionizing irradiation (4 Gy) followed by a recovery period of 12 h significantly increased the expression density of HLAE on primary macrovascular HUVECs (see Figure 19 a). Although these effects were similar to those induced by the contact of HUVECs with activated NK cells, they were less pronounced. Similar effects were observed for the immortalized macrovascular partner cell line EA.hy 926 (Figure 19 b). In contrast, ionizing irradiation had no significant effect on the expression density of HLAE on the immortalized microvascular HMECs, HLAE was only slightly down-regulated (Figure 19 c). None of the other cell surface markers, such as ULBP1-3, MICA/B and ICAM-1 (CD54), was found to be altered significantly following irradiation.

Co-incubation experiments (Figure 39) were performed with Granzyme B ELISPOT (on the left side) and ^{51}Cr release assays (on the right side) with non-irradiated (red and yellow) and irradiated (4 Gy, green and blue) ECs with un-stimulated (red and green) as well as with stimulated (yellow and blue) NK cells. The HUVECs are represented in Figure 39 a, the EA.hy 926 cells in Figure 39 b, and the HMECs in Figure 39 c. In line with the increased cell surface expression of HLAE, the lysis of irradiated HUVECs (Figure 39 a) and EA.hy 926 cells (Figure 39 b) by activated NK cells expressing NKG2A and NKG2C receptors decreased significantly, whereas that of HMECs with an approximately unaltered HLAE membrane expression remained unaffected (Figure 39 c). Un-stimulated NK cells did not affect the lysis of any of the EC types (Figure 39 a-c) and also did not significantly change the cell surface marker expression pattern as shown in Figure 35.

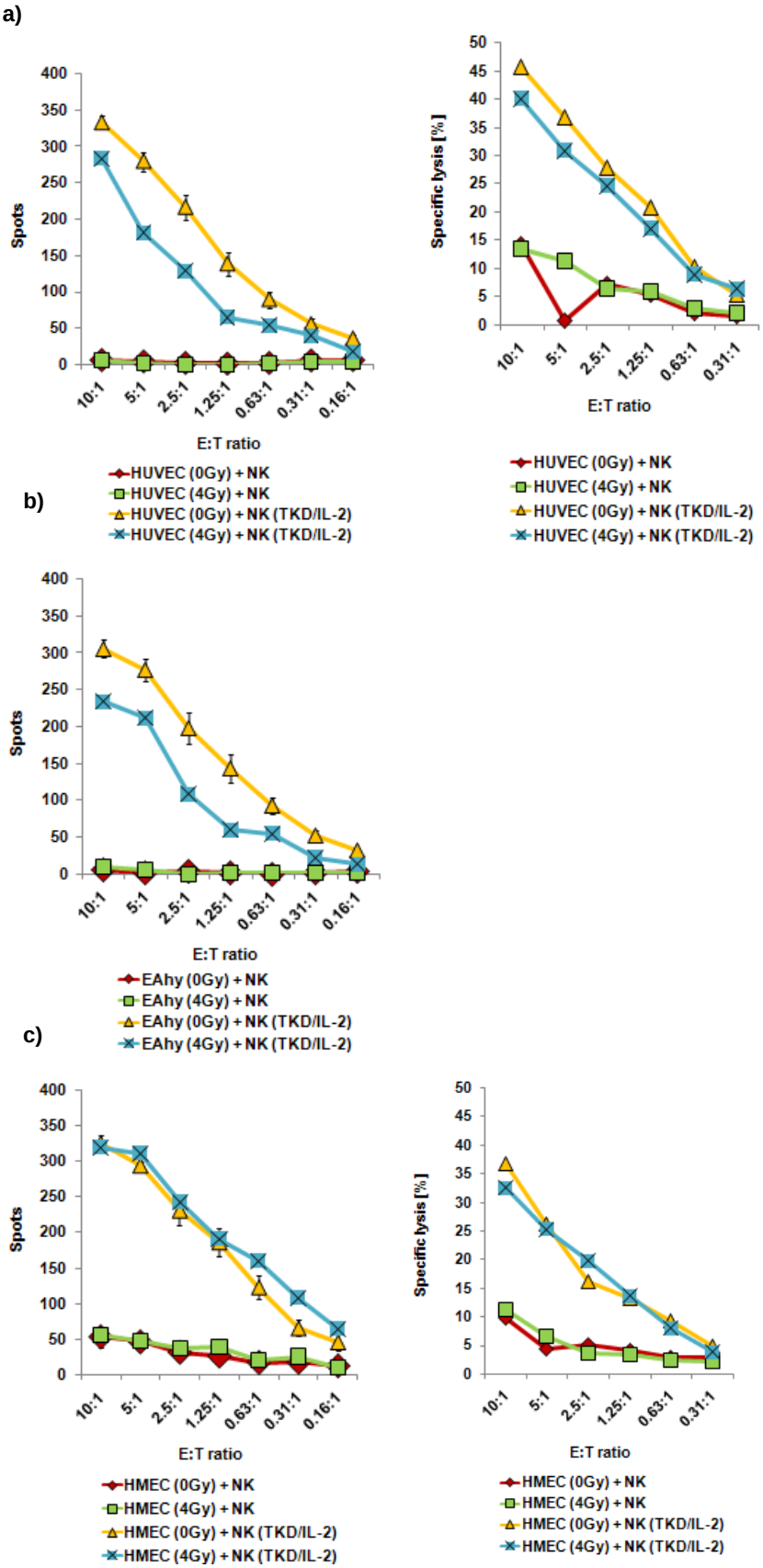

Figure 39: Granzyme B ELISPOT (left panel) and ^{51}Cr release assays (right panel) were performed with non-irradiated (red and yellow) and irradiated (4 Gy, green and blue) HUVECs (a), EA.hy 926 cells (b) and HMECs (c) with un-stimulated (red and green) as well as with stimulated (yellow and blue) NK cells. The results are shown as the mean +/- SEM of several independent experiments.

4 Discussion

Many experimental settings utilize immortalized and/or transformed ECs since primary ECs have only a limited lifespan and the purification of ECs is time consuming and complicate. The question arises, whether manipulations of ECs induced by immortalization alters the biological features of primary ECs. Therefore, herein, morphology, growth behavior, and phenotype of primary HUVECs were compared to that of immortalized HMECs and EA.hy 926 cells that are generated by a fusion of HUVECs with the epithelial lung tumor cell line A549-8.

The results of immunofluorescence studies and microscopical views of the cells during adherence under static cell culture conditions revealed no significant differences. However, under flow conditions, the HUVECs rapidly oriented towards the direction of the flow, whereas the EA.hy 926 cells appeared to have difficulties to tolerate the shear stress. EA.hy 926 cells also needed more time to become adherent to the surface of the chamber slides and the majority of the immortalized cells died within 2 days under flow conditions. These findings indicate that the manipulation caused by the immortalization affects cell functions such as the capacity to adhere to plastic surfaces and to align under flow conditions.

Differences and similarities in primary and immortalized ECs have already been discussed in previous work of others. It was shown that EA.hy 926 cells (Edgell et al 1983, Thornhill et al 1993) and HMECs (Xu et al 1994) are both positive for factor VIII-related antigen. Furthermore, Xu et al (1994) pointed out that HMECs are morphologically identical to their primary counterparts, namely the human dermal microvascular endothelial cells (HDMECs), and to HUVECs. Ades et al (1992) described that the immortalized HMECs maintain the cell morphology of their primary counterparts and share the phenotype regarding the strong expression of CD31 and ICAM-1. These results are in contradiction to my findings showing that HMECs express ICAM-1 only at low densities. The expression of ICAM-1 on HUVECs was also low.

Furthermore, the expression of other cell surface markers differed significantly within the different EC types. It is of particular interest that HUVECs were positive for MICA

and negative for HLAE in contrast to EA.hy 926 cells which were negative for MICA but positive for HLAE. Previous works (Zwirner et al 1998 and 1999) showed similar results with regard to the expression of MICA on HUVECs.

Most likely due to the fusion with the epithelial lung tumor cell line A549-8, EA.hy 926 cells also were found to be positive for the stress inducible markers ULBP3 and Hsp70. Immortalized HMECs were also positive for these two stress-related markers. Therefore, it is speculated that immortalized ECs might reflect a tumor-like phenotype. Interestingly, immortalized ECs differed also in the expression of the sphingolipid globoyltriaoslyceramide Gb3 (CD77) that has been identified as a tumor-specific lipid anchor for Hsp70 in the plasma membrane (Gehrmann et al 2008). Only tumor but not normal cells present Gb3 in lipid rafts in the plasma membrane. Similar to tumor cells, transformed HMECs express both, CD77 and Hsp70 in their plasma membrane. These findings provide another hint that, apart from their endothelial phenotype, HMECs show some characteristics that are typical for tumor cells.

In addition to differences in primary and immortalized ECs, also differences in micro- and macrovascular ECs were studied. In comparison to macrovascular EA.hy 926 cells, microvascular HMECs express the non-classical MHC molecule MICB. Since these differences in the cell surface expression pattern can be explained either by the origin of the vessels or by differences in the process of transformation, no final conclusion can be drawn with regard to this marker. Xu et al (1994) compared HMECs and HUVECs regarding their phenotypic features and concluded that HMECs reflect characteristics of both, micro- and macrovascular ECs.

The influence of culture conditions on the phenotype of ECs should also not be underestimated. Flow cytometry analysis revealed that the expression density of the adhesion molecule ICAM-1 (CD54) and HLAE was slightly increased when HUVECs were cultured under flow conditions. The increased cell surface density of CD54 in vivo might be attributed to a protection of the cells against shear stress, whereas the up-regulation of HLAE might be useful for the cells to mediate protection against the attack of activated NK cells in the blood stream.

Although MHC class I, MHC class I related chain MICA/B and ULBP1-3 are frequently up-regulated on tumor cells following environmental stress (Groh et al

1998), a sub-lethal irradiation dose of 4 Gy does not significantly increase the cell surface expression density of these markers on ECs.

In summary, these studies using transformed and primary ECs under static cell culture conditions demonstrate the limitations of in vitro experiments. Although not optimal, the cultivation of ECs under flow conditions is superior to that of cell cultures under static conditions. Furthermore, the process of immortalization of primary ECs also might have an impact on biological functions. Therefore, results of cultured ECs have to be considered with care regarding their clinical relevance. These findings are in accordance to the results of Luu et al (2010) who concluded that “the behaviour of cultured EC may depend as much on the physico-chemical culture conditions as on their origins”. Furthermore, no in vitro experimental system can replace animal models. This result is in line with findings of Sprague et al (2010) who showed that, although in vitro flow systems are mimicking the shear stress of the blood flow, the true complexity of the blood vessels and their microenvironment has to be studied in more sophisticated experimental approaches.

Previous studies (Botzler et al 1998, Multhoff et al 1999, Gastpar et al 2005) have shown that membrane-bound Hsp70 on tumor cells acts as a target structure for the recognition by activated but not resting NK cells. NK cells can be stimulated either with the full length Hsp70 protein, the C-terminal domain of Hsp70 or with a 14-mer peptide, termed TKD which is derived from the C-terminal substrate binding domain of Hsp70, in the presence of the pro-inflammatory cytokine IL-2 (Multhoff et al 2001, Gastpar et al 2004). In my experiments NK cells were stimulated with the Hsp70 peptide TKD plus IL-2 in order to stimulate the cytolytic function of NK cells against ECs.

Apparently, TKD/IL-2-stimulated NK cells exhibit higher expression densities of CD56 and CD94 compared to resting NK cells. These findings are in line with previously published results from our group. Gross, Schmidt-Wolf et al (2003) described that the mfi of CD94 and CD56 was only up-regulated on primary human NK cells but not on NK cell lines following stimulation with TKD/IL-2. Stangl et al (2008) also determined an increased cell surface expression density of CD56 and CD94 and a down-regulated expression of CD16 on NK cells upon stimulation with TKD/IL-2. Concomitantly, the production of the apoptosis inducing enzyme granzyme B was found to be up-regulated in NK cells. Elsner et al (2010) and Gross, Koelch et al

(2003) confirmed that a stimulation of NK cells with TKD/IL-2 causes an increased expression of intracellular granzyme B which was associated with an enhanced cytolytic activity of NK cells against Hsp70 membrane positive tumor cells. In summary, TKD/IL-2 stimulates the cytolytic activity of NK cells against Hsp70 membrane positive tumor cells concomitant with an up-regulated expression density of the NK cell receptors CD56 and CD94. The mechanism of killing was found to be associated with an elevated release of the apoptosis-inducing enzyme granzyme B by NK cells.

For a better understanding of the interaction of ECs and NK cells, the expression of activating and inhibitory NK cell ligands was studied on human primary and immortalized ECs before and after irradiation. The immunomodulatory functions on NK cells were monitored in parallel.

In previous studies different ECs were compared with regard to their interaction with leukocytes. Thornhill et al (1993) compared HUVECs and EA.hy 926 cells with respect to their leukocyte-EC adhesion mechanisms in the presence of IL-4, tumor necrosis factor (TNF), and interferon-γ. They concluded that EA.hy 926 cells and HUVECs behave similarly after incubation with TNF but not after incubation with IL-4 or interferon-γ. Lidington et al (1999) compared HMECs, EA.hy 926 cells, and HUVECs with respect to their interaction with immune effector cells. This group reported about differences between the cell lines with regard to their ability to respond to cytokines and their interaction with lymphocytes. Another group (Kitayama et al 1994) examined whether lymphokine-activated killer (LAK) cells could attack not only allogenic but also autologous ECs. They found that autologous as well as allogeneic ECs were attacked similarly by $CD16^+$ NK cells. Kotasek et al (1988) examined the mechanism of cultured endothelial cells following attack by lymphokine-activated killer (LAK) cells. Regarding cell morphology and phenotype this group presented similar results. Furthermore, damage in ECs was found after a LAK cell-based anti-tumor-therapy. Also Damle et al (1987), Miltenburg et al (1987), and Amador et al (1991) could show that activated lymphocytes could induce damage in vascular ECs. Although there are some specific differences in primary and immortalized ECs regarding their phenotype, most reports speculate about the possibility that activated lymphocytes can cause damage to the vasculature.

The MIC gene products and ULBP1-3 proteins act as activating ligands for the C-type lectin receptor NKG2D (Ebert et al 2008, Raulet 2003, Groh et al 2002, Gonzalez et al 2006) which is expressed on NK cells and via which activated NK cells can specifically kill their tumor target cells. Our group (Multhoff et al 1997, Gastpar et al 2004) has shown that in contrast to normal tissues, tumors frequently present the major stress-inducible heat shock protein 70 (Hsp70) on their plasma membrane. Similar to MICA/B and ULBP1-3 membrane-bound Hsp70 also serves as a recognition structure for TKD/IL-2 activated NK cells (Stangl et al 2006) on tumor cells in vitro and in tumor mouse models (Gross, Hansch et al 2003; Gross, Schmidt-Wolf et al 2003). Following activation, these NK cells show an elevated expression density of a panel of different receptors including the C-type lectin receptors CD94/NKG2A, CD94/NKG2C, NKG2D, and natural cytotoxicity receptors (NCRs) (Marin et al 2003).

Furthermore, the Hsp70 membrane density on tumor cells can be selectively enhanced by ionizing irradiation. In this work, it was of interest to study the role of membrane-bound Hsp70 as a recognition structure for NK cells on non-irradiated and irradiated primary and immortalized ECs. As expected, only immortalized ECs exhibited a membrane $Hsp70^{+}$ phenotype. It can be assumed that the fusion of primary HUVECs with the membrane $Hsp70^{+}$ tumor cell line A549-8 as well as the transformation of primary dermal microvascular ECs with the SV40 large T antigen results in a malignant transformation of ECs which enables the translocation of Hsp70 to the plasma membrane in a similar manner like in tumor cells. Therefore, it can be speculated that immortalized ECs might in part reflect the phenotype of tumor cells. In contrast to tumor cells, however, neither primary nor immortalized ECs exhibited a significant up-regulation of membrane Hsp70 density after ionizing irradiation.

In different assays HLAE could be proven to exert protective functions against the cytolytic attack of NK cells. When comparing the HLAE phenotype in micro- and macrovascular ECs and their susceptibility for NK cell mediated cytolysis, the absence of HLAE was found to be associated with a higher sensitivity towards activated NK cells. However, the balance of all cell surface markers, activating and inhibitory ligands, has to be considered. It has been previously described that the “NK cell function is the result of a fine tuning between opposite signals by inhibitory and/or activating receptors” (Pende et al 2002). Sutherland et al (2001 and 2002)

concluded that the expression of ULBPs or MICs by target cells can overcome an inhibitory signal and trigger NK cell cytotoxicity although it was formerly thought that inhibitory signals were dominant over signals generated by activating receptors. In this project the expression of activating ligands, such as MICA/B, ULBP1-3, and Hsp70, on ECs appeared to be of minor importance for NK cell mediated activities. Interestingly, the expression of HLAE by the HUVECs was up-regulated after co-incubation with stimulated NK cells. This change in the expression of HLAE, however, was transient. It dropped to baseline levels after further cultivation and following removal of the NK cells. Therefore, it was assumed that ECs actively up-regulate the expression of HLAE to protect themselves against the attack of activated NK cells. A sub-lethal irradiation initiated a selective up-regulation of HLAE on macrovascular ECs which correlated with a decreased susceptibility to NK cell mediated lysis. Interestingly, HLAE expression on immortalized microvascular ECs remained unchanged following irradiation and their lysis by activated NK cells remained unaltered.

Although the physiological relevance of these differences in the expression of HLAE on micro- and macrovasculature has not yet been completely understood, these findings might, among others, have future clinical implications for radiotherapy. In previous papers (Hantschel et al 2000, Multhoff et al 2000, Kleinjung et al 2003, Elsner et al 2007, Schmitt et al 2007, Milani et al 2009) the possibilities of anti-tumor therapies with NK cells against Hsp70 positive tumors have been described. Analyzing differences in activating and inhibitory NK ligands on ECs might be useful for the development of therapeutic strategies that combine irradiation and NK cell-based therapies. Also it will be of interest to study differences in ECs derived from normal and tumor tissues within one host organism.

Last but not least the effects of sub-lethal irradiation on the ECs have to be considered regarding radiation-induced cardiovascular diseases. Endothelial dysfunction, for example after irradiation, results in several diseases such as atherosclerosis or thrombosis. Epidemiological studies (Schultz-Hector et al 2007) have shown that radiation, even at low doses, significantly increases the risk for the development of myocardial infarction, more than ten years after treatment.

5 Summary

5.1 Summary

This work focused on studies analyzing the interaction of natural killer (NK) cells and irradiated or non-irradiated endothelial cells (ECs). Primary and immortalized, macro- and microvascular ECs were used. The macrovascular ECs were represented by primary human umbilical vein endothelial cells (HUVECs) and their immortalized fusion product EA.hy 926 cells (HUVECs fused with the epithelial lung tumor cell line A549-8). Microvascular ECs were represented by human dermal microvascular endothelial cells (HMECs) which were transfected with a PBR-322-based plasmid containing the coding region for the simian virus 40 A gene product, large T antigen. The different ECs were characterized morphologically and phenotypically under static culture conditions. With regard to their cell morphology and to the endothelial cell markers CD31 and factor VIII-related antigen, no significant differences were observed in the different ECs under static culture conditions. Under flow conditions using the pump system from ibidi (Martinsried, Germany), the primary HUVECs oriented rapidly towards the flow direction whereas the immortalized EA.hy 926 cells and HMECs did not show any alignment.

The expression of different cell surface markers (ULBP1-3, MICA/B, Hsp70, CD77, CD54, and HLAE), which act as activating or inhibitory ligands for NK cells, was analyzed on the different ECs by flow cytometry. The most important difference between the examined ECs was that HUVECs expressed the activating ligand MICA and not the inhibitory ligand HLAE, whereas the immortalized cell lines showed a strong expression of HLAE. After irradiation with a dose of 4 Gy, the expression of HLAE was significantly up-regulated on the EA.hy 926 cells and HUVECs. In HMECs the expression of HLAE was slightly down-regulated.

The studies of the interaction of ECs and NK cells were performed using un-stimulated and TKD/IL-2-stimulated NK cells. The ECs acted as target structure for stimulated NK cells. An active migration of activated but not of resting NK cells towards ECs was demonstrated by light microcopy and immunofluorescence

analysis. Time kinetics revealed that one EC was attacked by multiple activated NK cells and that cell aggregates were built. To quantify the killing activity of activated NK cells, cytotoxicity assays were performed. Granzyme B assays and ^{51}Cr release assays revealed that activated but not resting NK cells significantly kill ECs. By comparing the different ECs as target cells, it became apparent that primary HUVECs were lysed significantly better by activated NK cells than the two immortalized EC lines. This finding could be associated with a stronger expression of the inhibitory ligand HLAE by the immortalized cell lines. After irradiation with 4 Gy, the lysis of EA.hy 926 cells and HUVECs was reduced. The weaker lysability was found to be associated with an irradiation-induced increase in the expression of HLAE. In contrast, the lysis of irradiated HMECs that showed no significant differences in the expression of HLAE was comparable to the lysis of non-irradiated HMECs. Differences in the expression of activating ligands on ECs appear to have no effect on the killing activity of NK cells.

In conclusion, the interaction of NK cells and non-irradiated or irradiated ECs was found to be associated with differences in the expression of HLAE, in vitro. HLAE apparently has a protective role for endothelial cells towards the cytolytic activity of TKD/IL-2- activated NK cells.

5.2 Zusammenfassung

In dieser Arbeit ging es darum, die Interaktion von natürlichen Killer (NK)-Zellen mit unbestrahlten und bestrahlten Endothelzellen (ECs) zu untersuchen. Als ECs wurden sowohl primäre als auch immortalisierte makro- und mikrovaskuläre humane ECs verwendet. Als Vertreter der makrovaskulären ECs wurden primäre Endothelzellen aus der menschlichen Nabelschnurvene (Human Umbilical Vein Endothelial Cells, HUVECs) und deren Fusionsprodukt mit der epithelialen Lungentumor-Zelllinie A549-8, (EA.hy 926-Zellen) eingesetzt. Als mikrovaskuläre ECs wurden immortalisierte Endothelzellen aus der menschlichen Haut (Human Dermal Microvascular Endothelial Cells, HMECs) verwendet, die mit einem PBR-322 basiertem Plasmid, welches die kodierende Region des Simian-Virus 40 A Genprodukt, large T Antigen, enthält, transfiziert wurden. Zuerst wurden die ECs unter statischen Kulturbedingungen morphologisch und phänotypisch charakterisiert. Bezüglich der Morphologie waren keine signifikanten Unterschiede zu beobachten. Auch im Expressionsmuster der EC-Marker CD31 und des Faktor VIII-related Antigens sowie im Adhärenzverhalten auf Zellkulturschalen zeigten sich zwischen den verschiedenen EC-Typen keine Unterschiede. Unter Flussbedingungen im ibidi Pump System (Martinsried, Germany) allerdings richteten sich die primären HUVEC-Zellen rasch in Flussrichtung aus, während die immortalisierten EA.hy 926- und HMEC-Zelllinien keine Reaktion auf die Flussbedingungen zeigten.

Die Expression unterschiedlicher Oberflächenmarker (ULBP1-3, MICA/B, Hsp70, CD77, CD54 und HLAE), die als aktivierende oder inhibierende Liganden für NK-Zellen fungieren, wurde mit Hilfe der Durchflusszytometrie auf den unterschiedlichen ECs untersucht. Der stärkste Unterschied zwischen den ECs war, dass HUVEC-Zellen den aktivierenden Liganden MICA nicht aber den inhibierenden Liganden HLAE exprimierten, wohingegen die immortalisierten Zelllinien eine starke Expression von HLAE aufwiesen. Nach Bestrahlung mit einer Dosis von 4 Gy wurde die Expression von HLAE auf EA.hy 926-Zellen und HUVEC-Zellen signifikant hoch und bei HMEC-Zellen leicht herunter reguliert.

5 Summary

Die Untersuchungen der Interaktion zwischen den ECs und den NK-Zellen wurden sowohl mit unstimulierten als auch mit stimulierten (TKD/IL-2) NK-Zellen durchgeführt. Die ECs agierten als Zielstrukturen für stimulierte NK-Zellen. Eine aktive Migration von stimulierten nicht aber von unstimulierten NK-Zellen in Richtung der ECs konnte mit Hilfe von lichtmikroskopischen Aufnahmen und Immunfluoreszenzanalysen nachgewiesen werden. In kinetischen Analysen, die durch Filmaufnahmen dokumentiert wurden, konnte gezeigt werden, dass eine einzelne Endothelzelle von mehreren NK-Zellen attackiert wurde und dass sich dabei Zellaggregate bildeten. Um diese Beobachtungen zu quantifizieren, wurden Zytotoxizitäts-Versuche durchgeführt, nämlich Granzyme B ELISPOT Assays und ^{51}Cr Release Assays. Mit beiden Methoden konnte nachgewiesen werden, dass stimulierte NK-Zellen ECs signifikant stärker lysieren als ruhende NK-Zellen. Im Vergleich der ECs untereinander wurden die primären HUVEC-Zellen stärker lysiert als die zwei immortalisierten Endothelzelllinien. Dieser Befund konnte auf die stärkere Expression des inhibierenden Liganden HLAE auf den immortalisierten Zelllinien zurückgeführt werden. Nach Bestrahlung mit 4 Gy wurden die EA.hy 926-Zellen und die HUVEC-Zellen weniger stark lysiert. Dieser Befund korrelierte ebenfalls mit einer erhöhten Expression von HLAE. Im Gegensatz dazu war die Lyse bestrahlter HMEC-Zellen, die keine signifikanten Veränderungen in der HLAE-Expression zeigten, vergleichbar mit der Lyse nicht bestrahlter HMEC-Zellen. Die aktivierenden Liganden für NK-Zellen schienen keinen essentiellen Einfluss auf die Lysierbarkeit von ECs durch NK-Zellen zu besitzen.

Zusammenfassend kann man sagen, dass die Interaktion von NK-Zellen mit unbestrahlten und bestrahlten ECs in vitro zu einem hohen Maß über die Expression von HLAE gesteuert wird. HLAE besitzt offensichtlich eine protektive Rolle für Endothelzellen gegenüber der zytolytischen Aktivität von aktivierten NK-Zellen.

6 References

Ades EW, Candal FJ, Swerlick RA, George VG, Summers S, Bosse DC, Lawley TJ.
HMEC-1: establishment of an immortalized human microvascular endothelial cell line.
J. Invest. Dermatol. 99 (6): 683-690, 1992.

Ahmad M, Khurana NR, Jaberi JE.
Ionizing radiation decreases capillary-like structure formation by endothelial cells in vitro.
Microvasc. Res. 73 (1): 14-19, 2007.

Allavena P, Bianchi G, Paganin C, Giardina G, Mantovani A.
Regulation of adhesion and transendothelial migration of natural killer cells.
Nat. Immun. 15 (2-3): 107-116, 1996.

Amador JF, Vazquez AM, Cabrera L, Barral AM, Gendelman R, Jondal M.
Toxic effects of interleukin-2-activated lymphocytes on vascular endothelial cells.
Nat. Immun. Cell Growth Regul. 10 (4): 207-215, 1991.

Ando J, Yamamoto K.
Vascular mechanobiology – endothelial cell responses to fluid shear stress.
Circ. J. 73: 1983-1992, 2009.

Bahram S, Bresnahan M, Geraghty DE, Spies T.
A second lineage of mammalian major histocompatibility complex class I genes.
Proc. Natl. Acad. Sci. USA, Immunology 91 (14): 6259-6263, 1994.

Baudin B, Bruneel A, Bosselut N, Vaubourdolle M.
A protocol for isolation and culture of human umbilical vein endothelial cells.
Nature Protocols 2 (3): 481-485, 2007.

Bauer S, Groh V, Wu J, Steinle A, Phillips JH, Lanier LL, Spies T.
Activation of NK cells and T cells by NKG2D, a receptor for stress-inducible MICA.
Science 285 (5428): 727-729, 1999.

Biassoni R, Cantoni C, Falco M, Pende D, Millo R, Moretta L, Bottino C, Moretta A.
Human natural killer cell activating receptors.
Mol. Immunol. 37 (17): 1015-1024, 2000.

Biassoni R, Cantoni C, Marras D; Giron-Michel J, Falco M, Moretta L, Dimasi N.
Human natural killer cell receptors: insights into their molecular function and structure.
J. Cell. Mol. Med. 7 (4): 376-387, 2003.

Bielawska-Pohl A, Crola C, Caignard A, Gaudin C, Dus D, Kieda C, Chouaib S.
Human NK cells lyse organ-specific endothelial cells: analysis of adhesion and cytotoxic mechanisms.
J. Immunol 174: 5573-5582, 2005.

Biron CA.
Activation and function of natural killer cell responses during viral infections.
Curr. Opin. Immunol. 9: 24-34, 1997.

Bolland S, Ravetch JV.
Inhibitory pathways triggered by ITIM-containing receptors.
Adv. Immunol. 72: 149-177, 1999.

Borrego F, Kabat J, Kim DK, Lieto L, Maasho K, Pena J, Solana R, Coligan JE.
Structure and function of major histocompatibility complex (MHC) class I specific receptors expressed on human natural killer (NK) cells.
Mol. Immunol. 38 (9): 637-660, 2002.

Botzler C, Li G, Issels RD, Multhoff G.
Definition of extracellular localized epitopes of Hsp70 involved in an NK immune response.
Cell Stress Chaperones 3 (1): 6-11, 1998.

Braud VM, Jones EY, McMichael A.
The human major histocompatibility complex class Ib molecule HLA-E binds signal sequence-derived peptides with primary anchor residues at positions 2 and 9.
Eur. J. Immunol. 27: 1164-1169, 1997.

Braud VM, Allan DSJ, O´Callaghan CA, Söderström K, D´Andrea A, Ogg, GS, Lazetic S, Young NT, Bell JI, Phillips JH, Lanier LL, McMichael AJ.
HLA-E binds to natural killer cell receptors CD94/NKG2A, B and C.
Nature 391: 795-799, 1998.

Brooks AG, Posch PE, Scorzelli CJ, Borrego F, Coligan JE.
NKG2A complexed with CD94 defines a novel inhibitory natural killer cell receptor.
J. Exp. Med. 185 (4): 795-800, 1997.

Brunner KT, Mauel J, Cerottini JC, Chapuis B.
Quantitative assay of the lytic action of immune lymphoid cells on ^{51}Cr-labelled allogeneic target cells in vitro; inhibition by isoantibody and by drugs.
Immunol. 14: 181, 1968.

Carlos TM, Harlan JM.
Leukocyte-endothelial adhesion molecules.
Blood 84 (7): 2068-2101, 1994.

Cheung AL.
Isolation and culture of human umbilical vein endothelial cells (HUVEC).
Curr. Protoc. Microbiol. 4: A.4B.1–A.4B.8, 2007.

Cordes N, Park CC.
β1 integrin as a molecular therapeutic target.
Int. J. Radiat. Biol. 83 (11-12): 753-760, 2007.

Damle NK, Doyle LV, Bender JR, Bradley EC.
Interleukin 2-activated human lymphocytes exhibit enhanced adhesion to normal vascular endothelial cells and cause their lysis.
J. Immunol. 138 (6): 1779-1785, 1987.

Ebert EC, Groh V.
Dissection of spontaneous cytotoxicity by human intestinal intraepithelial lymphocytes: MIC on colon cancer triggers NKG2D-mediated lysis through Fas ligand.
Immunology 124: 33-41, 2008.

Edgell CJS, McDonald CC, Graham JB.
Permanent cell line expressing human factor VIII-related antigen established by hybridization.
Proc. Natl. Acad. Sci. USA, Cell Biology 80 (12): 3734-3737, 1983.

Elsner L, Muppala V, Gehrmann M, Lozano J, Mahlzahn D, Bickeböller H, Brunner E, Zientkowska M, Herrmann T, Walter L, Alves F, Multhoff G, Dressel R.
The heat shock protein HSP70 promotes mouse NK cell activity against tumors that express inducible NKG2D ligands.
J. Immunol. 179 (8): 5523-5533, 2007.

Elsner L, Flügge PF, Lozano J, Muppala V, Eiz-Vesper B, Demiroglu SY, Mahlzahn D, Herrmann T, Brunner E, Bickeböller H, Multhoff G, Walter L, Dressel R.
The endogenous danger signals HSP70 and MICA cooperate in the activation of cytotoxic effector functions of NK cells.
J. Cell. Mol. Med. 14 (4): 992-1002, 2010.

Gastpar R, Gross C, Rossbacher L, Ellwart J, Riegger J, Multhoff G.
The cell surface-localized heat shock protein 70 epitope TKD induces migration and cytolytic activity selectively in human NK cells.
J. Immunol. 172 (2): 972-980, 2004.

Gastpar R, Gehrmann M, Bausero MA, Asea A, Gross C, Schroeder JA, Multhoff G.
Heat shock protein 70 surface-positive tumor exosomes stimulate migratory and cytolytic activity of natural killer cells.
Cancer Res. 65 (12): 5238-5247, 2005.

Gehrmann M, Liebisch G, Schmitz G, Anderson R, Steinem C, De Maio A, Pockley G, Multhoff G.
Tumor-specific Hsp70 plasma membrane localization is enabled by the glycosphingolipid Gb3.
PLoS ONE 3 (4): e1925, 2008.

Gonzales S, Groh V, Spies T.
Immunobiology of human NKG2D and its ligands.
Curr. Top. Microbiol. Immunol. 298: 121-138, 2006.

Groh V, Bahram S, Bauer S, Herman A, Beauchamp M, Spies T.
Cell stress-regulated human major histocompatibility complex class I gene expressed in gastrointestinal epithelium.
Proc. Natl. Acad. Sci. USA, Immunology 93 (22): 12445-12450, 1996.

Groh V, Steinle A; Bauer S, Spies T.
Recognition of stress-induced MHC molecules by intestinal epithelial γδ T cells.
Science 279: 1737-1740, 1998.

Groh V, Wu J, Yee C, Spies T.
Tumour-derived soluble MIC ligands impair expression of NKG2D and T-cell activation.
Nature 419: 734-738, 2002.

Gross C, Hansch D, Gastpar R, Multhoff G.
Interaction of heat shock protein 70 peptide with NK cells involves the NK receptor CD94.
Biol. Chem. 384 (2): 267-279, 2003.

Gross C, Koelch W, De Maio A, Arispe N, Multhoff G.
Cell surface-bound heat shock protein 70 (Hsp70) mediates perforin-independent apoptosis by specific binding and uptake of granzyme B.
J. Biol. Chem. 278 (42): 41173-41181, 2003.

Gross C, Schmidt-Wolf IGH, Nagaraj S, Gastpar R, Ellwart J, Kunz-Schughart LAK, Multhoff G.
Heat shock protein 70-reactivity is associated with increased cell surface density of CD94/CD56 on primary natural killer cells.
Cell Stress Chaperones 8 (4): 348-360, 2003.

Hantschel M, Pfister K, Jordan A, Scholz R, Andreesen R, Schmitz G, Schmetzer H, Hiddemann W, Multhoff G.
Hsp70 plasma membrane expression on primary tumor biopsy material and bone marrow of leukemic patients.
Cell Stress Chaperones 5 (5): 438–442, 2000.

Houchins JP, Lanier LL, Niemi EC, Phillips JH, Ryan JC.
Natural killer cell cytolytic activity is inhibited by NKG2-A and activated by NKG2-C.
J. Immunol. 158 (8): 3603-3609, 1997.

Kitayama J, Tsuno N, Yasuhara H, Nagawa H, Kimura W, Kuroda A, Shibata Y, Juji T, Muto T.
Lysis of endothelial cells by autologous lymphokine-activated killer cells.
Cancer Immunol. Immunother. 38 (5): 317-322, 1994.

Kleinjung T, Arndt O, Feldmann HJ, Bockmühl U, Gehrmann M, Zilch T, Pfister K, Schönberger J, Marienhagen J, Eilles C, Rossbacher L, Multhoff G.
Heat shock protein 70 (Hsp70) membrane expression on head-and-neck cancer biopsy – a target for natural killer (NK) cells.
Int. J. Radiation Oncology Biol. Phys. 57 (3): 820–826, 2003.

Kotasek D, Vercellotti GM, Ochoa AC, Bach FH, White JG, Jacob HS.
Mechanism of cultured endothelial injury induced by lymphokine-activated killer cells.
Cancer Res. 48 (19): 5528-5532, 1988.

Kubin M, Cassiano L, Chalupny J, Chin W, Fanslow DCW, Müllberg J, Rousseau AM, Ulrich D, Armitage R.
ULBP1, 2, 3: novel MHC class I-related molecules that bind to human cytomegalovirus glycoprotein UL16, activate NK cells.
Eur. J. Immunol. 31 (5): 1428-1437, 2001.

Lanier LL.
NK cell receptors.
Annu. Rev. Immunol. 16: 359–393, 1998 a.

Lanier LL.
Activating and inhibitory NK cell receptors.
Adv. Exp. Med. Biol. 452: 13-18, 1998 b.

Lanier LL.
NK cell recognition.
Annu. Rev. Immunol. 23: 225–274, 2005.

Lawson C, Wolf S.
ICAM-1 signaling in endothelial cells.
Pharmacol. Rep. 61 (1): 22-32, 2009.

Lee N, Llano M, Carretero M, Ishitani A, Navarro F, López-Botet M, Geraghty DE.
HLA-E is a major ligand for the natural killer inhibitory receptor CD94/NKG2A.
Proc. Natl. Acad. Sci. USA, Immunology 95 (9): 5199-5204, 1998.

Lidington EA, Moyes DL, McCormack AM, Rose ML.
A comparison of primary endothelial cells and endothelial cell lines for studies of immune interactions.
Transpl. Immunol. 7 (4): 239-246, 1999.

López-Botet M, Bellón T, Llano M, Navarro F, García P, de Miguel M.
Paired inhibitory and triggering NK cell receptors for HLA class I molecules.
Hum. Immunol. 61: 7-17, 2000.

Luu NT, Rahman M, Stone PC, Rainger GE, Nash GB.
Responses of endothelial cells from different vessels to inflammatory cytokines and shear stress: evidence for the pliability of endothelial phenotype.
J. Vasc. Res. 47 (5): 451-461, 2010.

Maio M, Del Vecchio L.
Expression and functional role of CD54/Intercellular Adhesion Molecule-1 (ICAM-1) on human blood cells.
Leuk. Lymphoma 8 (1-2): 23-33, 1992.

Marin R, Ruiz-Cabello F, Pedrinaci S, Méndez R, Jiménez P, Geraghty DE, Garrido F.
Analysis of HLA-E expression in human tumors.
Immunogenetics 54: 767-775, 2003.

McQueen KL, Parham P.
Variable receptors controlling activation and inhibition of NK cells.
Curr. Opin. Immunol. 14 (5): 615–621, 2002.

Milani V, Stangl S, Issels R, Gehrmann M, Wagner B, Hube K, Mayr D, Hiddemann W, Molls M, Multhoff G.
Anti-tumor activity of patient-derived NK cells after cell-based immunotherapy- a case report.
J. Transl. Med. 7: 50, 2009.

Miltenburg AMM, Meijer-Paape ME, Daha MR, Paul LC.
Endothelial cell lysis induced by lymphokine-activated human peripheral blood mononuclear cells.
Eur. J. Immunol. 17: 1383-1386, 1987.

Moretta A, Bottino C, Vitale M, Pende D, Cantoni C, Mingari MC, Biassoni R, Moretta L.
Activating receptors and coreceptors involved in human natural killer cell-mediated cytolysis.
Annu. Rev. Immunol. 19: 197-223, 2001.

Multhoff G, Botzler C, Wiesnet M, Eissner G, lssels R.
$CD3^-$ large granular lymphocytes recognize a heat-inducible immunogenic determinant associated with the 72-kD heat shock protein on human sarcoma cells.
Blood 86 (4): 1374-1382, 1995.

Multhoff G, Botzler C, Jennen L, Schmidt J, Ellwart J, Issels R.
Heat shock protein 72 on tumor cells. A recognition structure for natural killer cells.
J. Immunol. 158 (9): 4341-4350, 1997.

Multhoff G, Mizzen L, Winchester CC, Milner CM, Wenk S, Eissner G, Kampinga HH, Laumbacher B, Johnson J.
Heat shock protein 70 (Hsp70) stimulates proliferation and cytolytic activity of natural killer cells.
Exp. Hematol. 27 (11): 1627–1636, 1999.

Multhoff G, Pfister K, Botzler C, Jordan A, Scholz R, Schmetzler H, Burgstahler R, Hiddemann W.
Adoptive transfer of human natural killer cells in mice with severe combined immunodeficiency inhibits growth of Hsp70-expressing tumors.
Int. J. Cancer 88 (5): 791-797, 2000.

Multhoff G, Pfister K, Gehrmann M, Hantschel M, Gross C, Hafner M, Hiddemann W.
A 14-mer Hsp70 peptide stimulates natural killer (NK) cell activity.
Cell Stress Chaperones 6 (4): 337-344, 2001.

Multhoff G.
Heat shock protein 70 (Hsp70): Membrane location, export and immunological relevance.
Methods 43 (3): 229-237, 2007.

Nerem RM.
Shear force and its effect on cell structure and function.
ASGSB Bull. 4 (2): 87-94, 1991.

Pende D, Rivera P, Marcenaro S, Chang CC, Biassoni R, Conte R, Kubin M, Cosman D, Ferrone S, Moretta L, Moretta A.
Major histocompatibility complex class I-related chain A and UL16-binding protein expression on tumor cell lines of different histotypes: analysis of tumor susceptibility to NKG2D-dependent natural killer cell cytotoxicity.
Cancer Res. 62 (21): 6178-6186, 2002.

Radons J, Stangl S, Multhoff G.
NK cell-based immunotherapies against tumors.
Central Eur. J. Med. 1(3): 179–204, 2006.

Raulet DH.
Roles of the NKG2D immunoreceptor and its ligands.
Nat. Rev. Immunol. 3: 781-790, 2003.

Resnick N, Yahav H, Shay-Salit A, Shushy M, Schubert S, Zilberman LCM, Wofovitz E.
Fluid shear stress and the vascular endothelium: for better and for worse.
Prog. Biophys. Mol. Biol. 81 (3): 177-199, 2003.

Rödel F, Frey B, Capalbo G, Gaipl U, Keilholz L, Voll R, Hildebrandt G, Rödel C.
Discontinuous induction of X-linked inhibitor of apoptosis in EA.hy.926 endothelial cells is linked to NF-kappaB activation and mediates the anti-inflammatory properties of low-dose ionizing-radiation.
Radiother. Oncol. 97 (2): 346-351, 2010.

Schmitt E, Gehrmann M, Brunet M, Multhoff G, Garrido C.
Intracellular and extracellular functions of heat shock proteins: repercussions in cancer therapy.
J. Leukoc. Biol. 81 (1): 15-27, 2007.

Schrambach S, Ardizzone M, Leymarie V, Sibilia J, Bahram S.
In vivo expression pattern of MICA and MICB and its relevance to auto-immunity and cancer.
PLos One 2(6): e518, 2007.

Schultz-Hector S, Trott KR.
Radiation-induced cardiovascular diseases: is the epidemiologic evidence compatible with the radiobiologic data?
Int. J. Radiation Oncology Biol. Phys. 67(1): 10-18, 2007.

Screpanti V, Wallin RPA, Ljunggren HG, Grandien A.
A central role for death receptor-mediated apoptosis in the rejection of tumors by NK cells.
J. Immunol. 167 (4): 2068-2073, 2001.

Shafer-Weaver K, Sayers T, Strobl S, Derby E, Ulderich T, Baseler M, Malyguine A.
The Granzyme B ELISPOT assay: an alternative to the ^{51}Cr-release assay for monitoring cell-mediated cytotoxicity.
J. Transl. Med. 1: 14, 2003.

Sprague B, Chesler NC, Magness RR.
Shear stress regulation of nitric oxide production in uterine and placental artery endothelial cells: experimental studies and hemodynamic models of shear stresses on endothelial cells.
Int. J. Dev. Biol. 54 (2-3): 331-339, 2010.

Springer TA.
Traffic signals for lymphocyte recirculation and leukocyte emigration: the multistep paradigm.
Cell. 76 (2): 301-314, 1994.

Stangl S, Wortmann A, Guertler U, Multhoff G.
Control of metastasized pancreatic carcinomas in SCID/beige mice with human IL-2/TKD-activated NK cells.
Immunol. 176: 6270-6276, 2006.

Stangl S, Gross C, Pockley AG, Asea AA, Multhoff G.
Influence of Hsp70 and HLA-E on the killing of leukemic blasts by cytokine/Hsp70 peptide-activated human natural killer (NK) cells.
Cell Stress Chaperones 13 (2): 221-230, 2008.

Steinle A, Li P, Morris DL, Groh V, Lanier LL, Strong RK, Spies T.
Interactions of human NKG2D with its ligands MICA, MICB, and homologs of the mouse RAE-1 protein family.
Immunogenetics 53 (4): 279-287, 2001.

Stephens HAF.
MICA and MICB genes: can the enigma of their polymorphism be resolved?
Trends Immunol. 22 (7): 378-385, 2001.

Sun JC, Lanier LL.
Natural killer cells remember: An evolutionary bridge between innate and adaptive immunity?
Eur. J. Immunol. 39 (8): 2059-2064, 2009.

Sutherland CL, Chalupny NJ, Cosman D.
The UL16-binding proteins, a novel family of MHC class I-related ligands for NKG2D, activate natural killer cell functions.
Immunol. Rev. 181: 185–192, 2001.

Sutherland CL, Chalupny NJ, Schooley K, VandenBos T, Kubin M, Cosman D.
UL16-binding proteins, novel MHC class I-related proteins, bind to NKG2D and activate multiple signaling pathways in primary NK cells.
J. Immunol. 168 (2): 671-679, 2002.

Thornhill MH, Li J, Haskard DO.
Leucocyte endothelial cell adhesion: a study comparing human umbilical vein endothelial cells and the endothelial cell line EA-hy-926.
Scand. J. Immunol. 38 (3): 279-286, 1993.

Trapani JA, Davis J, Sutton VR, Smyth MJ.
Proapoptotic functions of cytotoxic lymphocyte granule constituents in vitro and in vivo.
Curr. Opin. Immunol. 12 (3): 323–329, 2000.

Trinchieri G.
Biology of natural killer cells.
Adv. Immunol. 47: 187-376, 1989.

Ulbrecht M, Honka T; Person S, Johnson JP, Weiss EH.
The HLA-E gene encodes two differentially regulated transcripts and a cell surface protein.
J. Immunol. 149: 2945-2953, 1992.

Valés-Gómez M, Reyburn HT, Erskine RA, López-Botet M, Strominger JL.
Kinetics and peptide dependency of the binding of the inhibitory NK receptor CD94/NKG2-A and the activating receptor CD94/NKG2-C to HLA-E.
EMBO J. 18 (15): 4250-4260, 1999.

Verdier C, Couzon C, Duperray A, Singh P.
Modeling cell interactions under flow.
J. Math. Biol. 58 (1-2): 235-259, 2009.

Vivier E, Tomasello E, Paul P.
Lymphocyte activation via NKG2D: towards a new paradigm in immune recognition?
Curr. Opin. Immunol. 14 (3): 306-311, 2002.

Vivier E, Nunès JA, Vély F.
Natural killer cell signaling pathways.
Science 306: 1517-1519, 2004.

Weiss EH, Lilienfeld BG, Müller S, Müller E, Herbach N, Keler B, Wanke R, Schwinzer R, Seebach JD, Wolf E, Brem G.
HLA-E/human [beta]2-microglobulin transgenic pigs: protection against xenogeneic human anti-pig natural killer cell cytotoxicity.
Transplantation 87(1): 35-43, 2009.

Westgaard IH, Dissen E, Torgersen KM, Lazetic S, Lanier LL, Phillips JH, Fossum S.
The lectin-like receptor KLRE1 inhibits natural killer cell cytotoxicity.
J. Exp. Med. 197: 1551-1561, 2003.

Xu Y, Swerlick RA, Sepp N, Bosse D, Ades EW, Lawley TJ.
Characterization of expression and modulation of cell adhesion molecules on an immortalized human dermal microvascular endothelial cell line (HMEC-1).
J. Invest. Dermatol. 102 (6): 833-837, 1994.

Young EWK, Simmons CA.
Macro- and microscale fluid flow system for endothelial cell biology.
Lab Chip 10 (2): 143-160, 2010.

Zwirner NW, Fernández-Vina M, Stastny P.
MICA, a new polymorphic HLA-related antigen, is expressed mainly by keratinocytes, endothelial cells, and monocytes.
Immunogenetics 47 (2): 139-148, 1998.

Zwirner NW, Dole K, Stastny P.
Differential surface expression of MICA by endothelial cells, fibroblasts, keratinocytes, and monocytes.
Hum. Immunol. 60 (4): 323–330, 1999.

7 Acknowledgements

First of all, I owe my deepest gratitude to Prof. Dr. Gabriele Multhoff for providing me with this very interesting and fascinating topic for my thesis. Her enthusiastic discussions and constructive supports were always very helpful. Furthermore, I would like to thank her for encouraging and giving me the opportunity to publish my work.

I also want to thank Prof. Dr. Michael Molls for giving me the opportunity to perform my work in his Department of Radiotherapy and Radiooncology, Technische Universität München, Klinikum rechts der Isar.

I would like to show my gratitude to all members of the laboratory of Experimental Radiooncology/Radiobiology, especially to Dr. Mathias Gehrmann who took always the time to answer my questions and who introduced me into fluorescence microscopy and flow cytometry techniques. Furthermore, I would like to thank Stefan Stangl and Wolfgang Sievert for many helpful discussions. I am indebted to all of my colleagues to have the patience to avoid movements and temperature changes in the room in which my experiments were filmed under the microscope.

My thanks also to ibidi (Martinsried, Germany) for supporting me with latest updates of the flow system.

Last but not least I am very grateful to my family for its belief in me and its helpful suggestions.

Do 18. Juni, 15:30 Uhr

The human microvascular endothelial cell line HMEC presents activatory NK ligands

Authors: **Isabelle Riederer, Gabriele Multhoff**

Summary:

Endothelial cells are involved in many aspects of vascular biology. Dysfunctions are responsible for numerous diseases of the microvasculare system. For our assays we used dermal human microvascular endothelial cells (HMECs) which have been transfected with a PBR-322-based plasmid.

Although immortalized this cell line shows morphological and functional characteristics of primary endothelial cells such as a positive factor VIII and CD31 staining. The ibidi-system was used to maintain a continuous flow in the µ-Slide which contains the HMECs. This system mimicks blood flow in vessels and therefore endothelial cells can be examined under physiological conditions. We established cell culture kinetics under continuous flow with defined shear stress and performed long-term microscopic analysis over a period of 72 h. Our observation was that the HMECs appear more confluent in the flow system compared to negative control cells which were cultured without flow. This system also provides the possibility to study lymphocyte rolling and adhesion.

We examined cell surface markers on HMECs by flow cytometry which affect interaction with NK cells. HMECs present a variety of markers such as ULBP-1,2,3, MIC-A/B, Hsp70 on their cell surface which act as potential activatory ligands for NK cells. HLA-E, a negative regulatory ligand for NK cells was also found on HMECs. Functionally, a significant kill was observed after co-incubation of HMECs with TKD/IL-2-activated NK cells but not with unstimulated NK cells.

In conclusion we studied the phenotype of HMECs and correlated it with its lysability by NK cells.

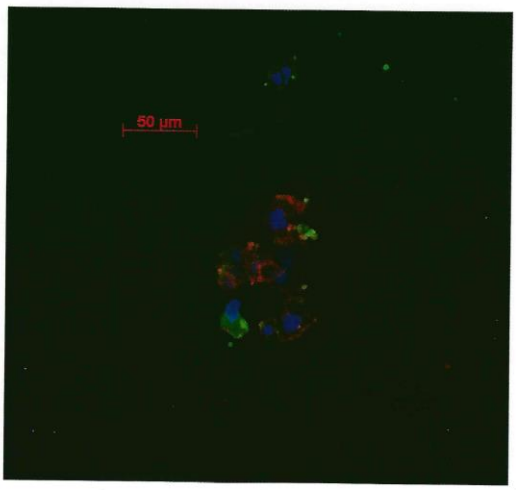

Quelle: Isabelle Riederer

Staining of HMECs with CD31-PE, Hsp70-FITC and nucleus (DAPI)

P6.09

Effects of irradiation on endothelial cells and interaction with the immune system

Gabriele Multhoff[1], Isabelle Riederer[1], Nikolaus Andratschke[1]

[1]Klinikum rechts der Isar, TU München Strahlentherapie

Endothelial cells are highly sensitive towards irradiation and also play key roles in tumorigenesis. Experimental findings suggest that radiation-induced focal decrease of the capillary density is an underlying cause of numerous diseases including myocardial failure.
For our assays we used dermal human microvascular endothelial cells (HMECs) as a model cell system. Although HMECs were immortalized by transfection they show morphological and functional characteristics of primary endothelial cells such as a positive factor VIII and a CD31 staining.
The ibidi-system was used to maintain a continuous flow in the µ-Slide which contains the HMECs. This system mimicks blood flow in vessels and therefore endothelial cells can be examined under physiological conditions. We established cell culture kinetics under continuous flow with defined shear stress and performed long-term microscopic analysis over a period of 72 h. Our observation was that the HMECs appear more confluent in the flow system compared to negative control cells which were cultured without flow. This system also provides the possibility to study lymphocyte rolling and adhesion.
We examined cell surface markers on HMECs by flow cytometry which affect interaction with NK cells. HMECs present a variety of markers such as ULBP-1,2,3, MIC-A/B, Hsp70 on their cell surface which act as potential activatory ligands for NK cells. HLA-E, a negative regulatory ligand for NK cells was also found on HMECs. Functionally, a significant kill was observed after co-incubation of HMECs with TKD/IL-2-activated NK cells but not with unstimulated NK cells.
In conclusion we studied the phenotype of HMECs and correlated it with its lysability by NK cells.

Effects of irradiation on endothelial cells and interaction with the immune system

[1]Isabelle Riederer, [1]Michael Molls, [1,2]Gabriele Multhoff

[1] Department of Radiotherapy and Radiooncology, Technische Universität München, Klinikum rechts der Isar and

[2] Helmholtz Center Munich, German Research Center for Environmental Health – Institute for Pathology, Munich, Germany

HelmholtzZentrum münchen
German Research Center for Environmental Health

Abstract

Endothelial cells are highly sensitive towards irradiation and also play key roles in tumorigenesis. Experimental findings suggest that radiation-induced focal decrease of the capillary density is an underlying cause of numerous diseases including myocardial failure.

For our assays we used dermal human microvascular endothelial cells (HMECs) as a model cell system. Although HMECs were immortalized by transfection they show morphological and functional characteristics of primary endothelial cells such as a positive factor VIII and a CD31 staining.

The ibidi-system was used to maintain a continuous flow in the µ-Slide which contains the HMECs. This system mimicks blood flow in vessels and therefore endothelial cells can be examined under physiological conditions. We established cell culture kinetics under continuous flow with defined shear stress and performed long-term microscopic analysis over a period of 72h. Our observation was that the HMECs appear more confluent in the flow system compared to negative control cells which were cultured without flow. This system also provides the possibility to study lymphocyte rolling and adhesion. We examined cell surface markers on HMECs by flow cytometry which affect interaction with NK cells. HMECs present a variety of markers such as ULBP-1,2,3, MIC-A/B, Hsp70 on their cell surface which act as potential activatory ligands for NK cells. HLA-E, a negative regulatory ligand for NK cells, was also found on HMECs. Functionally, a significant kill was observed after co-incubation of HMECs with TKD/ IL-2-actived NK cells but not with unstimulated NK cells.

In conclusion we studied the phenotype of HMECs and correlated it with its lysability by NK cells.

Aims

NK cell - HMEC interaction

Methods

Cell culture: The human microvascular endothelial cell line HMEC was cultured in MCDB 131 medium supplemented with EGF and hydrocortisol, 15% FCS.

Flow cytometry: Flow cytometry was performed with the fluorescence-labeled Abs directed against Hsp70 (cmHsp70.1), Gb3 (CD77), HLA-E, MICA/B and ULBP1-3.

NK cell stimulation: Human NK cells were stimulated with Hsp70 peptide TKD plus low dose IL-2 (100 IU/ml) for 4 days.

ELISPOT assay: Cytotoxicity against HMECs was measured by a standard granzyme B ELISPOT assay.

Flow system: Flow conditions were performed by using the ibidi-System. So the HMECs could be examined under nearly physiological conditions.

Irradiation: 24h after cell passaging HMECs were irradiated at 4 Gy. After a recovery period of 12h, cells were phenotypically characterized by flow cytometry.

Conclusion

- HMECs are targets for stimulated NK cells
- MIC-B acts as an activatory ligand for stimulated NK cells
- An up-regulated HLA-E density protects HMECs from killing by NK cells

Acknowledgments

This work was supported by grants from the DFG (MU1238 7/2 to G.M.), the BMBF (BioChance plus, 0313686A to G.M.), EU (TRANSNET 512253; STEMDIAGNOSTICS LSHB CT 2007 037703; CARDIORISK 211404 to G.M.), and by multimmune GmbH.

Results

HMECs are positive for factor VIII and CD31

HMEC: Human Microvascular Endothelial Cell line, transfected with a PBR-322 based plasmid.
HMECs are immortalized cells which show morphological and functional characteristics of primary ECs.

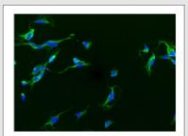

staining of HMECs with factor VIII (green) and DAPI (blue, nucleus)

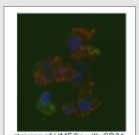

staining of HMECs with CD31-PE (red), Hsp70-FITC (green) and DAPI (blue)

Adherence and morphology of HMECs under flow

directly after seeding (0h)

60h after seeding without flow

20h after seeding plus 40h under flow

Activatory and inhibitory NK ligands on HMECs

Activatory markers:
MIC A/B
ULBP-1,2,3
Hsp70 (cmHsp70.1)

Inhibitory markers:
HLA -E

Hsp70 anchorage.
Globoyltriaosylceramide, Gb3 (CD77)

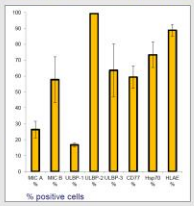

% positive cells

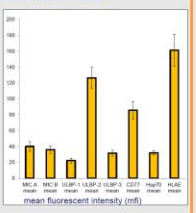

mean fluorescent intensity (mfi)

Interaction of NK cells with HMECs

visible light

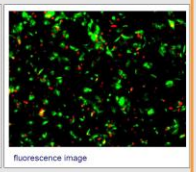

fluorescence image

Big adherent cells are HMECs (PKH67, green) and small round cells are NK cells (PKH26, red). Both photographs are taken 20h after co-incubation. NK cells are predominantly found in close proximity to the HMECs.

NK cells preferentially kill MIC-B positive HMECs

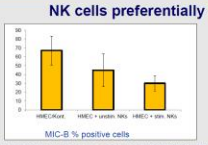

MIC-B % positive cells

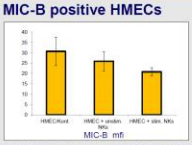

MIC-B mfi

Flow cytometry analysis was performed with HMECs without contact to NK cells as a control, with HMEC 24h after co-incubation with unstimulated NK cells and stimulated NK cells. NK cells attack especially MIC-B positive HMECs.

HLA-E is upregulated on HMECs after contact with NK cells

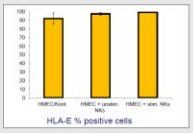

HLA-E % positive cells

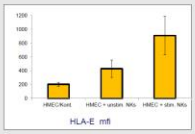

HLA-E mfi

24h after co-incubation of HMECs with NK cells (unstimulated, stimulated) the expression density of HLA -E is upregulated.

Granzyme B ELISPOT assay using unstimulated and stimulated NK cells

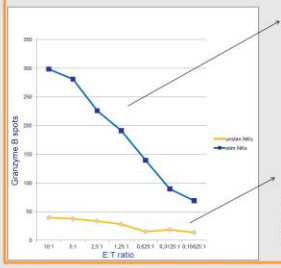

HMECs with stimulated NK cells 6h after co-incubation. Several NK cells attack one HMEC and build cell aggregates.

HMECs with unstimulated NK cells 6h after co-incubation. No cell aggregates are visible.

Radiation induced immunmodulation on HMECs

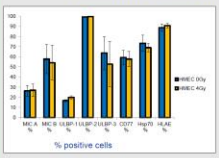

% positive cells

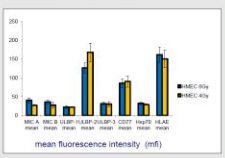

mean fluorescence intensity (mfi)

Irradiation at 4 Gy induces no significant changes in the expression of NK ligands on HMECs.

Granzyme B ELISPOT assay with stimulated NK cells against HMECs (0 Gy vs 4 Gy)

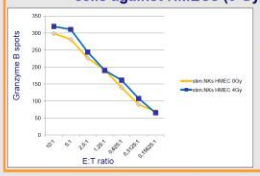

Irradiation of HMECs (4 Gy) does not significantly affect killing by stimulated NK cells.

OPEN ACCESS Freely available online

PLoS one

Irradiation-Induced Up-Regulation of HLA-E on Macrovascular Endothelial Cells Confers Protection against Killing by Activated Natural Killer Cells

Isabelle Riederer[1,2], Wolfgang Sievert[1,2], Günther Eissner[3], Michael Molls[1,2], Gabriele Multhoff[1,2]*

1 Department of Radiation Oncology, Klinikum rechts der Isar, Technische Universität München, Munich, Germany, **2** Clinical Cooperation Group (CCG) "Innate Immunity in Tumor Biology", Helmholtz Zentrum München, Munich, Germany, **3** Department of Cardiac Surgery, Klinikum der Universität München, Munich, Germany

Abstract

Background: Apart from the platelet/endothelial cell adhesion molecule 1 (PECAM-1, CD31), endoglin (CD105) and a positive factor VIII-related antigen staining, human primary and immortalized macro- and microvascular endothelial cells (ECs) differ in their cell surface expression of activating and inhibitory ligands for natural killer (NK) cells. Here we comparatively study the effects of irradiation on the phenotype of ECs and their interaction with resting and activated NK cells.

Methodology/Principal Findings: Primary macrovascular human umbilical vein endothelial cells (HUVECs) only express UL16 binding protein 2 (ULBP2) and the major histocompatibility complex (MHC) class I chain-related protein MIC-A (MIC-A) as activating signals for NK cells, whereas the corresponding immortalized EA.hy926 EC cell line additionally present ULBP3, membrane heat shock protein 70 (Hsp70), intercellular adhesion molecule ICAM-1 (CD54) and HLA-E. Apart from MIC-B, the immortalized human microvascular endothelial cell line HMEC, resembles the phenotype of EA.hy926. Surprisingly, primary HUVECs are more sensitive to Hsp70 peptide (TKD) plus IL-2 (TKD/IL-2)-activated NK cells than their immortalized EC counterpatrs. This finding is most likely due to the absence of the inhibitory ligand HLA-E, since the activating ligands are shared among the ECs. The co-culture of HUVECs with activated NK cells induces ICAM-1 (CD54) and HLA-E expression on the former which drops to the initial low levels (below 5%) when NK cells are removed. Sublethal irradiation of HUVECs induces similar but less pronounced effects on HUVECs. Along with these findings, irradiation also induces HLA-E expression on macrovascular ECs and this correlates with an increased resistance to killing by activated NK cells. Irradiation had no effect on HLA-E expression on microvascular ECs and the sensitivity of these cells to NK cells remained unaffected.

Conclusion/Significance: These data emphasize that an irradiation-induced, transient up-regulation of HLA-E on macrovascular ECs might confer protection against NK cell-mediated vascular injury.

Citation: Riederer I, Sievert W, Eissner G, Molls M, Multhoff G (2010) Irradiation-Induced Up-Regulation of HLA-E on Macrovascular Endothelial Cells Confers Protection against Killing by Activated Natural Killer Cells. PLoS ONE 5(12): e15339. doi:10.1371/journal.pone.0015339

Editor: Nils Cordes, Dresden University of Technology, Germany

Received August 20, 2010; **Accepted** November 9, 2010; **Published** December 16, 2010

Funding: The funders are EU-CARDIORISK (FP7-211403), DFG (SFB824/1), BMBDF-MOBITUM (01EZ0826), BMBF Kompetenzverbund Strahlenforschung (03NUK007E) and multimmune GmbH. The funders had no role in study design, data collection and analysis, decision to publish, or preparation of the manuscript. There are no current external sources for this study.

Competing Interests: The authors have declared that no competing interests exist.

* E-mail: gabriele.multhoff@lrz.tu-muenchen.de

Introduction

The endothelial cell (EC) monolayer which lines blood vessels performs multiple tasks including the regulation of tissue fluid homeostasis and blood cell transmigration. The interaction of ECs with leukocytes, such as activated NK cells, involves attachment and rolling which are predominantly mediated by selectins and carbohydrate-rich ligands, such as mucins [1–3]. Lymphocyte rolling might induce activation and facilitate the tight adhesion to ECs which is enabled by the integrin family of cell adhesion molecules [4]. The ligation, migration and extravasation of lymphocytes into the tissue has been postulated to be mediated by PECAM-1 (CD31) and involves the activation of integrins such as α4/β1 (VLA-4) [4,5], α4/β7 [5,6], α4/β2 (LFA-1, CD11a/CD18) [5–7], and αM/β2 (CR3, Mac-1, CD11b/CD18a) [7].

NK cells play pivotal roles in the early defence against viral infections and malignant transformations [8–10]. The functionality of NK cells is regulated by interactions of inhibitory and activating receptors [11,12] which belong either to the immunoglobulin (Ig)-like (KIR), Ig-like transcript (ILT), C-type lectin or natural cytotoxicity group, with the signals being derived from the target cell ligands [13]. Inhibitory receptors with specificity for classical and non-classical MHC class I molecules mediate protection for the target cells. HLA-E, a prominent member of the non-classical MHC (MHC class Ib), which is recognized by CD94/NKG2A (inhibitory) and CD94/NKG2C (activating) expressing NK cells, is characterized by a limited polymorphism and a tissue-specific and inducible expression pattern [14,15]. According to the "missing-self" theory [16], the partial or complete loss of MHC antigens can also render target cells susceptible to NK cells. The mechanism of killing by NK cells involves exocytosis of cytolytic granules containing apoptotic enzymes, such as granzymes and perforins and death receptor ligands such as Fas/Fas-ligand [17–24]. Our group has identified a

membrane form Hsp70 on tumor cells [25] as a tumor-specific recognition structure for a perforin-independent, granzyme B-mediated attack by allogeneic and autologous NK cells that have been pre-stimulated with Hsp70 peptide TKD plus low dose IL-2 [26,27].

Activated NK cells have been found to bind to the microvasculature of metastases [28] and to play a crucial role in the control of tumor angiogenesis [29,30]. In this context, we were interested to study the interactions of TKD/IL-2- stimulated NK cells with macro- and microvascular primary and immortalized ECs. An NK cell based phase I clinical study [31] which used *ex vivo* TKD/IL-2-activated NK cells to treat patients with colorectal and non-small cell lung (NSCLC) carcinoma has shown promising results with respect to the feasibility and safety of the procedure and its ability to enhance the capacity of patient-derived NK cells to kill membrane $Hsp70^+$ tumor cells *in vitro*. The goal of a subsequent proof-of-concept phase II clinical trial is to analyze the efficacy of TKD/IL-2-activated NK cells in NSCLC patients following radiochemotherapy as this has been shown to enhance the density of Hsp70 membrane expression on tumor cells (unpublished observations). Therefore, we were interested to study the surface expression of activating and inhibitory ligands on primary and immortalized macro- and microvascular ECs before and after irradiation.

Immortalized EC lines present Hsp70 on their plasma membrane and thus reflect a tumorigenic phenotype. The expression of ligands such as ULBP1-3 [32], MIC-A/-B, Hsp70, and HLA-E and the membrane-bound [33] form of the intercellular adhesion molecule ICAM-1 (CD54) was then correlated with the NK cell mediated cytotoxicity. Our findings suggest that HLA-E is a key player in the regulation of NK cell mediated killing of ECs. A movie showing the interaction of TKD/IL-2-activated NK cells and ECs indicates that a bulk of NK cells actively migrates towards ECs. Next, we studied the effects of ionizing irradiation on the expression of cell surface markers which might affect the killing activity of NK cells. We could demonstrate that an irradiation at 4 Gy results in a significantly up-regulated expression density of HLA-E on primary (HUVEC) and immortalized macrosvascular (EA.hy926) ECs, but not on immortalized microvascular HMEC. Despite a minor irradiation-induced increase in activating ligands, the significant increase in the HLA-E expression on macrovascular ECs led to a reduced lysis of HUVECs and EA.hy926 cells. The HLA-E expression density on the immortalized microvascular cell line HMEC did not change significantly by irradiation and thus the lysis remained unaltered.

Results

Comparative Analysis of the Phenotype of Human Primary and Immortalized Macro- and Microvascular ECs

The phenotype of the primary (HUVEC; Figure 1A) [34] and immortalized macro- (EA.hy926; Figure 1B) and immortalized microvascular (HMEC; Figure 1C) endothelial cells was determined by immunofluorescence microscopy and flow cytometry. All three endothelial cell types show a positive staining for the factor VIII-related antigen (Figure 1A–C) and strongly express the endothelial cell associated markers CD31 (platelet/endothelial cell adhesion molecule 1, PECAM-1), [35] and CD105 (endoglin) [36], a component of the TGF-beta 1 receptor complex, which is also involved in vascular remodelling (Table 1). Under shear stress induced by a flow system (IBIDI, Martinsried, Germany) for 12 h (Figure 1D; lower panel), but not under static culture conditions (Figure 1D; upper panel), HUVECs (Figure 1D, left), EA.hy926 cells (Figure 1D, middle) cells and to a lesser extent also HMECs (Figure 1D, right) exhibit the typical cobblestone morphology and a reorientation in line with the dynamic flow.

In contrast to the immortalized ECs, the primary macrovascular human umbilical vein endothelial cells (HUVECs) only present UL16 binding protein 2 (ULBP2), the major histocompatibility complex (MHC) class I chain-related protein MIC-A and classical MHC class I antigens (HLA-A, -B, -C) on their cell surface. A comparative analysis of the expression pattern of MIC-A, ICAM-1 (CD54) and HLA-E expression on ECs under static and flow conditions revealed no significant differences (data not shown).

In comparison to HUVECs, the immortalized EA.hy926 cell line expresses additional markers such as ULBP3, ICAM-1 (CD54) and the human leukocyte antigen E (HLA-E) on their cell membrane. The human microvascular endothelial cell line HMEC was immortalized by a transfection of primary dermal ECs with a PBR322 plasmid containing the coding region for the simian virus 40A gene product, large T antigen. This cell line resembles the phenotype of EA.hy926 cells with the exception that the MIC-A expression is substituted by MIC-B in HMECs. Although a translocation of the major stress-inducible heat shock protein 70 (Hsp70) to the plasma membrane [36,37] is typically associated with a tumorigenic phenotype, since normal cells are membrane $Hsp70^-$, a membrane $Hsp70^+$ phenotype was selectively detectable on immortalized EA.hy926 cells and HMECs using the cmHsp70.1 mAb (multimmune GmbH, Munich, Germany), but not on primary HUVECs. In contrast to the cmHsp70.1 mAb, other commercially available Hsp70-specific antibodies, such as SPA810, do not react with the membrane form of Hsp70 on tumor cells (manuscript submitted) or that on immortalized ECs.

Interaction of EC with Un-Stimulated and Stimulated NK Cells

The enrichment of NK cells was based on a negative selection procedure of peripheral blood mononuclear cells (PBMNCs) using Miltenyi microbeads coupled to anti-CD3 (T cell depletion) and anti-CD19 (B cell depletion) mAbs. Following the negative selection, an adherence step was included to reduce the number of $CD14^+$ monocytes and macrophages. The final population typically contained between 50 and 60% of $CD3^-$ NK cells, which were found to be positive for the neuronal cell adhesion molecule CD56 [38], the low affinity Fc-gamma receptor CD16 and the C-type lectin receptor CD94 (Figure 2). Enriched NK cells were either un-stimulated (Figure 2, grey bars) or were stimulated with Hsp70 peptide TKD plus low dose IL-2 (TKD/IL-2) for 4 days (Figure 2, black bars). Although no significant changes were observed with respect to the percentage of CD16, CD56 and CD94 positive cells, the stimulation with TKD/IL-2 resulted in a significant up-regulation in the expression density (mfi) of these antigens (Figure 2).

Differences in the adhesion of un-stimulated and TKD/IL-2-activated NK cells to HMECs under static conditions using microscopic and immunofluorescence analysis of PKH26GL-labeled NK cells (red fluorescence) and FITC-labeled (green fluorescence) HMECs are illustrated in Figure 3. Following a 4 h co-incubation, the number of ECs in culture wells containing activated NK cells (Figure 3B) was significantly reduced from 73 ± 5 to 37 ± 3 ECs per optical field ($p<0.05$; $n=3$), compared to culture wells containing resting NK cells (Figure 3A). Furthermore, the adhesion of activated NK cells to ECs was dramatically greater than that to resting NK cells. The close interaction of activated NK cells with ECs was confirmed using fluorescence microscopy. The adherence of activated PKH26GL-labeled NK cells (red) to

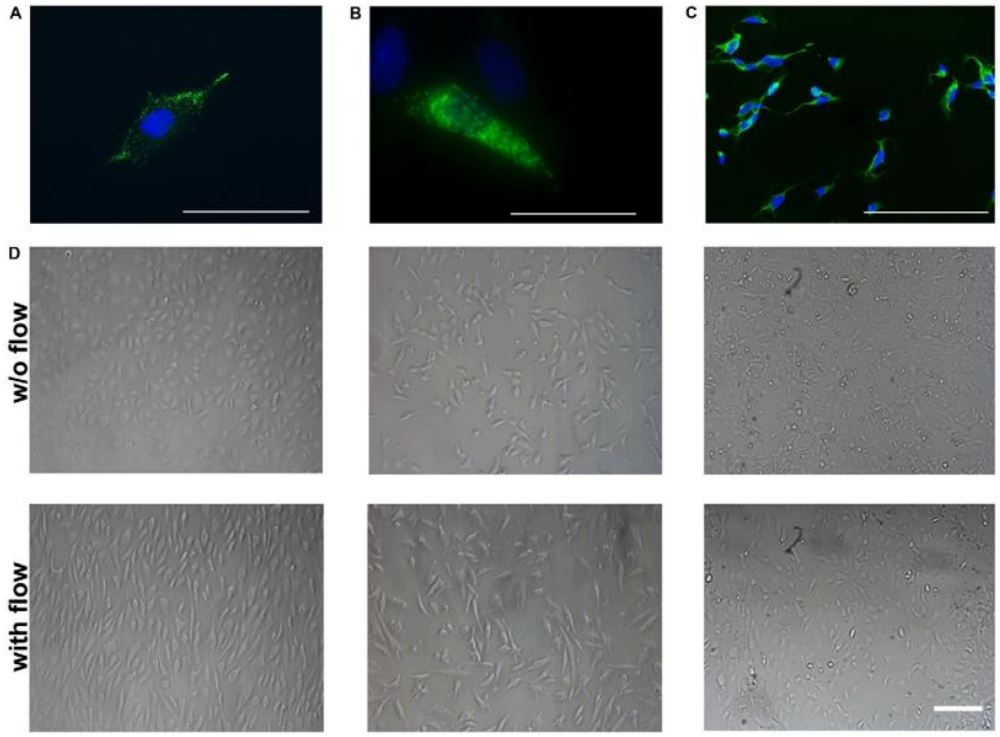

Figure 1. Von Willebrand staining and microscopic analysis of endothelial cells (ECs). Representative immunofluorescence images of primary macrovascular HUVECs (A), immortalized macrovascular EA.hy926 cells (B) and immortalized microvascular HMECs (C) stained for von Willebrand factor (FITC, green spectrum); nucleus is counter-stained with DAPI (blue spectrum); scale bar, 100 µm. (D) Microscopic analysis of HUVECs (left panel), EA.hy926 cells (middle panel) and HMECs (right panel) under static (upper panel) and under flow conditions for 12 h (lower panel), scale bar, 200 µm. Under flow the ECs show the typical cobblestone morphology.
doi:10.1371/journal.pone.0015339.g001

FITC-labeled HMECs (green) was visualized in an orange spectrum (Figure 3D). In contrast, no co-localization was detectable if HMECs were co-cultured for 4 h with resting NK cells (Figure 3C). Movies illustrating the differences in the kinetics of the adherence and the concerted attack of HMECs by TKD/IL-2-stimulated NK cells in comparison to resting NK cells are included in the supplementary information. It appears that activated (video S2 and video S3), but not resting NK cells (video S1), actively migrate towards HMECs and that this interaction results in the detachment and elimination of HMECs.

HLA-E Expression Partially Protects EA.hy926 Cells and HMECs from Lysis by Activated NK Cells

We have previously shown that TKD/IL-2-activated NK cells kill their tumor target cells via a perforin-independent, granzyme B mediated lysis [27]. HUVECs, EA.hy926 cells and HMECs were sensitive to granzyme B mediated apoptosis by TKD/IL-2-activated NK cells (Figure 4A), whereas none of the three ECs were lysed to a significant extent by resting NK cells (data not shown). However, the lysis of primary macrovascular HUVECs by activated NK cells was always considerably greater than that of its corresponding immortalized cell line EA.hy926 and the immortalized microvascular cell line HMEC (Figure 4A/B). This finding was not expected, since the immortalized ECs express ULBP3 and membrane Hsp70, in addition to ULBP1 and MIC-A/-B as activating ligands for TKD/IL-2-stimulated NK cells. We therefore assumed that the increased susceptibility of HUVECs to activated NK cells was most likely due to the absence of the inhibitory ligand HLA-E. A comparison of the lysis of HUVECs and HMECs in a standard ^{51}Cr release assay confirmed the data that were obtained using the granzyme B ELISPOT assay (Figure 4B).

Phenotypic Changes of Cell Surface Markers on ECs after Contact with Activated NK Cells

The proportion of marker positive target cells and the cell surface density of the markers following co-incubation of the ECs with resting and activated NK cells for 12 h were analyzed by flow cytometry in the separately gated cell populations. Apart from MIC-A, ICAM-1 (CD54) and HLA-E, none of the cell surface markers appeared to be affected by the contact with NK cells. The cell surface density of CD31 and CD105, as typical EC-related markers, also remained unchanged (data not shown). As summarized in Figure 5A (left panel), the percentage of MIC-A$^+$

Table 1. Comparative analysis of the expression of activating and inhibitory cell surface markers on primary and immortalized ECs.

	Primary macrovascular	Immortalized	Immortalized microvascular	Expression Pattern
ECs	**HUVEC**	**EA.hy926**	**HMEC**	**HUVEC/ EA.hy926/ HMEC**
Marker	**% (mean fluorescence intensity)**			**++ >70% + >20% − >10%**
CD31	89±4 (89)	96±7 (96)	97± (92)	++/++/++
CD105	97±6 (97)	99±0.1 (99)	99±2 (98)	++/++/++
ULBP1	0±1 (66)	0±0 (46)	4±1 (43)	−/−/−
ULBP2	48±7 (59)	96±2 (63)	98±1 (131)	+/++/++
ULBP3	6±3 (52)	58±11 (52)	51±11 (62)	−/+/+
MIC-A	73±6 (107)	21±4 (46)	8±3 (116)	++/+/−
MIC-B	3±1 (47)	2±1 (25)	36±10 (37)	−/−/+
HLA-E	1±0 (11)	86±3 (162)	83±4 (201)	−/++/++
W6/32	97±2 (48)	98±9 (75)	95±7 (67)	++/++/++
cmHsp70.1	6±4 (12)	58±5 (69)	48±6 (54)	−/+/+
SPA810	2± (51)	1± (91)	2± (44)	−/−/−
CD54	5±2 (88)	13±2 (46)	21±3 (49)	−/+/+

doi:10.1371/journal.pone.0015339.t001

primary HUVECs slightly dropped, as did the proportion of MIC-A^+ in its corresponding immortalized partner cell line EA.hy926. The cell surface density of MIC-A on the surviving cell fraction remained unaltered in HUVECs and EA.hy926 cells (Figure 5A, right panel). The microvascular cell line HMEC, which contains a very low proportion of MIC-A^+ cells showed a decrease in the surface density of this marker (Figure 5A, right panel), and there was also a small reduction in the proportion of MIC-B^+ cells (data not shown). With respect to the intercellular adhesion molecule ICAM-1 (CD54), all three EC types reacted similarly by significantly up-regulating the percentage of cells expressing this adhesion molecule and its cell surface density following contact with activated NK cells (Figure 5B). The most striking difference between the EC types was observed with respect to the expression of HLA-E. After contact with activated NK cells, but not with resting NK cells, the percentage of HLA-E^+ HUVECs increased from below 5% up to nearly 100% within 12 h (Figure 5C). Since the doubling time of HUVECs is slow (24 h), these results suggest that HLA-E is actively up-regulated in primary macrovascular ECs. In contrast, almost all EA.hy926 cells and HMECs initially showed a membrane HLA-E^+ phenotype and contact with activated NK cells only enhanced the density of HLA-E expression (Figure 5C). In contrast to TKD/IL-2-activated NK cells, resting NK cells had no influence on the viability of the ECs, nor did they alter the expression of MIC-A, ICAM-1 (CD54) and HLA-E.

The dramatic up-regulation of ICAM-1 (CD54) and HLA-E on HUVECs was transient, since the levels of these proteins on the cell surface dropped to the very low baseline levels following the removal of activated NK cells (Figure 5D). Similar effects were seen with the increased density of these antigens on the immortalized EC types (data not shown).

An Irradiation-Induced Up-Regulation of HLA-E Decreases Sensitivity to Activated, NKG2A and NKG2C Expressing NK Cells

Exposure to ionizing irradiation (4 Gy) followed by a recovery period of 12 h significantly increased the expression density of HLA-E on primary macrovascular HUVECs (Figure 6A) and also the percentage of HLA-E positive cells (from below 5 up to 27%). Similar effects were observed for the immortalized macrovascular partner cell line EA.hy926 (Figure 6B). Although these effects were similar to those induced by the contact of HUVECs with activated NK cells, they were less pronounced. In contrast, ionizing irradiation had no effect on the expression density of HLA-E on immortalized microvascular HMECs (Figure 6C). None of the other cell surface markers, such as MHC class I, ULBP1-3, MIC-

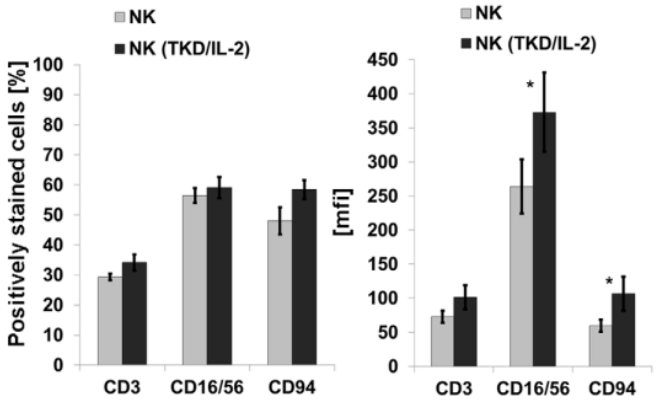

Figure 2. Phenotyping of effector cells. Comparative analysis of T (CD3) and NK (CD16/56, CD94) cell specific markers on NK cell enriched PBMNC preparations with and without stimulation with TKD (2 μg/ml) plus low dose IL-2 (100 IU/ml) for 4 days. Left panel, proportion of marker positively stained cells in %; right panel, mean fluorescence intensity (mfi) values. Mean fluorescence values differing significantly between un-stimulated and stimulated NK cells are marked with *, $p<0.05$.
doi:10.1371/journal.pone.0015339.g002

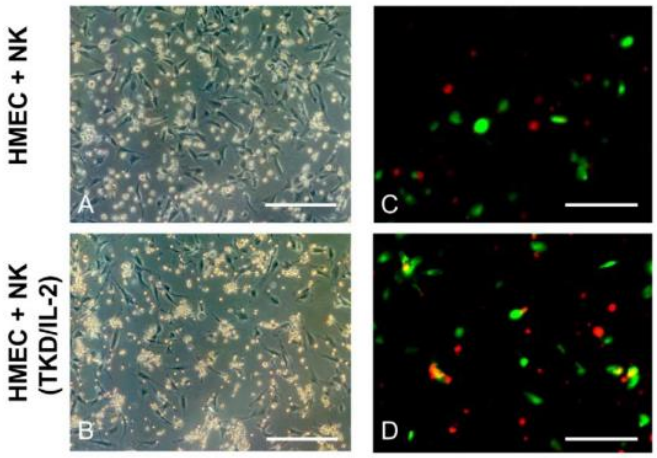

Figure 3. Representative microscopic images of the adherence of TKD/IL-2-activated NK cells to HMECs. A confluent monolayer of HMECs was co-cultured for 4 h either with resting (A) and TKD/IL-2-activated NK cells (B). Pictures were taken using a Zeiss Axiovert 200 inverted fluorescence microscope. The amount of adherent HMECs was drastically reduced after a co-incubation with activated (B) compared to resting NK cells (A). The number of HMECs co-cultured for 4 h with activated NK cells significantly dropped from 73±5 to 37±3 cells, as determined by counting of an optical field ($n = 3$, $p<0.05$). Scale bar, 50 μm. Representative immunofluorescence images of TKD/IL-2-activated NK cells to HMECs. The specific adhesion of activated NK cells, labeled with PKH26GL in red, to HMECs, labeled with FITC in green, is illustrated in orange (D). No co-staining of red and green labels was seen when resting NK cells were used (C). Pictures were taken using a Zeiss Axiovert 200 inverted fluorescence microscope.
doi:10.1371/journal.pone.0015339.g003

A/-B and ICAM-1 (CD54), were found to be altered significantly following irradiation. In line with the increased cell surface expression of HLA-E, the lysis of irradiated HUVECs (Figure 7A) and EA.hy926 cells (Figure 7B) by activated NK cells expressing NKG2A and NKG2C receptors decreased significantly, whereas that of HMECs with an unaltered HLA-E membrane expression remained unaffected (Figure 7C). Un-stimulated NK cells did not affect the lysis of any of the EC types (Figure 7A–C) and also did not change the cell surface marker expression pattern as shown in Figure 5A–C.

Pre-incubation of TKD/IL-2-activated NK cells with NKG2A and NKG2C antibodies and irradiated HUVECs (4Gy) with HLA-E antibodies, demonstrated that the lysis of irradiated HUVECs was significantly enhanced if NK cells had been pre-incubated with the agonistic NKG2C mAb (Figure 8). Furthermore, the blocking of the inhibitory ligand HLA-E on irradiated

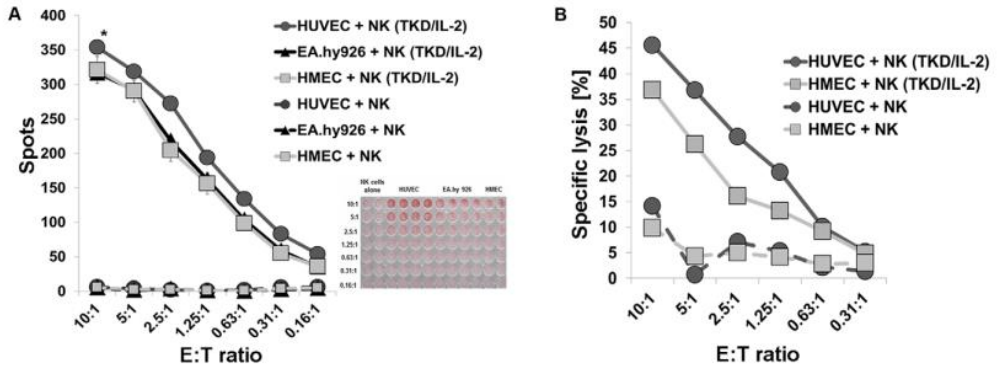

Figure 4. Granzyme B and ^{51}Cr release assay of ECs by resting and activated NK cells. Granzyme B ELISPOT assay (4 h) of resting and TKD/IL-2-activated NK cells attacking HUVECs, EA.hy926 cells and HMECs (A). The effector to target (E:T) ratios ranged between 10:1 to 0.16:1. The data represent mean values of at least 3 independent experiments. The differences in lysis of HUVECs compared to that of EA.hy926 cells and HMECs was significantly different *, $p<0.05$ at all E:T ratios. Standard ^{51}Cr release assay (4 h) comparing the lysis of HUVECs and HMECs by resting and TKD/IL-2-activated NK cells at effector to target ratios ranging from 10:1 to 0.31:1 (B). The data are from one typical experiment, therefore no statistical analysis has been performed.
doi:10.1371/journal.pone.0015339.g004

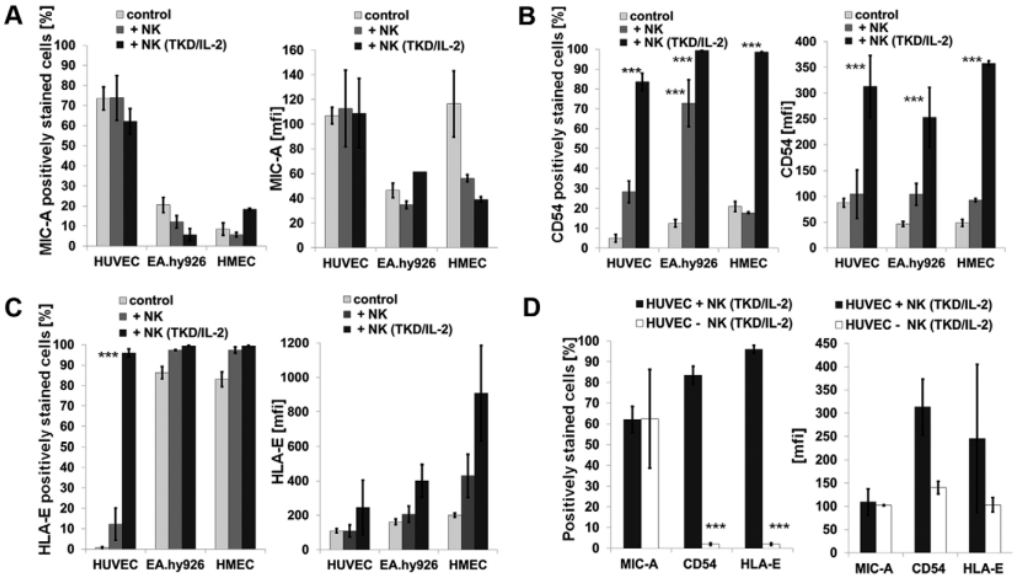

Figure 5. Phenotyping of ECs after contact with resting and activated NK cells. Comparative analysis of the proportion of HUVECs, EA.hy926 cells and HMECs expressing MIC-A (A), CD54 (B) and HLA-E (C) (left panel) and mean fluorescence intensity values of expression (mfi; right panel) in the absence of NK cells (light grey bars) and after a 12 h co-culture with resting (dark grey bars) or TKD/IL-2-activated (black bars) NK cells. Cell surface marker expression was determined by flow cytometry; ECs and NK cell populations were gated separately based on differences in the forward (FSC) and side scatters (SSC). Asterisks mark values significantly different to control values, ***, $p<0.001$, as determined by the Mann-Whitney test using the SPSS software. The expression of the cell surface markers indicated above on HUVECs in the presence of TKD/IL-2-activated NK cells (black bars) and after removal of the NK cells (white bars) was determined by flow cytometry. In the absence of NK cells the elevated levels in the expression of CD54 and HLA-E positively stained HUVECs dropped to initially low levels (D). Asterisks mark values which are significantly different to control values, ***, $p<0.001$, as determined by the Mann-Whitney test using the SPSS software.
doi:10.1371/journal.pone.0015339.g005

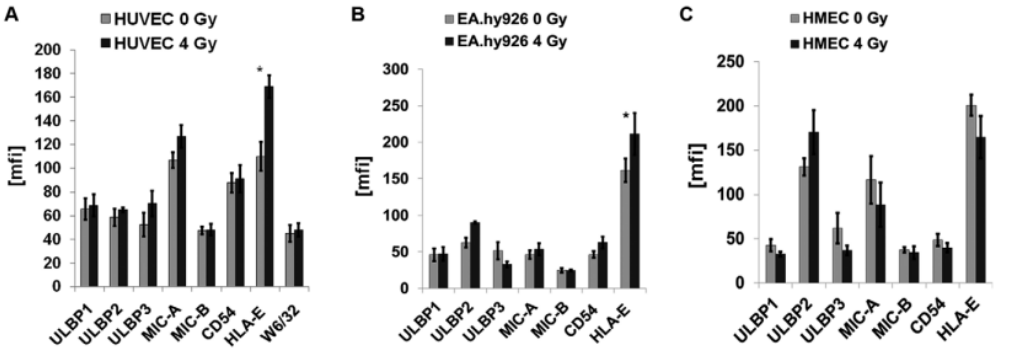

Figure 6. Phenotyping of ECs before and after irradiation at 4 Gy. Comparative analysis of the mean fluorescence intensity values for ULBP1-3, MIC-A/-B, CD54 (ICAM-1) and HLA-E expression on HUVECs (A), EA.hy926 cells (B) and HMECs (C) after ionizing irradiation at the sub-lethal dose of 4 Gy followed by a recovery period of 12 h. The MHC class I expression, as determined by W6/32 mAb, was measured only on HUVECs. The expression density of HLA-E was found to be significantly reduced on HUVECs and EA.hy926 cells (*, $p<0.05$), but not on HMECs following irradiation. No significant changes were observed with respect to other cell surface markers such as ULBP1-3, MIC-A/-B, CD54 and MHC class I antigens.
doi:10.1371/journal.pone.0015339.g006

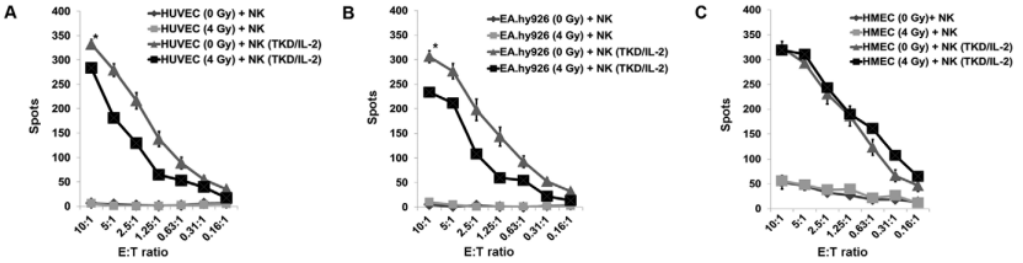

Figure 7. Comparative analysis of the lysis of non-irradiaited and irradiated ECs. Comparative analysis of the lysis of non-irradiated and irradiated (4 Gy) HUVECs (A), EA.hy926 cells (B) and HMECs (C) by un-stimulated and TKD/IL-2-stimulated NK cells. The data represent the mean values of three independent experiments and were obtained using 4 h granzyme B ELISPOT assays. The effector to target ratios ranged from 10:1 to 0.16:1. An asterisk marks values which are significantly different to values derived with non-irradiated target cells *, $p<0.05$ at all E:T ratios.
doi:10.1371/journal.pone.0015339.g007

HUVECs using an HLA-E specific antibody results in a significantly enhanced lysis (Figure 8). In contrast, the lysis of irradiated HUVECs was not significantly affected by pre-incubating activated NK cells with the NKG2A mAb.

Discussion

Herein, we have studied the expression of activating and inhibitory NK target ligands on human primary and immortalized ECs before and after irradiation and monitored its immunomodulatory functions. Although MHC class I, MHC class I related chain MIC-A and MIC-B and ULBP1-3 are frequently up-regulated on tumor cells by environmental stress [39], our findings indicate that a sub-lethal irradiation dose of 4 Gy does not significantly increase their cell surface expression on ECs. The MIC gene products [40] and ULBP1-3 proteins act as activating ligands for the C-type lectin receptor NKG2D [41–45] which is expressed on NK cells and via which activated NK cells can specifically kill their tumor target cells. We have previously shown that in contrast to normal tissues, tumors frequently present the major stress-inducible heat shock protein 70 (Hsp70) on their plasma membrane [37,46]. Similar to MIC-A/-B and ULBP1-3 membrane Hsp70 also serves as recognition structure for NK cells that have been activated by the Hsp70 peptide TKD plus IL-2 (TKD/IL-2) [47], both on tumor cells *in vitro* and in tumor mouse models [48,49]. Following activation, these NK cells show an elevated expression density of a panel of different receptors including the C-type lectin receptors CD94/NKG2A, CD94/NKG2C, NKG2D and natural cytotoxicity receptors (NCRs)

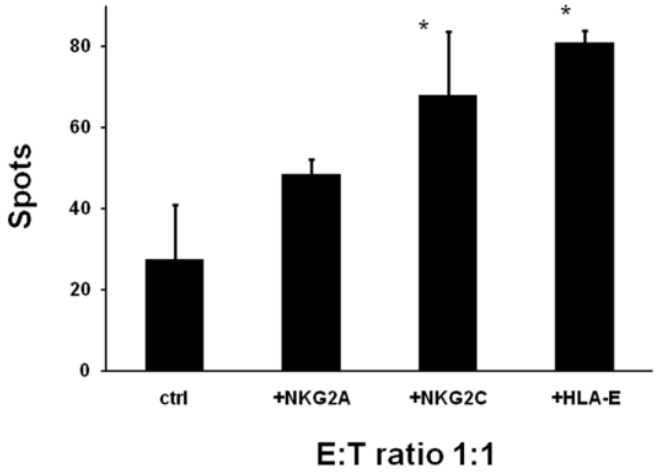

Figure 8. Blocking of lysis of irradiated ECs by antibodies directed against NK effector and target cells. Activation/inhibition of the granzyme B ELISPOT assay by antibodies directed against NKG2A, NKG2C or HLA-E. Comparative analysis of the lysis of irradiated (4 Gy) HUVECs either untreated or pre-incubated with HLA-E antibody by TKD/IL-2-stimulated NK cells that were pre-incubated either with NKG2A or NKG2C antibodies for 30 min. 50±3.5% expressed NKG2A and 68±15% of activated NK cells expressed NKG2C; 81±2.8% of irradiated HUVECs expressed HLA-E after contact with activated NK cells. The data represent the mean values of three experiments and were obtained using 4 h granzyme B ELISPOT assays. The effector to target (E:T) ratio was 1:1. An asterisk marks values which are significantly different to values derived with non-irradiated target cells *, $p<0.05$.
doi:10.1371/journal.pone.0015339.g008

[52,53]. Furthermore, the Hsp70 membrane density on tumor cells can be selectively enhanced by ionizing irradiation. Here, we were interested to study the role of membrane Hsp70 as a recognition structure for NK cells on non-irradiated and irradiated ECs. As expected, only immortalized ECs exhibited a membrane $Hsp70^+$ phenotype. We assume that the fusion of primary HUVECs with the membrane $Hsp70^+$ tumor cell line A549-8, as well as the transformation of primary dermal microvascular ECs with the SV40 large T antigen, result in a malignant transformation of ECs which enables the translocation of Hsp70 to the plasma membrane in a manner which is analogous to that apparent for tumor cells. We therefore speculate that immortalized ECs might in part reflect the phenotype of a tumor cell. However, in contrast to tumor cells, neither primary and nor immortalized ECs exhibited significant up-regulation of membrane Hsp70 density after ionizing irradiation (data not shown).

Although HLA-E transcripts are always present in ECs [14], the HLA-E surface expression is highly variable. HLA-E is known to act as a negative regulatory signal for NK cells expressing the inhibitory receptor CD94/NKG2A and thus might confer immune regulatory functions [50,51]. Trophoblasts and tumor cells protect themselves against the attack by the innate immune system via the expression of HLA-E [52,53]. We have previously shown that transfection of HLA-E down-regulates the cytolytic response of TKD/IL-2-activated NK cells against tumor cells [54]. Along with these findings, HLA-E also plays a protective role against NK cells in the field of xenotransplantation. HLA-E transgenic pigs expressing human HLA-E on PBMNC and ECs were found to be protected against NK cell mediated killing [55]. When comparing the HLA-E phenotype in macro- and microvascular ECs with their susceptibility for NK cell mediated cytolysis, the absence of HLA-E was found to be associated with a higher sensitivity towards activated NK cells. In contrast, the expression of activating ligands, such as MIC-A/-B, ULBP1-3 and Hsp70 on ECs appears to be of minor importance for this NK cell mediated activity. A sub-lethal irradiation initiated a selective up-regulation of HLA-E on macrovascular ECs which correlated with a decreased susceptibility to NK cell mediated lysis. In line with these findings, treating of NK cells with an agonistic antibody directed against the activating NK cell receptor NKG2C and ECs with an antibody inhibiting HLA-E increased the lysis of irradiated, HLA-E expressing primary, macrovascular HUVECs. Since the lysis of irradiated HUVECs was not significantly affected by an antibody directed against the inhibitory receptor NKG2A, we speculate that the activating NKG2C receptor is dominant over the effects of the inhibitory receptor NKG2A.

Interestingly, HLA-E expression on immortalized microvascular ECs remained unchanged following irradiation and their lysis by activated NK cells remained unaltered. Although the physiological relevance of these differences in the HLA-E expression on macro- and microvasculature has yet to be elucidated, these findings might, among others, have future clinical implications for radiotherapy. Analyzing differences in activating and inhibiting NK ligands on ECs might be useful for therapeutic strategies that combine irradiation and NK cell-based therapies. Also it will be interesting to see the outcome of direct comparisons between normal ECs and ECs from malignant tumor samples of the same tissue which are currently being undertaken in our laboratory.

Materials and Methods

Cells

Human umbilical vein ECs (HUVEC) [34] are the most common source of primary macrovascular ECs used for in vitro studies. HUVECs were prepared by digestion using 0.1% collagenase/trypsin solution (Sigma-Aldrich Corp., St. Louis, MO, USA) and grown to confluence. The cells were cultured in T25 flasks at a density of 1×10^6 cells per ml in ECGM medium supplemented with 10% v/v FCS and Supplement Mix containing 100 IU/ml polymyxin B in an incubator at 37°C in a humidified atmosphere with 5% CO_2. Cells were passaged twice a week and harvested by incubation with trypsin/EDTA for 1 min at 37°C. Cells undergo senescence at passages 8–10.

The cell line EA.hy926 results from a fusion of HUVECs with the epithelial lung tumor cell line A549-8 [56]. The cell line EA.hy926 was kindly provided by Dr. Cora-Jean S. Edgell (University of North Carolina, Chapel Hill, USA). The cells were grown in DMEM medium supplemented with 10% v/v FCS, 2 µM glutamine, 100 µM hypoxanthine, 0.4 µM aminopterin, 16 µM thymidine and 50 mg/l gentamicin at 37°C in a humidified atmosphere with 5% CO_2.

The human microvascular endothelial cell line CDC/EU.-HMEC-1, further referred as HMEC, was derived by transfecting human dermal microvascular ECs using a PBR-322 plasmid containing the coding region for the simian virus 40 A gene product (SV40), large T antigen to immortalize them [57]. The cell line was cultured in MCDB 131 medium (Gibco BRL, Karlsruhe, Germany) supplemented with 15% v/v FCS, 2 µM glutamine (Gibco BRL), 100 µM hydrocortisone (Sigma Aldrich, Deisenhofen, Germany), 10 ng/ml Epidermal growth factor (EGF, Becton Dickinson, Heidelberg, Germany) and 1% w/v penicillin/streptomycin (Gibco BRL, Karlsruhe, Germany) as antibiotics at 37°C in a humidified atmosphere with 5% CO_2.

Irradiation of ECs

Macro- and microvascular primary and immortalized ECs (HUVECs, EA.hy926 cells and HMECs) were cultured to 75% confluence and then irradiated with a single dose of 4 Gy at a dose rate of 1 Gy/min (Gulmay Isodose Control, Solingen, Germany). After a recovery period of 12 h, supernatants were centrifuged to remove the detached cells. The surviving cell fraction was used for further analysis. The total number of the attached and detached cells was counted.

Von Willebrand Factor Staining

For the von Willebrand (factor VIII-related antigen) staining, cells were seeded into 8-well µ-slide. After adherence, the cells were fixed with methanol-acetone (1:1) at room temperature for 2 min and rinsed with PBS. Samples were incubated with polyclonal rabbit antibody against human factor VIII-related antigen (Sigma Aldrich, Deisenhofen, Germany) at 37°C for 45 min, rinsed with PBS and incubated with goat-anti-rabbit FITC (fluorescein-isothiocyanate)-labeled secondary antibody (Sigma Aldrich, Deisenhofen, Germany) at 37°C for another 30 min. Cells were then washed with PBS/10% v/v FCS and cell nuclei were stained with 1 µg/ml diamidinophenylindole (DAPI, Roche, Mannheim, Germany).

Flow Cytometry

Cells were detached from the culture flasks using trypsin/EDTA (Gibco BRL, Karlsruhe, Germany) at 37°C for 1 min. After two washings in ice-cold PBS/FCS (1% v/v) cells were incubated for 30 min at 4°C with the following fluorescence-conjugated monoclonal antibodies (mAbs): anti-CD31 (Becton Dickinson, Heidelberg, Germany), anti-ULBP1-3, anti-MICA/B (BAMO1, IgG1; BAMO2, IgG2a, Bamomab, Munich, Germany), anti-HLA-E (MEM-06, Biozol, Eching, Germany), anti-MHC class I (W6/32, Sigma, Missouri, USA), anti-Hsp70 (cmHsp70.1, multi-

mmune GmbH, Munich, Germany; SPA810, Stressgen via Assay Designs, Ann Arbor, MI, USA), anti-CD54 (Dianova, Hamburg, Germany). After another two washing steps viable, propidium iodide-negative cells were gated and analyzed on a FACSCalibur flow cytometer (Becton Dickinson, Heidelberg, Germany).

^{51}Cr Release and Granzyme B ELISPOT Assays and Inhibition/Activation studies

Briefly, viable ECs were labeled with 0.1 µCi of $Na_2{}^{51}CrO_4$ (Hartmann Analytic GmbH, Braunschweig, Germany) at 37°C for 2 h. After two washes with RPMI 1640 medium, ^{51}Cr-labeled target cells (1×10^4) were transferred into triplicate wells of a 96-well plate. Human NK cells which were isolated using a standard CD3/CD19 depletion protocol (Miltenyi, Dreieich, Germany), followed by an adherence selection of CD14$^+$ cells. Un-stimulated NK cells or NK cells stimulated with TKD (2 µg/ml) and IL-2 (100 IU/ml) were then added to the ECs at various effector to target (E:T) cell ratios. After a 4 h co-incubation, supernatants (100 µl) were harvested and their radioactivity determined was using a gamma counter (Coulter). Specific lysis was calculated using the formula: % specific lysis = (experimental release – spontaneous release)/(maximum release –spontaneous release) ×100. The spontaneous release for each target cell ranged between 10 and 15%.

For the granzyme B ELISPOT assay, 96-well ELISPOT plates (Millipore GmbH, Schwalbach, Germany) were coated with capture antibody by an overnight incubation at 4°C, after which they were blocked using 10% v/v FCS. The effector and target cells (3×10^3) were added at different E:T ratios as indicated. After 4 h incubation at 37°C and 2 washing steps, a biotinylated detecting antibody (2 µg/ml) was added. After additional 2 washes, the presence of granzyme B was visualized using 3-amino-9-ethyl-carbazole substrate solution (25 min). Spots were counted and data were analyzed using an Immuno Spot Series 3A Analyzer (CTL-Europe GmbH, Aalen, Germany).

For inhibition/activation studies effector (TKD/IL-2-activated NK cells) or target (HUVECs) cells were pre-incubated with unlabeled NKG2A, NKG2C (MAB1059, MAB1381, 5 µg/ml each, R&D systems, Minneapolis, MN, USA) or HLA-E (MEM-06, Biozol, Eching, Germany, 5 µg/ml) antibodies for 30 min at room temperature and then used in the granzyme B ELISPOT assay at an E:T ratio of 1:1.

Statistical Analysis

Means between two groups were tested for differences using the t-test or the non-parametric Mann Whitney rank sum test, means of more than two groups were compared using the Analysis of variance (ANOVA).

IBIDI Movie

Due to the better availability of EC lines compared to primary ECs, HMECs were used as target cells for the videos. Killing of HMECs by resting and TKD/IL-2-activated human NK cells at an effector to target (E:T) ratio of 5:1. Briefly, 5,000 HMEC were seeded into µ Dishes $^{35\ mm,\ low}$ with Culture Insert (IBIDI, Martinsried; Germany) in a volume of 70 µl RPMI-1640 medium supplemented with 10% v/v FCS and cultured overnight. The supernatant was removed and 25,000 NK cells (resting or IL-2 activated for 4 days) were added in a volume of 70 µl fresh medium. Killing of target cells was filmed for 6 h. Time interval, 20 s; number of slides, 1200; totally elapsed 6 h, magnification, 10×, MV; format, mpg.

Supporting Information

Video S1 Movie illustrating the attack of HMECs by resting NK cells. Resting NK cells co-cultured with HMECs at an E:T ratio of 10:1 for 6 h at a magnification of 10x.
(MP4)

Video S2 Movie illustrating the attack of HMECs by TKD/IL-2-activated NK cells. TKD/IL-2-activated NK cells co-cultured with HMECs at an E:T ratio of 10:1 for 6 h at a magnification of 10x.
(MP4)

Video S3 Movie illustrating the attack of HMECs by TKD/IL-2-activated NK cells. TKD/IL-2-activated NK cells co-cultured with HMECs at an E:T ratio of 10:1 for 6 h at a magnification of 20x.
(MP4)

Author Contributions

Conceived and designed the experiments: GM. Performed the experiments: IR WS GE. Analyzed the data: MM GE GM. Contributed reagents/materials/analysis tools: GM. Wrote the paper: GM.

References

1. Springer TA (1994) Traffic signals for lymphocyte recirculation and leukocyte emigration: the multistep paradigm. Cell 76: 301–314.
2. Carlos TM, Harlan JM (1994) Leukocyte-endothelial adhesion molecules. Blood 84: 2068–2101.
3. Allavena P, Bianchi G, Paganin C, Giardina G, Mantovani A (1996) Regulation of adhesion and transendothelial migration of natural killer cells. Nat Immun 15: 107–116.
4. Cordes N, Park CC (2007) Beta 1 integrin as a molecular therapeutic target. Int J Radiat Biol 83: 753–760.
5. Berlin C, Bargatze RF, Campbell JJ, von Andrian UH, Szabo MC, et al. (1995) Alpha 4 integrins mediate lymphocyte attachment and rolling under physiologic flow. Cell 80: 413–422.
6. Berlin C, Berg EL, Briskin MJ, Andrew DP, Kilshaw PJ, et al. (1993) Alpha 4 beta 7 integrin mediates lymphocyte binding to the mucosal vascular addressin MAdCAM-1. Cell 74: 185–195.
7. Smith CW, Marlin SD, Rothlein R, Toman C, Anderson DC (1989) Cooperative interactions of LFA-1 and Mac-1 with intercellular adhesion molecule-1 in facilitating adherence and transendothelial migration of human neutrophils in vitro. J Clin Invest 83: 2008–2017.
8. Trinchieri G (1989) Biology of natural killer cells. Adv Immunol 47: 187–376.
9. Bielawska-Pohl A, Crola C, Caignard A, Gaudin C, Dus D, et al. (2005) Human NK cells lyse organ-specific endothelial cells: analysis of adhesion and cytotoxic mechanisms. J Immunol 174: 5573–5582.
10. Biron CA (1997) Activation and function of natural killer cell responses during viral infections. Curr Opin Immunol 9: 24–34.
11. Biassoni R, Cantoni C, Marras D, Giron-Michel J, Falco M, et al. (2003) Human natural killer cell receptors: insights into their molecular function and structure. J Cell Mol Med 7: 376–387.
12. Westgaard IH, Dissen E, Torgersen KM, Lazetic S, Lanier LL, et al. (2003) The lectin-like receptor KLRE1 inhibits natural killer cell cytotoxicity. J Exp Med 197: 1551–1561.
13. Lanier LL (2008) Up on the tightrope: natural killer cell activation and inhibition. Nat Immunol 9: 495–502.
14. Ulbrecht M, Honka T, Person S, Johnson JP, Weiss EH (1992) The HLA-E gene encodes two differentially regulated transcripts and a cell surface protein. J Immunol 149: 2945–2953.
15. Braud V, Jones EY, McMichael A (1997) The human major histocompatibility complex class Ib molecule HLA-E binds signal sequence-derived peptides with primary anchor residues at positions 2 and 9. Eur J Immunol 27: 1164–1169.
16. Karre K, Ljunggren HG, Piontek G, Kiessling R (1986) Selective rejection of H-2-deficient lymphoma variants suggests alternative immune defence strategy. Nature 319: 675–678.
17. Hayakawa Y, Kelly JM, Westwood JA, Darcy PK, Diefenbach A, et al. (2002) Cutting edge: tumor rejection mediated by NKG2D receptor-ligand interaction is dependent upon perforin. J Immunol 169: 5377–5381.

18. Kagi D, Ledermann B, Burki K, Seiler P, Odermatt B, et al. (1994) Cytotoxicity mediated by T cells and natural killer cells is greatly impaired in perforin-deficient mice. Nature 369: 31–37.
19. Wallin RP, Screpanti V, Michaelsson J, Grandien A, Ljunggren HG (2003) Regulation of perforin-independent NK cell-mediated cytotoxicity. Eur J Immunol 33: 2727–2735.
20. Ebert EC, Groh V (2008) Dissection of spontaneous cytotoxicity by human intestinal intraepithelial lymphocytes: MIC on colon cancer triggers NKG2D-mediated lysis through Fas ligand. Immunology 124: 33–41.
21. Parham P (2004) Killer cell immunoglobulin-like receptor diversity: balancing signals in the natural killer cell response. Immunol Lett 92: 11–13.
22. Froelich CJ, Orth K, Turbov J, et al. (1996) New paradigm for lymphocyte granule-mediated cytotoxicity. Target cells bind and internalize granzyme B, but an endosomolytic agent is necessary for cytosolic delivery and subsequent apoptosis. J Biol Chem 271: 29073–29079.
23. Chowdhury D, Lieberman J (2008) Death by a thousand cuts: granzyme pathways of programmed cell death. Annu Rev Immunol 26: 389–420.
24. Hoves S, Trapani JA, Voskoboinik I (2010) The battlefield of perforin/granzyme cell death pathways. J Leuko Biol 87: 237–243.
25. Gastpar R, Gehrmann M, Bausero MA, Asea A, Gross C, et al. (2005) Heat shock protein 70 surface-positive tumor exosomes stimulate migratory and cytolytic activity of natural killer cells. Cancer Res 65: 5238–5247.
26. Multhoff G, Pfister K, Gehrmann M, Hantschel M, Gross C, et al. (2001) A 14-mer Hsp70 peptide stimulates natural killer (NK) cell activity. Cell Stress Chaperones 6: 337–344.
27. Gross C, Koelch W, DeMaio A, Arispe N, Multhoff G (2003) Cell surface-bound heat shock protein 70 (Hsp70) mediates perforin-independent apoptosis by specific binding and uptake of granzyme B. J Biol Chem 278: 41173–41181.
28. Chen WS, Kitson RP, Goldfarb RH (2002) Modulation of human NK cell lines by vascular endothelial growth factor and receptor VEGFR-1 (FLT-1). In Vivo 16: 439–445.
29. Giron-Michel J, Fogli M, Gaggero A, et al. (2003) Detection of a functional hybrid receptor gammac/GM-CSFRbeta in human hematopoietic CD34+ cells. J Exp Med 197: 763–775.
30. Strasly M, Cavallo F, Geuna M, et al. (2001) IL-12 inhibition of endothelial cell functions and angiogenesis depends on lymphocyte-endothelial cell cross-talk. J Immunol 166: 3890–3899.
31. Krause SW, Gastpar R, Andreesen R, Gross C, Ullrich H, et al. (2004) Treatment of colon and lung cancer patients with ex vivo heat shock protein 70-peptide-activated, autologous natural killer cells: a clinical phase I trial. Clin Cancer Res 10: 3699–3707.
32. Lilienfeld BG, Schildknecht A, Imbach LL, et al. (2008) Characterization of porcine UL16-binding protein 1 endothelial cell surface expression. Xenotransplantation 15: 136–144.
33. Videm V, Albrigtsen M (2008) Soluble ICAM-1 and VCAM-1 as markers of endothelial activation. Scand J Immunol 67: 523–531.
34. Gifford SM, Grummer MA, Pierre SA, Austin JL, Zheng J, et al. (2004) Functional characterization of HUVEC-CS: Ca2+ signaling, ERK 1/2 activation, mitogenesis and vasodilator production. J Endocrinol 182: 485–499.
35. Newman PJ, Berndt MC, Gorski J, White GC, 2nd, Lyman S, et al. (1990) PECAM-1 (CD31) cloning and relation to adhesion molecules of the immunoglobulin gene superfamily. Science 247: 1219–1222.
36. Barabara NP, Wrana JL, Letarte M (1999) Endoglin is an accessory protein that interacts with the signaling receptor complex of multiple members of the transforming growth factor beta superfamily. J Biol Chem 274: 584–594.
37. Multhoff G, Botzler C, Jennen L, Schmidt J, Ellwart J, et al. (1997) Heat shock protein 72 on tumor cells: a recognition structure for natural killer cells. J Immunol 158: 4341–4350.
38. Robertson MJ, Ritz J (1990) Biology and clinical relevance of human natural killer cells. Blood 76: 2421–2438.
39. Groh V, Steinle A, Bauer S, Spies T (1998) Recognition of stress-induced MHC molecules by intestinal epithelial gammadelta T cells. Science 279: 1737–1740.
40. Bahram S, Bresnahan M, Geraghty DE, Spies T (1994) A second lineage of mammalian major histocompatibility complex class I genes. Proc Natl Acad Sci USA 91: 6259–6263.
41. Ebert EC, Groh V (2008) Dissection of spontaneous cytotoxicity by human intestinal intraepithelial lymphocytes: MIC on colon cancer triggers NKG2D-mediated lysis through Fas ligand. Immunology 124: 33–41.
42. Raulet DH (2003) Roles of the NKG2D immunoreceptor and its ligands. Nat Rev Immunol 3: 781–790.
43. Groh V, Wu J, Yee C, Spies T (2002) Tumour-derived soluble MIC ligands impair expression of NKG2D and T-cell activation. Nature 419: 734–38.
44. Gonzalez S, Groh V, Spies T (2006) Immunobiology of human NKG2D and its ligands. Curr Top Microbiol Immunol 298: 121–138.
45. Pende D, Rivera P, Marcenaro S, et al. (2002) Major histocompatibility complex class I-related chain A and UL16-binding protein expression on tumor cell lines of different histotypes: analysis of tumor susceptibility to NKG2D-dependent natural killer cell cytotoxicity. Cancer Res 62: 6178–6186.
46. Gastpar R, Gross C, Rossbacher L, Ellwart J, Riegger J, et al. (2004) The cell surface-localized heat shock protein 70 epitope TKD induces migration and cytolytic activity selectively in human NK cells. J Immunol 172: 972–980.
47. Stangl S, Wortmann A, Guertler U, Multhoff G (2006) Control of metastasized pancreatic carcinomas in SCID/beige mice with human IL-2/TKD-activated NK cells. J Immunol 176: 6270–6276.
48. Gross C, Hansch D, Gastpar R, Multhoff G (2003) Interaction of heat shock protein 70 peptide with NK cells involves the NK receptor CD94. Biol Chem 384: 267–279.
49. Gross C, Schmidt-Wolf IG, Nagaraj S, Ellwart J, Kunz-Schughart L, et al. (2003) Heat shock protein 70-reactivity is associated with increased cell surface density of CD94/CD56 on primary natural killer cells. Cell Stress Chaperones 8: 348–360.
50. Braud VM, Allan DS, O'Callaghan CA (1998) HLA-E binds to natural killer cell receptors CD94/NKG2A, B and C. Nature 391: 795–799.
51. Lee N, Llano M, Carretero M, Ishitani A, Navarro F, et al. (1998) HLA-E is a major ligand for the natural killer inhibitory receptor CD94/NKG2A. Proc Natl Acad Sci USA 95: 5199–5204.
52. King AG, Johanson K, Frey CL, DeMarsh PL, White JR, et al. (2000) Identification of unique truncated KC/GRO beta chemokines with potent hematopoietic and anti-infective activities. J Immunol 164: 3774–3782.
53. Marin R, Ruiz-Cabello F, Pedrinaci S, Mendez R, Jimenez P, et al. (2003) Analysis of HLA-E expression in human tumors. Immunogenetics 54: 767–775.
54. Stangl S, Gross C, Pockley AG, Asea A, Multhoff G (2008) Influence of Hsp70 and HLA-E on the killing of leukemic blasts by cytokine/Hsp70 peptide-activated human NK cells. Cell Stress Chaperones 13: 221–230.
55. Weiss EH, Lilienfeld BG, Muller S, Muller E, Herbach N, et al. (2009) HLA-E/human beta2-microglobulin transgenic pigs: protection against xenogeneic human anti-pig NK cytotoxicity. Transplantation 87: 35–43.
56. Edgell CJ, Mc Donald CC, Graham JB (1983) Permanent cell line expressing human factor VIII-related antigen established by hybridization. Proc Natl Acad Sci USA 80: 3734–3737.
57. Ades EW, Candal FJ, Swerlick RA, George VG, Summers S, et al. (1992) HMEC-1: establishment of an immortalized human microvascular endothelial cell line. J Invest Dermatol 99: 683–690.

Targeting membrane heat-shock protein 70 (Hsp70) on tumors by cmHsp70.1 antibody

Stefan Stangl[a,1], Mathias Gehrmann[a,1], Julia Riegger[a], Kristin Kuhs[a], Isabelle Riederer[a], Wolfgang Sievert[a], Kathrin Hube[a], Ralph Mocikat[b], Ralf Dressel[c], Elisabeth Kremmer[b], Alan G. Pockley[d], Lars Friedrich[e], Laszlo Vigh[f], Arne Skerra[e], and Gabriele Multhoff[a,2]

[a]Department of Radiation Oncology, Klinikum rechts der Isar, Technische Universität München, and Clinical Cooperation Group "Innate Immunity in Tumor Biology," [b]Institute of Molecular Immunology, Helmholtz-Zentrum München, Deutsches Forschungszentrum für Gesundheit und Umwelt, 81675 Munich, Germany; [c]Department of Cellular and Molecular Immunology, University of Göttingen, 37073 Göttingen, Germany; [d]Department of Oncology, The Medical School, University of Sheffield, Sheffield S10 2RX, United Kingdom; [e]Lehrstuhl für Biologische Chemie, Technische Universität München, 85354 Freising-Weihenstephan, Germany; and [f]Biological Research Centre, Institute of Biochemistry, Hungarian Academy of Sciences, 6701 Szeged, Hungary

Edited* by Eva Kondorosi, Institute for Plant Genomics, Human Biotechnology and Bioenergy, Szeged, Hungary, and approved December 6, 2010 (received for review October 31, 2010)

Immunization of mice with a 14-mer peptide TKDNNLLGRFELSG, termed "TKD," comprising amino acids 450–461 ($aa_{450-461}$) in the C terminus of inducible Hsp70, resulted in the generation of an IgG1 mouse mAb cmHsp70.1. The epitope recognized by cmHsp70.1 mAb, which has been confirmed to be located in the TKD sequence by SPOT analysis, is frequently detectable on the cell surface of human and mouse tumors, but not on isogenic cells and normal tissues, and membrane Hsp70 might thus serve as a tumor-specific target structure. As shown for human tumors, Hsp70 is associated with cholesterol-rich microdomains in the plasma membrane of mouse tumors. Herein, we show that the cmHsp70.1 mAb can selectively induce antibody-dependent cellular cytotoxicity (ADCC) of membrane Hsp70$^+$ mouse tumor cells by unstimulated mouse spleen cells. Tumor killing could be further enhanced by activating the effector cells with TKD and IL-2. Three consecutive injections of the cmHsp70.1 mAb into mice bearing CT26 tumors significantly inhibited tumor growth and enhanced the overall survival. These effects were associated with infiltrations of NK cells, macrophages, and granulocytes. The Hsp70 specificity of the ADCC response was confirmed by preventing the antitumor response in tumor-bearing mice by coinjecting the cognate TKD peptide with the cmHsp70.1 mAb, and by blocking the binding of cmHsp70.1 mAb to CT26 tumor cells using either TKD peptide or the C-terminal substrate-binding domain of Hsp70.

immunotherapy | syngeneic tumor model | tumor antibody dependent cellular cytotoxicity | epitope mapping | surface antigen

Although the combination of mAbs with standard therapies plays a pivotal role in the treatment of cancer (1–4), the therapeutic success of this strategy is restricted by the availability of tumor-specific antibodies. Global profiling of the surface proteome of human tumors has revealed an abundancy of stress proteins in the plasma membrane (5, 6). Herein, we describe the generation of a mouse mAb directed against a 14-mer peptide TKDNNLLGRFELSG (TKD) of the major stress-inducible heat-shock protein 70 (Hsp70, Hsp70-1, Hsp72, HspA1A #3303), which is present on the cell surface of human tumor cell lines (7). Screening of a large number of primary human tumor biopsies and the corresponding normal tissues has indicated that carcinomas, but none of the tested normal tissues, frequently present Hsp70 on their cell surface (8, 9). Moreover, a membrane Hsp70$^+$ tumor phenotype has been found to be associated with a significantly decreased overall survival in patients with lower rectal and lung carcinomas. The expression of this molecule might therefore serve as a negative prognostic marker (9) in these patient groups. It has been hypothesized that membrane Hsp70 might support the spread of distant metastasis or might confer resistance to standard therapies (10).

The TKD sequence, which is exposed to the extracellular milieu of tumors, resides in the C-terminally localized oligomerization domain of the Hsp70 molecule (11). Furthermore, this TKD peptide in combination with low-dose IL-2 has been found to stimulate the migratory and cytolytic activity of NK cells against membrane Hsp70$^+$ tumor cells (12). In contrast to other commercially available Hsp70 antibodies, the cmHsp70.1 mAb uniquely identifies the membrane form of Hsp70 on viable tumor cells with an intact plasma membrane in vitro.

We have recently shown that the cmHsp70.1 mAb also binds to the CT26 mouse colon tumor cells in vivo (13). Herein, we demonstrate that consecutive injections of the cmHsp70.1 mAb into mice bearing CT26 tumors can significantly reduce the mass of membrane Hsp70$^+$ tumors and increase overall survival during therapy via the induction of antibody-dependent cellular cytotoxicity (ADCC). The in vitro ADCC activity could be further enhanced by using TKD/IL-2–activated NK cells as effector cells instead of unstimulated mouse spleen cells. These findings suggest that membrane Hsp70 could serve as a unique immunotherapeutic target for a broad spectrum of different tumor entities.

Results

Monoclonal Antibody cmHsp70.1 Binds to Membrane Hsp70$^+$ Human and Mouse Tumors. The epitope of the cmHsp70.1 mAb, which was generated by immunizing mice with the 14-mer peptide TKD, was confirmed by SPOT analysis and peptide blocking studies (Fig. S1). Viable human tumor cell lines, such as colon (CX2), breast (MDA436, MCF-7), and lung (A549) carcinomas and malignant melanomas (Malme, Mel Ei, Mel Ho, Parl, A375, Sk Mel29) bind cmHsp70.1 mAb, but not the Hsp70-specific SPA810 mAb (Fig. 1*A*). The cmHsp70.1 mAb also stains immortalized endothelial cells (EA.hy926, HMEC), but not their nontransformed, isogenic counterparts (primary ECs) (Fig. 1*B*, *Upper* two panels). Similar to the human tumor cell lines, single-cell suspensions of primary human gastrointestinal and pancreatic tumor samples ($n = 229$) also frequently (more than 40% of all tested tumor cases) bind cmHsp70.1 mAb, whereas the corresponding reference tissues are always membrane Hsp70$^-$.

With respect to mouse tumors, the cmHsp70.1 mAb binds to CT26 colon (61%) (Fig. 1 *C* and *D*) and highly malignant B16F10 mouse melanoma cells (74%) (Fig. 1*B*, *Lower Right*), whereas only a minor population of the isogenic, low-malignant counterpart B16F0 (14%) (Fig. 1*B*, *Lower Left*), 1048 pancreatic carci-

Author contributions: G.M. designed research; S.S., M.G., J.R., K.K., I.R., W.S., K.H., R.M., R.D., E.K., A.G.P., and L.F. performed research; E.K., L.V., and A.S. contributed new reagents/analytic tools; S.S., M.G., I.R., W.S., R.D., E.K., A.G.P., L.V., A.S., and G.M. analyzed data; and G.M. wrote the paper.

The authors declare no conflict of interest.

*This Direct Submission article had a prearranged editor.

Freely available online through the PNAS open access option.

[1]S.S. and M.G. contributed equally to this work.

[2]To whom correspondence should be addressed. E-mail: gabriele.multhoff@lrz.tu-muenchen.de.

This article contains supporting information online at www.pnas.org/lookup/suppl/doi:10.1073/pnas.1016065108/-/DCSupplemental.

IMMUNOLOGY

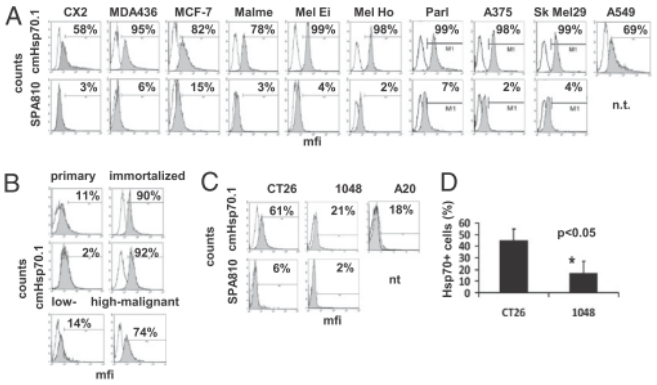

Fig. 1. Representative flow cytometric histograms of membrane Hsp70 expression on human and mouse tumor cell lines. (*A*) Human CX2 (colon), MDA436 (breast), MCF-7 (breast), Malme, Mel Ei, Mel Ho, Parl, A375, Sk Mel29 (all malignant melanomas), A549 (lung) carcinoma, (*B*) primary and immortalized endothelial cells, and (*C*) mouse CT26 (colon), 1048 (pancreas), A20 (B lymphoma), B16F0 (low-malignant melanoma), and (*B*) B16F10 (high-malignant, metastatic melanoma), tumor cell lines were analyzed by flow cytometry using either cmHsp70.1-FITC (*Upper*) or SPA810-FITC (*Lower*) mAb. Results are expressed as log green fluorescence intensity vs. relative cell numbers. The IgG1 isotype-matched control is indicated in white and membrane Hsp70 staining in gray histograms. The whole staining procedure was performed at 4 °C and only viable, 7-AAD$^-$ cells were gated upon and analyzed. (*B*) Comparison of the membrane Hsp70 expression in isogenic human and mouse cells. Human primary endothelial cells (ECs, *Top* and *Middle*) were compared with their corresponding immortalized partner cell lines EA.hy926, a fusion product of human umbilical vein ECs (HUVEC) with A549 lung carcinoma cells, and HMEC, which was derived by a transfection of primary ECs with SV40 large T antigen, were stained with cmHsp70.1 mAb, as described above. Furthermore, the low-malignant mouse melanoma cell line B16F0 (*Left*) was compared with the high-malignant, metastatic tumor cell line B16F10. The IgG1 isotype-matched control is indicated in white and membrane Hsp70 staining using cmHsp70.1 mAb in gray histograms. (*D*) The flow cytometric analysis of CT26 and 1048 tumor cell lines using cmHsp70.1-FITC mAb was repeated six times. The differences in membrane Hsp70 positivity in CT26 and 1048 tumor cell lines was significant (*$P < 0.05$).

noma (21%) (Fig. 1 *C* and *D*), and A20 B-lymphoma cells (18%) (Fig. 1*C*) are membrane Hsp70$^+$. The staining of cytosolic Hsp70 was excluded in all experiments, as only viable, 7-AAD$^-$ tumor cells with intact plasma membranes were gated and analyzed.

Monoclonal Antibody cmHsp70.1 Initiates ADCC in Membrane Hsp70$^+$ Tumors in Vitro. Measurements using fluorescence-conjugated marker beads revealed that ≈10,000 Hsp70 molecules are present on the plasma membrane of CT26 mouse tumor cells (13). Despite this relatively low surface density, 50 μg/mL cmHsp70.1 mAb could induce significant ADCC-mediated killing of CT26 carcinoma cells by unstimulated mouse spleen effector cells at E:T ratios ranging from 50:1 to 6.25:1 (Fig. 2*A*) ($P < 0.05$). The 1048 carcinoma cells that contained only a small proportion of Hsp70$^+$ cells were not sensitive to ADCC (Fig. 2*A*). As a control, the capacity of other mouse IgG1 antibodies (SPA810, Ox7.11) and the cmHsp70.1 Fab fragment to induce ADCC was assessed and compared with that of cmHsp70.1 mAb. As shown in Fig. 2*B*, neither SPA810 mAb nor cmHsp70.1 Fab induced any significant ADCC against membrane Hsp70$^+$ CT26 tumor cells. Similar negative findings were obtained if mouse BW cells (hybrid cross between New Zealand Black and White mice) transfected with theta (56% membrane theta$^+$ cells) were used as target cells for ADCC (Fig. 2*C*). In the same experiment, cmHsp70.1 mAb induces significant ADCC in CT26 colon adenocarcinoma cells (60% membrane Hsp70$^+$ cells) (Fig. 2*C*).

To determine whether preactivating mouse spleen cells with TKD (2 μg/mL) plus IL-2 (100 IU/mL) improves the killing of membrane Hsp70$^+$ CT26 cells in vitro, ADCC experiments were repeated using unstimulated and preactivated effector cells. The stimulation of mouse spleen cells with TKD/IL-2 significantly increased the proportion of CD49b$^+$ NK cells and CD25$^+$ cells (Table 1) ($P < 0.05$) and the lysis of CT26 cells (Fig. 2*D*) ($P < 0.01$). An element of this increase in cytolysis could be explained by a direct killing of membrane Hsp70$^+$ tumor cells by TKD/IL-2–activated NK cells (12), as it was apparent in the absence of the

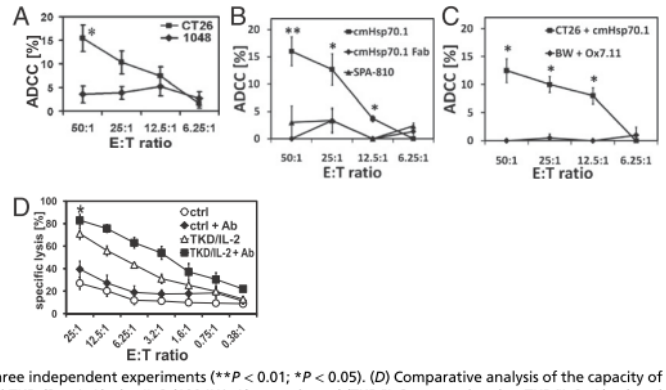

Fig. 2. Comparative analysis of ADCC using different IgG1 mAbs and cmHsp70.1 Fab fragment. (*A*) In vitro ADCC of membrane Hsp70$^+$ mouse CT26 colon (60%, filled squares) and membrane Hsp70$^-$ 1048 pancreatic carcinoma cells (filled diamonds), using 50 μg/mL Hsp70.1 mAb and unstimulated mouse spleen cells at E:T ratios ranging from 50:1 to 6.25:1. (*B*) In comparison with cmHsp70.1 mAb (filled squares), no significant ADCC was induced in mouse CT26 colon carcinoma cells (61% cmHsp70.1$^+$) using the non-binding IgG1 mAb SPA810 (filled circles) or cmHsp70.1 Fab fragment (filled triangles). (*C*) The IgG1 Ox7.11 mAb, which detects the theta antigen on 56% of the BW mouse tumor cells, does not induce ADCC in BW mouse tumor cells (filled triangles). Specific ADCC was measured using 50 μg/mL antibody or Fab fragment, respectively; unstimulated mouse spleen cells at E:T ratios ranging from 50:1 to 6.25:1 were used as effector cells. Specific lysis mediated by the direct cytotoxic effect of NK cells in the absence of cmHsp70.1 mAb was subtracted. The phenotypes of the effector cells are summarized in Table 2. Data are means ± SE of at least three independent experiments (**$P < 0.01$; *$P < 0.05$). (*D*) Comparative analysis of the capacity of unstimulated (ctrl, open circles; ctrl+Ab, filled diamonds) and TKD (2 μg/mL) plus IL-2 (100 IU/mL) preactivated (TKD/IL-2, open triangles; TKD/IL-2+Ab, closed squares) mouse spleen cells to kill CT26 carcinoma cells. The ADCC experiment was performed either in the absence (open symbols) and presence (+Ab; closed symbols) of 50 μg/mL cmHsp70.1 mAb. Lysis is mediated by ADCC in the presence of cmHsp70.1 mAb and by a direct cytotoxic effect of mouse NK cells in the absence of mAb, at E:T ratios ranging from 25:1 to 0.38:1. Data are means ± SE of at least three independent experiments. Lysis of activated effector cells in the absence and presence of cmHsp70.1 mAb was significantly different (*$P < 0.05$, all E:T ratios). ADCC was calculated using the formula: percent of specific lysis = (experimental release − spontaneous release)/(maxiumum release − spontaneous release) × 100.

Table 1. Proportion (%) of marker-positive cells in unstimulated and TKD/IL-2 preactivated mouse spleen cells

Antigen	Proportion of antigen-positive cells (%)	
	Unstimulated	TKD/IL-2–stimulated
CD8 (T cells)	11.2 ± 1.3	13.8 ± 3.4
CD4 (T cells)	21.1 ± 0.9	15.4 ± 5.9
CD205 (granulocytes)	6.4 ± 3.3	12.0 ± 5.4
CD11c (APC)	6.4 ± 3.2	8.4 ± 5.5
Ly6G/Ly6C (Gr-1)	8.7 ± 4.7	7.5 ± 3.0
B220 (B cells)	62.9 ± 5.4	61.0 ± 5.3
CD11b (APC)	14.6 ± 2.9	18.2 ± 4.9
CD49b (NK cells)	12.8 ± 4.7	22.5 ± 4.0*
CD25 (activation marker)	6.9 ± 4.7	9.7 ± 7.1*

*$P < 0.05$, corrected for multiple testing.

cmHsp70.1 mAb (Fig. 2*D*). However, the presence of cmHsp70.1 mAb further enhanced the cytolytic activity of unstimulated and TKD/IL-2–stimulated mouse spleen cells against membrane Hsp70$^+$ CT26 cells. The differences in the killing of CT26 tumor cells by TKD/IL-2–activated mouse spleen cells in the presence and absence of cmHsp70.1 mAb can be viewed in a movie which illustrates two major findings: the targeted migration of effector cells toward membrane Hsp70$^+$ tumor cells, which is enhanced in the presence of the cmHsp70.1 mAb and the concerted attack of tumor cells by effector cells (Movie S1).

ADCC in Tumor-Bearing Mice. An intraperitoneal injection of 2.5×10^4 CT26 mouse colon tumor cells suspended in 100 μL PBS resulted in rapidly growing tumors with a tumor take of 100%. A comparative phenotyping of cultured CT26 and single-cell suspensions derived from CT26 tumor-bearing mice on day 14 revealed the proportion of membrane Hsp70$^+$ cells to be significantly greater in the latter (46.2 ± 9%, $n = 6$ vs. 69.8 ± 14%, $n = 7$; $P < 0.05$).

Based on our observation that the cmHsp70.1 mAb initiates ADCC in membrane Hsp70$^+$ CT26 cells in vitro, the capacity of this antibody to induce tumor killing in CT26 tumor-bearing mice was evaluated. The tumor weights in mice that received two and three consecutive intravenous injections of cmHsp70.1 mAb (20 μg per injection) on days 3, 5, and 7 were significantly lower than those in mice receiving an isotype-matched control antibody (1.7 ± 0.63 g vs. 0.59 ± 0.32 g and 0.44 ± 0.29 g, respectively, $P < 0.05$) (Fig. 3*A*).

Immunohistochemical studies of consecutive CT26 tumor sections following one to three injections of cmHsp70.1 mAb revealed a dramatic increase in F4/80$^+$ macrophages and Ly6G/Ly6C$^+$ granulocytes, and a moderate increase in Ly49b$^+$ CD56$^+$ NK cells within the tumor (Fig. 3*B* and Table 2). CD3$^+$ T cells began to infiltrate tumor tissue from day 21 onwards (Table 2).

Growth curves of CT26 tumors after subcutaneous injection of 1×10^6 cells after one and three intravenous injections of cmHsp70.1 mAb (20 μg per injection) on days 4, 7, and 10 revealed that three repeated injections of cmHsp70.1 mAb resulted in a significant growth delay (Fig. 3*C*) ($P < 0.05$), which correlated with an increased overall survival (Fig. 3*D*) ($P < 0.05$). In line with these findings, overall survival was also greater in mice with intraperitoneal CT26 tumors (Fig. 4*A*, filled squares) ($n = 24$, $P < 0.0001$) than their IgG1 isotype-matched control antibody treated counterparts (Fig. 4*A*, open circles) ($n = 14$). In contrast, an identical treatment regimen had no significant effect ($P = 0.310$) on the survival of mice bearing A20 B-cell lymphomas, which lack membrane Hsp70 expression (Fig. 4*B*). Furthermore, the decrease in tumor weight after three intravenous injections of cmHsp70.1 mAb was associated with a significant increase in serum levels of Hsp70 on day 14 (154 ± 41.7 pg/mL vs. 1,434.5 ± 786 pg/mL, $n = 4$, $P < 0.01$), as measured by ELISA.

TKD Peptide Is the Target for ADCC. Coinjection of cmHsp70.1 mAb (20 μg per injection) with an excess of Hsp70 peptide TKD (50 μg per injection) into CT26 tumor-bearing mice (intraperitoneally) on days 3, 5, and 7 completely reversed the antitumoral effect of the antibody therapy ($P < 0.02$) (Fig. 5*A*). This finding indicated that the TKD peptide, which contains the epitope of the cmHsp70.1 mAb, competes with membrane Hsp70 on the cell surface of mouse tumors for binding in vivo.

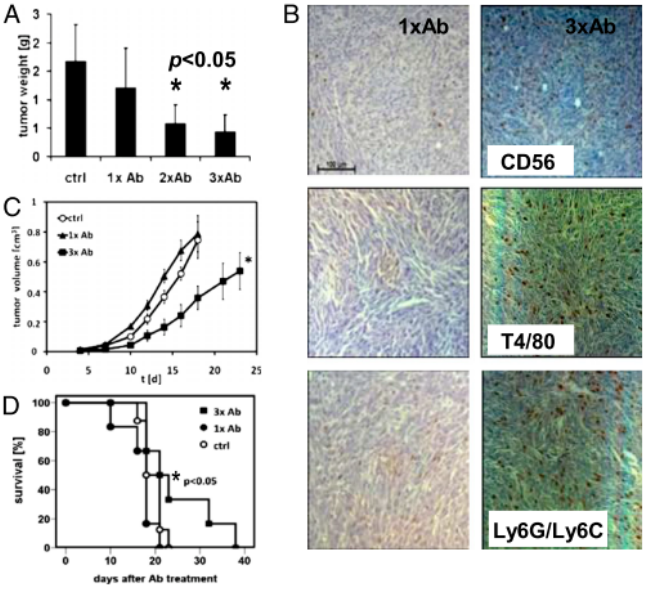

Fig. 3. Reduction in tumor weight and the delay of CT26 tumor growth in BALB/c mice after one to three injections of cmHsp70.1 mAb is associated with an infiltration of immunocompetent effector cells. (*A*) Two and three consecutive injections of cmHsp70.1 mAb (intravenously) result in a significant reduction in tumor weight (*$P < 0.05$). The cmHsp70.1 mAb (20 μg per injection) was injected intravenously on days 3, 5, and 7 following intraperitoneal injection of 2.5×10^4 CT26 tumor cells. Mice were killed on day 14 and tumor weights were determined. Data are means of six to nine animals (*$P < 0.05$). (*B*) Representative photomicrographs of CT26 tumor sections after one (1 × Ab; *Left*) and three consecutive injections of cmHsp70.1 mAb (3 × Ab; *Right*) on days 3, 5, and 7 (20 μg per injection). Infiltration of NK cells (CD56; *Top*), monocytes (T4/80; *Middle*) and granulocytes (Ly6G/Ly6C; *Bottom*) was determined on consecutive sections of CT26 tumors derived from mice on day 14. Semiquantitative data are summarized in Table 2. (Scale bar, 100 μm.) (*C*) Three (filled square) but not one (filled triangle) injections of cmHsp70.1 mAb (i.v.) result in a significant growth delay of subcutaneously injected CT26 tumors (*$P < 0.05$). The cmHsp70.1 mAb (20 μg per injection) was injected intravenously on days 4, 7, and 10 following subcutaneous injection of 1×10^6 CT26 tumor cells. Tumor weight was measured in each mouse every second day after the last antibody injection (*$P < 0.05$ for all time points from day 10 onwards). (*D*) Control mice (open circles) and mice that were injected only once with mAb cmHsp70.1 (filled circles, day 5) became moribund from day 18 onwards, whereas mice that were injected three times (filled squares, day 4, 7, 10) with cmHsp70.1 mAb showed a significant increase in overall survival (*$P < 0.05$). Each datapoint represents measurements of six to nine mice.

Table 2. Semiquantitative analyses of the lymphocytic and granulocytic infiltration of CT26 tumors after one to three injections of the cmHsp70.1 mAb

Marker	Treatment with cmHsp70.1 mAb			
	Ctrl	1×	2×	3×
CD3ε (T cells)	—	—	—	+
Ly49b/CD56 (NK cells)	+	+	++	+++
F4/80 (macrophages)	++	++	++	+++
Ly6G/Ly6C (Gr-1) (granulocytes/macrophages)	+	++	++	+++

BALB/c mice were injected (intraperitoneally) with CT26 tumor cells (2.5×10^4) on day 0 and injected with cmHsp70.1 mAb (20 μg per injection) on days 3, 5, and 7. Mice were killed on day 21 and at least six consecutive tumor sections (5 μm) were examined immunohistochemically using antibodies directed against T cells (CD3ε), NK cells (Ly49b), monocytes (F4/80), and granulocytes (Ly6G/Ly6C). The results indicate the number of infiltrating cells within a defined tumor section of 1 cm^2; —, no infiltration (<10); +, weak infiltration (10–50); ++, intermediate infiltration (50–200); +++, strong infiltration (<200). Representative images of consecutive tumor sections stained with Ly49, CD56, F4/80, and Ly6G/Ly6C antibodies are illustrated in Fig. 3*B*.

The specificity of the interactions was further confirmed by determining whether the binding of cmHsp70.1 mAb to the cell surface of cultured CT26 tumor cells could be blocked by the TKD peptide, which represents the immunogen (Fig. S1), but not by a 14-mer scrambled NGL(NGLTLKNDFSRLEG) peptide consisting of the same amino acid residues in a different order. The proportion of membrane $Hsp70^+$ cells decreased in a concentration-dependent manner from 59% (white graph) to 44% (gray graph; 12.5 μg/mL) and from 60% (white graph) to less than 15% (gray graph; 25 μg/mL) (Fig. 5*B*). In contrast, no inhibition in binding was apparent when the same concentrations of NGL peptide were used for the blocking experiments (Fig. 5*B*, *Right*). As a control, the binding of cmHsp70.1 mAb to CT26 cells was also significantly inhibited using the C-terminal substrate binding domain of Hsp70 ($P < 0.05$) (Fig. 5*C*). All blocking studies were performed at 4 °C because of the rapid internalization of cmHsp70.1 mAb at higher temperatures (13).

Discussion

Hsp70 mediates the stability of tumor cells following environmental stress (14, 15), and it is commonly regarded as an intracellular molecule. However, it is now apparent that a membrane form of Hsp70 is frequently expressed on a broad variety of human tumors, but not on the corresponding normal tissues. This membrane expression can be specifically detected using the cmHsp70.1 mAb, which has been generated using the human 14-mer TKD sequence as an immunogen. Because the human and murine TKD sequences only differ in one amino acid (16) (human T**K**DNNLLGRFELSG; mouse T**R**DNNLLGRFELSG), we also screened mouse tumor cell lines for their capacity to express the membrane form of Hsp70. Similar to human tumors (7, 8), the mouse colon tumor cell line CT26 (17) was also membrane $Hsp70^+$. The depletion of cholesterol from the plasma membrane reduced the membrane density of Hsp70 on CT26 mouse colon tumor cells (Fig. S2), whereas changes in the salt concentration or the pH—indicative of receptor-mediated associations—had no effect. These data demonstrate that the membrane form of Hsp70 in mice also appears to be located in cholesterol-rich microdomains (18, 19). Although the cmHsp70.1 mAb can specifically detect membrane Hsp70 expression on viable tumor cells, other commercially available Hsp70-specific antibodies cannot.

We have previously reported that a membrane $Hsp70^+$ phenotype serves as a negative prognostic marker for patients with lower rectal and lung carcinomas (9). Herein, we have demonstrated that immortalized, oncogenic-transformed and highly metastatic tumors, but not their primary counterparts and low-malignant cells, present Hsp70 on their cell surface. The study therefore assessed the capacity of membrane Hsp70 to act as a tumor-specific target for antibody-mediated killing of highly aggressive tumors using a syngeneic CT26 mouse-colon tumor model. Despite the relatively low density of Hsp70 molecules that are presented on the cell surface of CT26 mouse tumor cells (≈10,000 per cell), and that IgG1 has a low capacity to induce ADCC (20) and complement-dependent cytotoxicity (21) in mice, the cmHsp70.1 mAb mediates specific killing in membrane $Hsp70^+$ CT26 tumors. In contrast, other IgG1 control antibodies directed against theta or the Fab fragment of cmHsp70.1 mAb had no such effect. Furthermore, binding of cmHsp70.1 mAb to membrane $Hsp70^+$ tumors did not enhance the intracellular Hsp70 levels

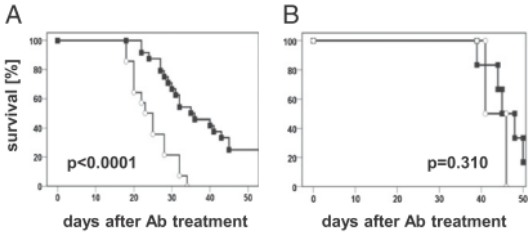

Fig. 4. (*A*) Kaplan-Meyer curves of overall survival of mice treated with an isotype-matched control antibody or cmHsp70.1 mAb on days 3, 5, and 7 after intraperitoneal injection of 2.5×10^4 CT26 tumor cells (20 μg per injection). The overall survival of mice (3 × Ab cmHsp70.1, filled squares; $n = 24$) treated with cmHsp70.1 mAb was significantly higher than that of animals (ctrl, open circles; $n = 14$) that received the IgG1 isotype-matched control antibody ($P < 0.0001$). (*B*) In contrast, the cmHsp70.1-mAb treatment (3 × Ab cmHsp70.1, filled squares) had no significant effect on the survival of mice bearing membrane $Hsp70^-$ A20 lymphomas ($n = 12$) compared with mice receiving the IgG1 isotype-matched control antibody (ctrl, open circles; $n = 4$, $P = 0.310$).

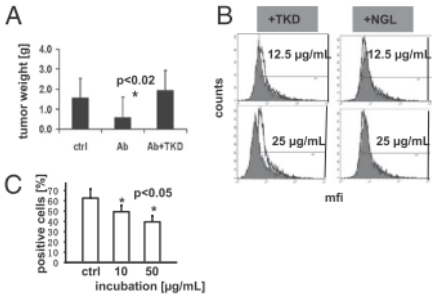

Fig. 5. (*A*) Coinjection of an excess of the Hsp70 peptide TKD with the cmHsp70.1 mAb completely inhibits the significant antitumoral effect of the latter (*$P < 0.02$). The cmHsp70.1 mAb (20 μg per injection) was coinjected intravenously on days 3, 5, and 7 together with 50 μg TKD following intraperitoneal injection of 2.5×10^4 CT26 tumor cells; media, $n = 21$; Ab, $n = 22$; Ab+TKD, $n = 21$. Mice were killed on day 14 and tumor weights were determined. (*B*) Binding of cmHsp70.1-FITC mAb to CT26 tumor cells was inhibited by the coincubation with an excess of TKD peptide. As a control, the scrambled NGL peptide was used. Tumor cells were coincubated either with cmHsp70.1-FITC mAb (5 μg/mL; white histogram) or with cmHsp70.1-FITC mAb (5 μg/mL) plus TKD (gray histogram; *Left*) or NGL peptide (gray histogram; *Right*) at concentrations of 12.5 and 25 μg/mL, respectively. The data illustrate one representative experiment out of three independent experiments, all of which show similar results. (*C*) Binding of cmHsp70.1-FITC to CT26 tumor cells was inhibited significantly (*$P < 0.05$) by the coincubation with the C-terminal substrate-binding domain of Hsp70 in a concentration dependent manner (10 and 50 μg/mL).

(Fig. S2), and thus a cmHsp70.1 mAb-based therapy is not likely to enhance protection of tumors against Hsp70-mediated apoptosis.

We have previously demonstrated that the incubation of lymphocytes with Hsp70 peptide TKD in the presence of low-dose IL-2 results in an enhanced cytolytic and migratory capacity of NK cells toward membrane $Hsp70^+$ tumor cells in vitro and in vivo (12, 22). The direct cytolytic effects of TKD/IL-2–activated NK cells against membrane $Hsp70^+$ mouse tumors were clearly detectable in the current study, as has previously been described for human tumors (12, 23, 24). In a clinical phase I trial, the tolerability, feasibility and safety of adoptively transferred, autologous TKD/IL-2–activated NK cells has been shown in patients having colorectal and lung carcinomas (23). Here, we show that the in vitro cytotoxic effects of TKD/IL-2–activated NK cells against membrane $Hsp70^+$ tumor cells can be further improved by the addition of cmHsp70.1 mAb. This process is most likely mediated by ADCC. The cmHsp70.1 mAb-induced killing of membrane Hsp70 CT26 tumor cells involves an enhanced migratory capacity of effector cells and a direct cytotoxic attack.

Three intravenous injections of relatively low amounts of unconjugated cmHsp70.1 mAb into tumor-bearing mice induced an infiltration of innate immune cells and significantly reduced the growth of CT26 tumors. The finding that the membrane Hsp70-positivity of CT26 tumors derived from mice autopsies was greater than that of in vitro cultured CT26 cells might explain the cmHsp70.1 mAb-mediated ADCC effect.

We have also previously reported that membrane $Hsp70^+$ tumors actively release Hsp70 surface-positive lipid vesicles (25), which have the biophysical characteristics of exosomes (26, 27) and that these can attract activated, but not resting NK cells. The current study found a significant increase in circulating Hsp70 in those mice in which tumor growth was inhibited. Whether this serum Hsp70 originates from exosomes or from necrotic tumor material has not yet been elucidated. Furthermore, ongoing studies are evaluating whether the administration of low-dose IL-2 into tumor-bearing mice might further improve the antitumoral effect of cmHsp70.1 mAb via the in vivo activation of mouse NK cells.

Remarkably, three consecutive intravenous injections of relatively low amounts of cmHsp70.1 mAb not only delayed the growth of subcutaneous- and intraperitoneal-residing CT26 tumors, but also significantly prolonged the survival of the mice. The Hsp70-specificity of this approach is supported by the finding that cmHsp70.1 mAb had no effect on tumor growth or the survival of mice bearing membrane $Hsp70^-$ A20 B-cell lymphomas. Moreover, coincubating membrane $Hsp70^+$ tumors with an excess of TKD peptide or the C-terminal substrate-binding domain and cmHsp70.1 mAb blocked the antibody binding in vitro, and TKD peptide also completely reversed the antitumoral effect in vivo. These data confirm that the TKD peptide sequence represents the recognition site of cmHsp70.1 mAb (Fig. S1).

As radiochemotherapy has been shown to enhance the cell-surface density of Hsp70 on tumors (10, 28–30), we speculate that a combined approach consisting of an Hsp70 mAb-based immunotherapy, which involves activated NK cells, as has been shown for a Her2-targeted ADCC (31), might provide a previously unexplored strategy to improve the clinical outcome of patients undergoing standard radiochemotherapy or with distant metastases. This proposition is in line with the observation that a metastasis-free survival rate of patients can be associated with an enhanced NK cell activity (32). The clinical relevance of our data are further supported by published observations on the ADCC activity of trastuzumab in metastatic breast cancer patients (33). In this study, the in vitro ADCC activity toward Her2 overexpressing tumor cells, which was quantitatively comparable to that which was seen against Hsp70 membrane-positive tumor cells in the current study, could be correlated to the short-term antitumor responses in trastuzumab-treated breast cancer patients (33).

Materials and Methods

Human Tumor Cell Lines, Mouse Tumor Cell Lines, and Primary Cells. Human tumor cell lines: CX2 (colon), MCF-7, MDA436 (breast), and A549 (lung) carcinoma cell lines (Tumorbank Deutsches Krebsforschungszentrum, Heidelberg, Germany), Malme, Mel Ei, Mel Ho, Parl, A375 and Sk Mel29 malignant melanomas (J. Johnson, Institute of Immunology, Ludwig-Maximilians-Universität Munich, Germany) (34). Mouse tumor cell lines: CT26 (colon, CT26.WT; ADCC CRL-2638, BALB/c) (17), 1048 (pancreatic), A20 (B-cell lymphoma, BALB/c) (35), B16F0 (low malignant, C57BL/6), B16F10 (high malignant, C57BL/6), BW transfected with the theta antigen (E. Kremmer, Helmholtz-Zentrum München, Munich, Germany). Cells were cultured in RPMI 1640 or DMEM supplemented with 10% (vol/vol) heat-inactivated FCS, 2 mM L-glutamine, 1 mM sodium-pyruvate and antibiotics (100 IU/mL penicillin, 100 μg/mL streptomycin) at 37 °C in 5% (vol/vol) CO_2. Single-cell suspensions were derived by short-term (less than 1 min) treatment with 0.25% (wt/vol) Trypsin-0.53 mM EDTA.

Primary macrovascular HUVECs and their isogenic EC counterparts EA.hy.926, which results from a fusion of HUVECs with the epithelial lung-carcinoma cell line A549, and HMEC, which were obtained by a transfection of primary microvascular ECs with the coding region for the simian virus 40A gene product (SV40) large T antigen, were cultured in ECGM medium supplemented with Supplement Mix (Sigma Aldrich). Cell-culture reagents were purchased from Life Technologies and Sigma Aldrich.

Tumor specimens and corresponding normal tissues were obtained from patients at the University Regensburg, Germany between February 2002 and January 2004. Fresh biopsy material was washed in antibiotic (penicillin/streptomycin) containing DMEM and single-cell suspensions were prepared by mincing the tissue and forcing it through a sterile mesh. The corresponding normal tissue was derived from the same patients at a distance of at least 0.2 cm from the tumor. The study was approved by the Institutional Review Board of the Medical Faculty of the University Hospital Regensburg, Germany and all patients included in the study provided signed informed consent.

Flow Cytometry and Blocking of Binding. The membrane Hsp70 phenotype on tumor cells was determined by flow cytometry using either the FITC-conjugated cmHsp70.1 mAb (IgG1; Multimmune GmbH), which is directed against the extracellular exposed sequence of membrane Hsp70 or the SPA810 mAb (IgG1; Stressgen via Assay Designs). Briefly, after incubation of viable cells (0.2×10^6 cells) with the primary antibodies for 30 min at 4 °C and following two washing steps, 7-AAD$^-$ viable cells were analyzed using a FACSCalibur flow cytometer (BD Biosciences). An isotype-matched (IgG1) control antibody was used to determine nonspecific binding to cells. Blocking of the antibody binding was performed by coincubating viable tumor cells (0.2×10^6 cells) using cmHsp70.1-FITC mAb (5 μg/mL) and an excess of TKD or scrambled NGL peptide (12.5 and 25 μg/mL) or the C-terminal substrate binding domain of Hsp70 (aa 383–548, 10 and 50 μg/mL).

The proportion of lymphocyte subpopulations, monocytes, granulocytes, and their expression of the activation marker CD25 (α chain of the IL-2 receptor) was determined using FITC/PE-labeled mAb directed against CD4, CD8, CD205, CD11c, Ly6G/Ly6C (Gr-1), B220, CD11b, CD49b, CD56 and CD25 (BD Biosciences).

Animals. BALB/c mice were obtained from an animal breeding colony (Harlan Winkelmann) and maintained in pathogen-free, individually ventilated cages (Tecniplast). Animals were fed with sterilized, laboratory rodent diet (Meika) and were used for experiments between 6 and 12 wk of age. All animal experiments were approved by the "Regierung von Oberbayern" and were performed in accordance with institutional guidelines of the Klinikum rechts der Isar, Technische Universität München.

Stimulation of Mouse Spleen Cells for ADCC. Freshly isolated BALB/c mouse spleen cells (5×10^6 cells/mL) were cultured in RPMI medium 1640 containing 10% (vol/vol) FCS alone (unstimulated) or medium containing low-dose IL-2 (100 IU/mL) plus TKD peptide (2 μg/mL) (Bachem) at 37 °C for 4 d. TKD is a GMP-grade 14-mer peptide of the C-terminal substrate binding domain of human Hsp70 (TKDNNLLGRFELSG, $aa_{450–463}$), which is known to selectively induce the reactivity of human NK cells against membrane $Hsp70^+$ tumor cells (12). The TKD equivalent region in the mouse (TRDNNLLGRFELSG) exhibits only one conservative amino acid exchange at position 2 (K-R) and this sequence stimulates mouse NK cells, even in the absence of IL-2 (16).

ADCC and Blocking Assays. ADCC was measured using a standard 4 h ^{51}Cr-release assay (36, 37). For blocking, labeled target cells were preincubated with the cmHsp70.1 mAb, the IgG1 isotype-matched control mAbs, SPA810 mAb, the theta-specific Ox7.11 (50 μg/mL, each), or the cmHsp70.1 Fab fragment (50 μg/mL). The degree of ADCC-dependent cytotoxicity was calculated, from which the lysis mediated by NK cells in the absence of cmHsp70.1 mAb/isotype control was subtracted. The spontaneous release for each target cell ranged

between 10 and 15%. Complement-dependent cytotoxicity was performed using identical experimental conditions, but in the absence of effector cells.

Intraperitoneal and Subcutaneous Injection of Tumor Cells. Tumor cells were thawed from a common frozen stock and cultured in vitro for 2 to 3 d before use. Next, 2.5×10^4 CT26 or 8×10^5 A20 cells (35) were injected intraperitoneally. For the growth-delay experiments, 1×10^6 CT26 cells were injected subcutaneously (neck) in BALB/c mice using a 1-mL plastic syringe and a 22-gauge needle. The injection was visually controlled using a 7× Stereomicroscope (Zeiss). The cmHsp70.1 mAb was injected either once on day 4 or on days 4, 7, and 10 after subcutaneous tumor injection and the tumor volume was determined every second day using a caliper and confirmed using ultrasound (GE Healthcare).

Injection of Antibodies and the 14-mer Hsp70 Peptide TKD. For the immunotherapeutic approach, mice were injected with unconjugated cmHsp70.1 mAb (i.v., 20 μg mAb per injection) or an IgG1 isotype-matched control antibody on days 3, 5, and 7 after the injection of CT26 cells (i.p., 2.5×10^4). For the inhibition assays, 20 μg cmHsp70.1 mAb was coinjected with an excess of the TKD peptide (TKDNNLLGRFELSG; 50 μg/mL per injection; purity >97%, EMC Microcollections GmbH) on days 3, 5, and 7 after an intraperitoneal tumor cell injection.

Autopsy. Control mice and cmHsp70.1 mAb treated mice were killed by craniocervical dislocation. The peritoneal cavity was macroscopically inspected for tumor dissemination and the primary tumors were excised in total, and their weights determined.

Immunohistochemistry. After weighing, tumors were cut into 4-mm thick pieces, fixed in Bouin's solution containing 71.5% (vol/vol) picric acid, 23.8% (wt/vol) formaldehyde, 4.7% (vol/vol) acetic acid, and embedded in paraffin. Consecutive section-pairs of the tumors (5 μm) were prepared from the ventral margin of each piece for a distance of 250 μm. The morphology of the excised tumors was visualized using standard H&E and Masson-Goldner staining. Nuclei were costained in 1% (wt/vol) Mayer's Hematoxylin (Dako). For the immunohistochemistry, endogenous peroxidase activity was blocked using freshly prepared 1% (vol/vol) H_2O_2 containing 0.1% (wt/vol) NaN_3. For the detection of effector cells, sections were heated for 30 min at 97 °C and then incubated with anti-NK cell (clone DX5, 1:25, rat–anti-mouse CD49b, IgM; Biozol; clone 12F11, 1:100, rat–anti-mouse CD56; BD Biosciences), anti-T cell (clone 145–2C11, 1:50, hamster–anti-mouse CD3ε, IgG; Biolegend; clone SP7, 1:100, rabbit–anti-goat CD3; Abcam), anti-macrophage (clone BM8, 1:50, rat–anti-mouse F4/80, IgG2a; ACRIS Antibodies GmbH, 1:50), anti-granulocyte/macrophage (clone RB6-8C5, 1:50, rat–anti-mouse Gr-1 Ly6C/Ly6G, IgG2bκ; Biolegend) mAbs or the appropriate isotype-matched control reagent overnight at 4 °C. After washing, sections were incubated for 2 h at room temperature with a rabbit anti-rat or rabbit anti-hamster HRP-conjugated secondary polyclonal antibody preparations as appropriate (Dako) followed, after washing, by diaminobenzidine (Dako) as the chromogen. Sections were counter stained with 1% (wt/vol) Mayer's Hematoxylin (Dako) for 30 s and analyzed on an Axiovert 25 microscope (Zeiss).

Statistical Analysis. Comparative analysis of in vitro data was undertaken using a nonparametric log-rank test (Mann-Whitney). Survival times were estimated from Kaplan-Meyer curves by log-rank test (38).

ACKNOWLEDGMENTS. The authors thank Nicola Dierkes and Anett Lange for excellent technical and editorial assistance, and Integrated BioDiagnostics (Martinsried, Germany) for technical support. This work was supported by the Deutsche Forschungsgemeinschaft (DFG) SFB824/1, DFG-Cluster of Excellence: Munich-Centre of Advanced Photonics, Bundesministerium für Bildung und Forschung (MOBITUM, 01EZ0826; Kompetenzverbund Strahlenforschung, 03NUK007E), the European Union (EU-STEMDIAGNOSTICS, FP7-037703; EU-CARDIORISK, FP7-211403), and Multimmune GmbH.

1. Adams GP, Weiner LM (2005) Monoclonal antibody therapy of cancer. *Nat Biotechnol* 23:1147–1157.
2. Scallon BJ, et al. (2006) A review of antibody therapeutics and antibody-related technologies for oncology. *J Immunother* 29:351–364.
3. Bonner JA, et al. (2006) Radiotherapy plus cetuximab for squamous-cell carcinoma of the head and neck. *N Engl J Med* 354:567–578.
4. Edwards JC, et al. (2004) Efficacy of B-cell-targeted therapy with rituximab in patients with rheumatoid arthritis. *N Engl J Med* 350:2572–2581.
5. Ferrarini M, Heltai S, Zocchi MR, Rugarli C (1992) Unusual expression and localization of heat-shock proteins in human tumor cells. *Int J Cancer* 51:613–619.
6. Shin BK, et al. (2003) Global profiling of the cell surface proteome of cancer cells uncovers an abundance of proteins with chaperone function. *J Biol Chem* 278:7607–7616.
7. Multhoff G, et al. (1995) A stress-inducible 72-kDa heat-shock protein (HSP72) is expressed on the surface of human tumor cells, but not on normal cells. *Int J Cancer* 61:272–279.
8. Hantschel M, et al. (2000) Hsp70 plasma membrane expression on primary tumor biopsy material and bone marrow of leukemic patients. *Cell Stress Chaperones* 5:438–442.
9. Pfister K, et al. (2007) Patient survival by Hsp70 membrane phenotype: Association with different routes of metastasis. *Cancer* 110:926–935.
10. Gehrmann M, et al. (2005) Dual function of membrane-bound heat shock protein 70 (Hsp70), Bag-4, and Hsp40: protection against radiation-induced effects and target structure for natural killer cells. *Cell Death Differ* 12(1):38–51.
11. Fouchaq B, Benaroudj N, Ebel C, Ladjimi MM (1999) Oligomerization of the 17-kDa peptide-binding domain of the molecular chaperone HSC70. *Eur J Biochem* 259:379–384.
12. Multhoff G, et al. (2001) A 14-mer Hsp70 peptide stimulates natural killer (NK) cell activity. *Cell Stress Chaperones* 6:337–344.
13. Stangl S, et al. (2010) In vivo imaging of CT26 mouse tumors by using cmHsp70.1 monoclonal antibody. *J Cell Mol Med*, 10.1111/j.1582-4934.2010.01067.x.
14. Horváth I, Vigh L (2010) Cell biology: Stability in times of stress. *Nature* 463:436–438.
15. Horváth I, Multhoff G, Sonnleitner A, Vigh L (2008) Membrane-associated stress proteins: More than simply chaperones. *Biochim Biophys Acta* 1778:1653–1664.
16. Zhang H, Liu R, Huang W (2007) A 14-mer peptide from HSP70 protein is the critical epitope which enhances NK activity against tumor cells in vivo. *Immunol Invest* 36:233–246.
17. Wang M, et al. (1995) Active immunotherapy of cancer with a nonreplicating recombinant fowlpox virus encoding a model tumor-associated antigen. *J Immunol* 154:4685–4692.
18. Gehrmann M, et al. (2008) Tumor-specific Hsp70 plasma membrane localization is enabled by the glycosphingolipid Gb3. *PLoS One* 3:e1925.
19. Sugawara S, et al. (2009) Binding of *Silurus asotus* lectin to Gb3 on Raji cells causes disappearance of membrane-bound form of HSP70. *Biochim Biophys Acta* 1790(2):101–109.
20. Steplewski Z, Lubeck MD, Koprowski H (1983) Human macrophages armed with murine immunoglobulin G2a antibodies to tumors destroy human cancer cells. *Science* 221:865–867.
21. Houghton AN, et al. (1985) Mouse monoclonal IgG3 antibody detecting GD3 ganglioside: A phase I trial in patients with malignant melanoma. *Proc Natl Acad Sci USA* 82:1242–1246.
22. Stangl S, Wortmann A, Guertler U, Multhoff G (2006) Control of metastasized pancreatic carcinomas in SCID/beige mice with human IL-2/TKD-activated NK cells. *J Immunol* 176:6270–6276.
23. Krause SW, et al. (2004) Treatment of colon and lung cancer patients with ex vivo heat shock protein 70-peptide-activated, autologous natural killer cells: A clinical phase I trial. *Clin Cancer Res* 10:3699–3707.
24. Milani V, et al. (2009) Anti-tumor activity of patient-derived NK cells after cell-based immunotherapy—A case report. *J Transl Med* 7:50.
25. Gastpar R, et al. (2005) Heat shock protein 70 surface-positive tumor exosomes stimulate migratory and cytolytic activity of natural killer cells. *Cancer Res* 65:5238–5247.
26. Bausero MA, Gastpar R, Multhoff G, Asea A (2005) Alternative mechanism by which IFN-gamma enhances tumor recognition: Active release of heat shock protein 72. *J Immunol* 175:2900–2912.
27. Lancaster GI, Febbraio MA (2005) Exosome-dependent trafficking of HSP70: A novel secretory pathway for cellular stress proteins. *J Biol Chem* 280:23349–23355.
28. Gehrmann M, Radons J, Molls M, Multhoff G (2008) The therapeutic implications of clinically applied modifiers of heat shock protein 70 (Hsp70) expression by tumor cells. *Cell Stress Chaperones* 13(1):1–10.
29. Kleinjung T, et al. (2003) Heat shock protein 70 (Hsp70) membrane expression on head-and-neck cancer biopsy-a target for natural killer (NK) cells. *Int J Radiat Oncol Biol Phys* 57:820–826.
30. Farkas B, et al. (2003) Heat shock protein 70 membrane expression and melanoma-associated marker phenotype in primary and metastatic melanoma. *Melanoma Res* 13 (2):147–152.
31. Carson WE, et al. (2001) IL-2 enhances NK cell response to Herceptin-coated Her2/*neu*-positive breast cancer cells. *Eur J Immunol* 31:3016–3025.
32. Kondo E, et al. (2003) Preoperative natural killer cell activity as a prognostic factor for distant metastasis following surgery for colon cancer. *Dig Surg* 20:445–451.
33. Beano A, et al. (2008) Correlation between NK function and response to trastazumab in metastic breast cancer patients. *J Transl Med* 6:25.
34. Dressel R, Johnson JP, Günther E (1998) Heterogeneous patterns of constitutive and heat shock induced expression of HLA-linked HSP70-1 and HSP70-2 heat shock genes in human melanoma cell lines. *Melanoma Res* 8(6):482–492.
35. Kim KJ, Kanellopoulos-Langevin C, Merwin RM, Sachs DH, Asofsky R (1979) Establishment and characterization of BALB/c lymphoma lines with B cell properties. *J Immunol* 122:549–554.
36. Nishioka Y, et al. (1997) Combined therapy of multidrug-resistant human lung cancer with anti-P-glycoprotein antibody and monocyte chemoattractant protein-1 gene transduction: The possibility of immunological overcoming of multidrug resistance. *Int J Cancer* 71(2):170–177.
37. MacDonald HR, Engers HD, Cerottini JC, Brunner KT (1974) Generation of cytotixic T lymphocytes in vitro. *J Exp Med* 140:718–730.
38. Kaplan E, Meyer P (1958) Non-parametric estimation from incomplete observations. *J Am Stat Assoc* 53:457–481.

Endothelial cells cultured under flow

[1]Isabelle Riederer, [1]Michael Molls, [1]Wolfgang Sievert, [1,2]Gabriele Multhoff

[1] Department of Radiation Oncology, Technische Universität München, Klinikum rechts der Isar and
[2] Helmholtz Center Munich, German Research Center for Environmental Health, CCG – Innate Immunity in Tumor Biology, Munich, Germany

HelmholtzZentrum münchen
German Research Center for Environmental Health

Abstract

Introduction: By using a novel flow system of ibidi® GmbH (Martinsried, Germany) we established a method to mimick blood flow in macro- and microvascular vessels .
Material & Methods: Primary and immortalized endothelial cells were cultured under continous flow with defined shear stress and microscopic images were taken over a period of 72 h. The ibidi® system consists of an air pressure pump, fluid unit, and µ-slides in which the cells are cultured. After an overnight incubation (37°C, 5% CO_2) of endothelial cells in µ-slides the system is started by a stepwise increase of the flow rate in order to adapt the cells to shear stress. Via the software provided by ibidi® (Pump control v 1.4.0) different parameters can be adjusted to control pressure and shear stress rate. The pump system can produce negative and positive pressure in both reservoirs of the fluid unit and thus the medium is transported from one to the other reservoir through the µ-slide. Valve switch effects guarantee a continuous unidirectional flow of the medium through the µ-slide.
Three different human endothelial cells were used for our studies: primary macrovascular human umbilical vein endothelial cells (HUVECs) and their corresponding immortalized partner cell line EA.hy 926, a fusion product of HUVECs with lung carcinoma cells, and immortalized dermal human microvascular endothelial cells (HMECs) which were transfected with a PBR-322-based SV40 plasmid.
Results: Under confluent growth conditions, all endothelial cell lines are positively stained for factor VIII-related antigen (data not shown) and show the typical cobblestone formation. Under flow, primary HUVECs but not immortalized endothelial cell lines show a parallel orientation in direction of the flow. HUVECs have the capacity to migrate against the flow direction and also proliferate during flow. Under static growth conditions the parallel cell orientation disappears within hours.
HMECs grow faster and become more confluent under flow than under static cell culture conditions.
In contrast, EA.hy 926 cells lose adherence to plastic and undergo apoptotic cell death within two days under flow conditions.
Conclusion: The ibidi® system provides a suitable tool to mimick blood flow for primary HUVECs but not for immortalized endothelial cell lines (EA.hy.926; HMECs).

Acknowledgments: This work was supported by grants from EU-CARDIORISK 211404 and in parts by the DFG (SFB824 to G.M.), the BMBF (MOBITUM, 01EZ0826; m4, 01EX1021C; Strahlenkompetenz, 03NUK007E), and by multimmune GmbH. We thank Anett Lange for excellent editorial assistance.

ibidi® flow system

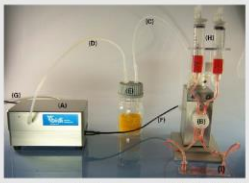

The ibidi® pump system. (A) air pressure pump, (B) fluid unit, (C, D) air pressure tubings, (E) dry bottle with silicate, (F) electric cable, (G) USB cable, (H) perfusion set, (I) µ-slide. (origin: ibidi®)

Generation of unidirectional flow

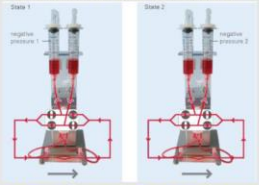

The principle of flow. Air pressure moves the medium from one reservoir to the other through a µ-slide. By regular valve switching continuous unidirectional flow is assured. (origin: ibidi®)

µ-slide

View of a µ-slide containing cells under flow. (origin: ibidi®)

Input mask of the software PumpControl v. 1.4.0

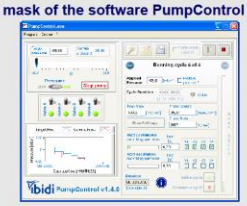

Input mask of the software "PumpControl v. 1.4.0" provided by ibidi® for adjustment of specific parameters like cycle duration, shear stress and flow rate. (origin ibidi®)

Characterization of the µ-slides and some parameters for the flow system

µ-slide	Cell number	Growth area	Volume / Height of the channel
µ-Slides I[0.4]	1-2 x 10^5	2.5 cm^2	100 µl / 400 µm
µ-Slide VI	0.25 x 10^5	0.6 cm^2	30 µl / 400 µm

Characteristics of two µ-slide types.

Cycle duration	Shear stress	Flow rate (circa)
5 h	1 dyne/cm^2	0.8 ml/min
5 h	2.5 dyne/cm^2	2 ml/min
infinite	5 dyne/cm^2	4ml/min

Defined parameters for the flow system.

Comparison of the morphology of HUVECs, EA.hy 926, and HMECs under flow

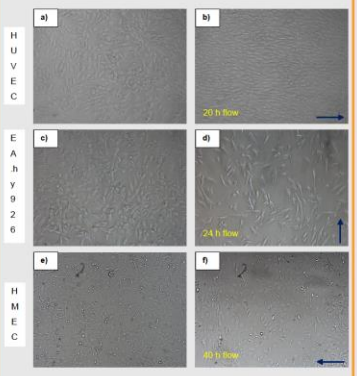

HUVECs (a, b), EA.hy 926 cells (c, d), and HMECs (e, f) under static (a, c, e) or flow (b, d, f) conditions. The flow direction is marked with an arrow. The cells were seeded 24 h before starting the flow. The duration of the flow is printed on the images.

Morphology of HUVECs before, during, and after flow

HUVECs before flow (a), during flow (24 h) (b), and 2 h after flow (c).

Cell proliferation of HUVECs under flow conditions

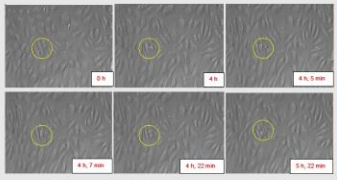

Details of the proliferation of HUVECs under flow conditions